Technology Collaboration Programme on Heat Pumping Technologies (HPT TCP)

Annex 40

Heat Pump Concepts for Nearly Zero-Energy Buildings

Task 3: Heat pump technology developments and heat pump testing platforms

Final Report

Operating Agent: Switzerland

2016

Report no. HPP-AN40-3

Published by

IEA Heat Pump Centre
Box 857, SE-501 15 Borås
Sweden
Phone: +46 10 16 55 12
Fax: +46 33 13 19 79

Production

IEA Heat Pump Centre, Borås, Sweden

ISBN 978-91-88349-82-8
Report No. HPP-AN40-3

Preface
This project was carried out within the Technology Collaboration Programme on Heat Pumping Technologies (HPT TCP) which is an Implementing agreement within the International Energy Agency, IEA.

The IEA
The IEA was established in 1974 within the framework of the Organization for Economic Cooperation and Development (OECD) to implement an International Energy Programme. A basic aim of the IEA is to foster cooperation among the IEA participating countries to increase energy security through energy conservation, development of alternative energy sources, new energy technology and research and development (R&D). This is achieved, in part, through a programme of energy technology and R&D collaboration, currently within the framework of over 40 Implementing Agreements.

The Technology Collaboration Programme on Heat Pumping Technologies (HPT TCP)
The Technology Collaboration Programme on Heat Pumping Technologies (HPT TCP) forms the legal basis for the Heat Pumping Technologies Programme. Signatories of the TCP are either governments or organizations designated by their respective governments to conduct programmes in the field of energy conservation.

Under the TCP collaborative tasks or “Annexes” in the field of heat pumps are undertaken. These tasks are conducted on a cost-sharing and/or task-sharing basis by the participating countries. An Annex is in general coordinated by one country which acts as the Operating Agent (manager). Annexes have specific topics and work plans and operate for a specified period, usually several years. The objectives vary from information exchange to the development and implementation of technology. This report presents the results of one Annex. The Programme is governed by an Executive Committee, which monitors existing projects and identifies new areas where collaborative effort may be beneficial.

The IEA Heat Pump Centre
A central role within the HPT TCP is played by the Heat Pump Centre (HPC). Consistent with the overall objective of the HPT TCP the HPC seeks to advance and disseminate knowledge about heat pumps, and promote their use wherever appropriate. Activities of the HPC include the production of a quarterly newsletter and the webpage, the organization of workshops, an inquiry service and a promotion programme. The HPC also publishes selected results from other Annexes, and this publication is one result of this activity.

For further information about the IEA Heat Pumping Technologies Programme and for inquiries on heat pump issues in general contact the Heat Pump Centre at the following address:
IEA Heat Pump Centre
Box 857
SE-501 15 BORÅS
Sweden
Phone: +46 10 16 55 12

Schweizerische Eidgenossenschaft
Confédération suisse
Confederazione Svizzera
Confederaziun svizra
Bundesamt für Energie BFE

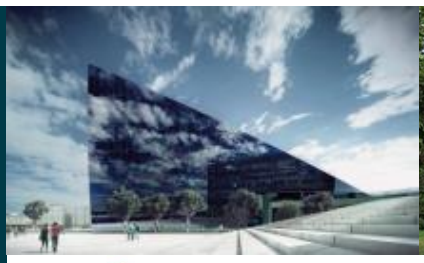

Schweizerische Eidgenossenschaft
Confédération suisse
Confederazione Svizzera
Confederaziun svizra
Bundesamt für Energie BFE

HSR
HOCHSCHULE FÜR TECHNIK
RAPPERSWIL
FHO Fachhochschule Ostschweiz

IEA HPT Annex 40 Heat pump concepts Nearly Energy Buildings

Heat pump concepts for Nearly Zero Energy Buildings

Heat pump technology developments and heat pump testing platforms

Editor
Carsten Wemhoener
Institute of Energy Technologies
HSR University of Applied Sciences Rapperswil
carsten.wemhoener@hsr.ch

IEA HPT Annex 40 Final Report Task 3

August 2016

International Energy Agency
Heat Pumping Technologies

Imprint

IEA HPT Annex 40 "Heat pump concepts for nearly zero energy buildings"
The work presented here is a contribution to the Annex 40 in the Heat Pump Technologies (HPT) Implementing Agreement of the International Energy Agency (IEA)

Operating Agent (Switzerland):
Institute of Energy Technologies, HSR University of Applied Sciences Rapperswil
Prof. Carsten Wemhoener, carsten.wemhoener@hsr.ch

Canada:
CANMET Energy, Natural ressources Canada, Varennes:
Roberto Sunyé, Ph.D., Roberto.Sunye@RNCan-NRCan.gc.ca
Laboratoire des technologies de l`énergie (LTE), Hydro Quebec, Shawinigan
Vasile Minea, PhD, minea.vasile@lte.ireq.ca

Finland:
Green Net Finland, Vantaa: Suvi Häkämies, suvi.hakamies@greennet.fi
Aalto University, Aalto: Juha Jokisalo
Finnish Heat Pump Association SULPU: Jussi Hirvonen
VTT Technical Research Centre of Finland Ltd, Helsinki: Satu Paiho

Germany:
Fraunhofer Institute of Solar Energy systems (FhG-ISE), Freiburg (Brsg.)
Dr.-Ing. Doreen Kalz, doreen.kalz@ise.fraunhofer.de, Dominic Wystrcil, Simon Winiger

Japan:
Graduate School of Engineering, Nagoya University, Nagoya
Prof. Dr. Eng. Masaya Okumiya, okumiya@davinci.nuac.nagoya-u.ac.jp
Graduate School of Design and Architecture, Nagoya City University, Nagoya
Prof. Dr. Eng. Gyuyoung Yoon, yoon@sda.nagoya-cu.ac.jp

The Netherlands:
Platform 31, Den Haag: Ivo Opstelten, Niels Sijpheer
TNO, Delft: Wouter Borsboom
Netherlands Enterprise Agency (RVO), Utrecht: Raymond Beuken, raymond.beuken@rvo.nl

Norway:
SINTEF Energy, Trondheim: Maria Justo Alonso maria.justo.alonso@sintef.no
COWI AS and NTNU, Trondheim: Dr. Ing. Jørn Stene, jost@cowi.no
The Norwegian University of Science and Technology (NTNU), Trondheim: Laurent Georges

Sweden:
SP Technical Research Institute of Sweden, Borås: Svein Ruud, svein.ruud@sp.se

Switzerland:
Institute of Energy in Building, Univ. of Applied Sciences Northwestern Switzerland, Muttenz
Prof. Dr. Thomas Afjei, thomas.afjei@fhnw.ch, Andreas Müller
Institute of Energy Technologies, HSR Univ. of Applied Sciences Rapperswil
Reto Kluser, Raphael Schweizer, Roman Schwarz, Loris Steinmann

USA:
Oak Ridge National Laboratory (ORNL), Oak Ridge, Tennessee
Van D. Baxter, baxtervd@ornl.gov
National Institute of Standards and Technologies (NIST), Gaitherbourg, Maryland
Vance W. Payne, Ph.D., vance.payne@nist.gov
Center of Environmental Energy Engineering (CEEE), University of Maryland
Prof. Reinhard Radermacher, Ph. D., raderm@umd.edu, Jiazhen Ling, Ph. D.

Abstract

Since the mid of the 1990ties low energy buildings with a significantly reduced energy consumption down to ultra-low energy standard (typical space heating energy need of 15 kWh/(m^2a)) have been realised. Based on the political strategies for the building sector in terms of meeting the climate protection targets, the building concepts are currently extended to derive a nearly zero energy balance, which requires on the one hand an energy-efficient building envelope and on the other hand energy-efficient building system technologies amended by an on-site renewable energy production.
IEA HPT Annex 40 is to investigate heat pumps for the application in nearly zero energy buildings. Due to the unique features of the heat pump, the application in nearly zero energy buildings can be particularly beneficial. Besides the high performance of the heat pump in combination with adapted systems of low supply temperatures, which can be installed in buildings with high performance building envelopes due to the low space heating loads, also the integration options of heat pumps with other building technologies can be an advantage of the heat pump application in these buildings.
In the Task 3 of the IEA HPT Annex 40 technology development of heat pumps adapted to the application in nearly or net zero energy buildings have been performed. These developments are related to different aspects.

- Performance improvements of the different operation modes which can be covered by the heat pump, e.g. space heating, space cooling, domestic hot water (DHW) and dehumidification
- Multifunctional operation of heat pumps for different building services, also in simultaneous operation mode, e.g. combined space cooling and DHW production
- Integration options of the heat pump with other building system technology, e.g. solar components, which are installed in the building envelope and which could be used as heat source and heat sink.
- Design and commissioning of test houses and platforms which enable the test of nZEB technology under reproducible conditions

Due to these developments, the heat pump application in nZEB can be even better performing than in the application in normal low energy buildings. On the other hand, it can be easier to reach the nZEB balance by application of adapted heat pumps with better performance, since less energy has be generated on-site to reach the balance.
This report on Task 3 covers the technology developments performed under IEA HPT Annex 40. It is partly linked also to lab-testing and field testing of components as well as to simulation work done for the prototypes and has therefore also a connection to the field testing performed in Task 4 of the Annex and the case studies by simulations in Task 2.

The results presented in this report relate to the

- Development of integrated heat pump (IHP) variants at Oak Ridge National Laboratory (ORNL) in the USA
- Integration of heat pumps and solar components as solar assisted heat pumps at CANMET Energy of Natural Resources Canada and in Switzerland
- Development of high performance dehumidification units for air-conditioning, e.g. in office buildings in Japan
- Commission and monitoring at the net Zero Energy Residential Testing Facility (NZERTF) at the campus of the National Institute of Standards and Technologies (NIST)

Contents

1 Solar assisted heat pumps in Canada

1.1 Solar assisted heat pump with ice slurry storage

Since 2009, Natural Resources Canada/CanmetENERGY-Varennes has worked to develop a new solar heat pump concept using ice slurry latent thermal storage (Tamasauskas et al., 2015). The integration of an ice storage in a solar system has the following three advantages, which increases the performance of the components:

- Increased energy storage densities
- Stable heat pump source temperatures
- Improved solar collector efficiencies

1.1.1 Solar heat pump concept

The investigated solar heat pump concept using an ice slurry storage has two distinct solar loops in order to operate in its most energy-efficient configuration. The principle concept of the system is shown in Fig. 1.

In one loop, the Solar Loop A, the collectors operate in series with the ice storage tank, offering improved solar collector efficiencies due to cold operation temperatures of the collector, increased thermal gains and extended collector utilisation periods in winter months, when solar radiation and ambient temperatures are lower. In this operation mode, the collector is used to regenerate the ice slurry storage, which is used as source of the heat pump.

In the other Solar Loop B, the collectors operate in series with the warm water tank, which can reduce the heat pump operation at higher temperature level, when ambient conditions allow the collectors to directly meet building thermal demands.

The system is able to switch between the two loops throughout the day as appropriate. Flow rates for the two solar loop circulation pumps are identical and set proportional to the total collector area.

In heating mode, the warm water storage is charged by the heat pump, which used water from the ice storage as heat source. The heating system is supplied by water from the top of the storage. DHW is preheated by a vertical coil inside the storage. Back-up heating is provided by direct electrical heating.

In cooling mode, the heat pump is operated during he night (10 PM to 6 AM) to generate ice in the storage, which serves as cold storage. Condenser heat is either rejected to the warm water storage depending on capacity or to an air-cooled remote outdoor air condenser. During daytime the DHW needs are met by charging the hot water storage with solar energy.

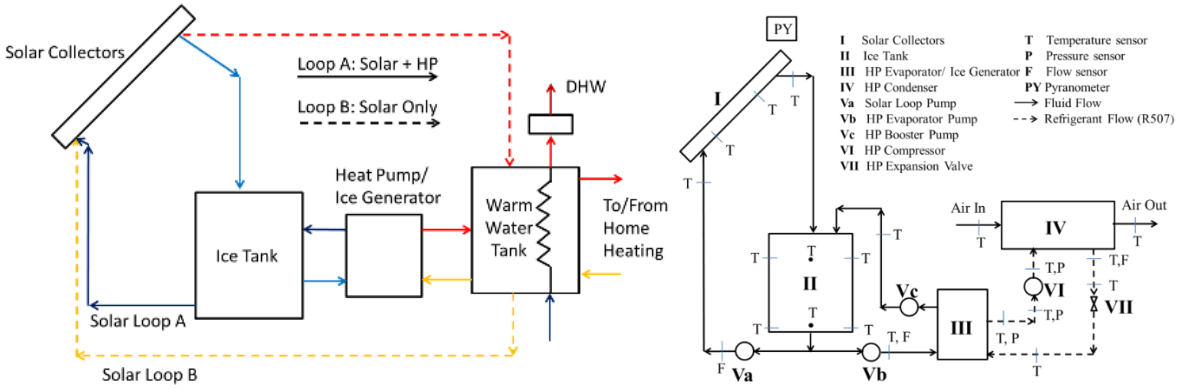

Fig. 1: Principle system configuration of the solar assisted heat pump (left) and simplified diagram of ice slurry test bench (right)

1.1.2 Test bench

A test bench has been developed at the NRCan/CanmetENERGY facility near Montreal in order to examine the potential of this system in reducing heating related energy use. Besides the approval of the concept, the test bench served different other purposes, among these the test of the Solar loop A, validation of simulations models, development of operational strategies and in-depth system analysis.

A simplified diagram of the developed test bench is provided in Fig. 1 (right), indicating all major equipment and measurement points. The test bench has been modified in sight of the concept, so it contains only one solar loop (Solar Loop A) and uses a water-air heat pump instead of a water-water heat pump. As working fluid, a propylene glycol mixture was used.

The test bench consists of several main components responsible for the supply, storage, and delivery of thermal energy.

- Four glazed flat plate solar collectors of total gross area of 11.9 m^2. Freezing risk is prevented by a drain back system.
- An ice tank of a total volume of 5 $m^{3.}$ The tank fluid mass is 3,695 kg, and consists of an initial 4% (by mass) propylene glycol/water solution. The freeze point of the solution is -1.1 °C (30 °F) when there is no ice, and decreases to approximately -2.0 °C (28.4 °F) at a 40% ice mass fraction. The tank is not mixed: Ice and fluid are allowed to separate via gravity into two distinct layers. Fluid returning from the solar loop is reintroduced into the tank using a distributor, which aims for an even delivery of flow across the top of the tank.
- Heat Pump/Ice Generator: The heat pump used in the test bench consists of an evaporator/ice generator coupled with a compressor and an air-cooled condensing unit. R-507a is used as the refrigerant. The rated heating capacity is approximately 17.8 kW (61 MBH) and the COP is 4.0 at design conditions (an inlet evaporator temperature of 0 °C and an inlet condenser temperature of 25 °C).

1.2 Validation of simulation results

One purpose of the test bench was to build and validate simulation models of the systems. Modelling was done in TRNSYS v17 (Klein et al., 2010). Both standard and custom components have been used for the simulation. The developed test bench energy model was validated using measured data from the Spring and Autumn of 2014. Special focus was given to validating the solar and heat pump loops, responsible for the supply and delivery of thermal energy within the system.

The following figures show comparison for the collector and the heat pump loop for October 23rd, 2014. Data for this day was selected because (i) it demonstrates the performance of the system at lower solar radiation values, and (ii) both the solar and heat pump loops were operated within a short time frame. Similar results were obtained for other days examined. Validation of the ice storage tank model is contained in Tamasauskas et al. (2012b).

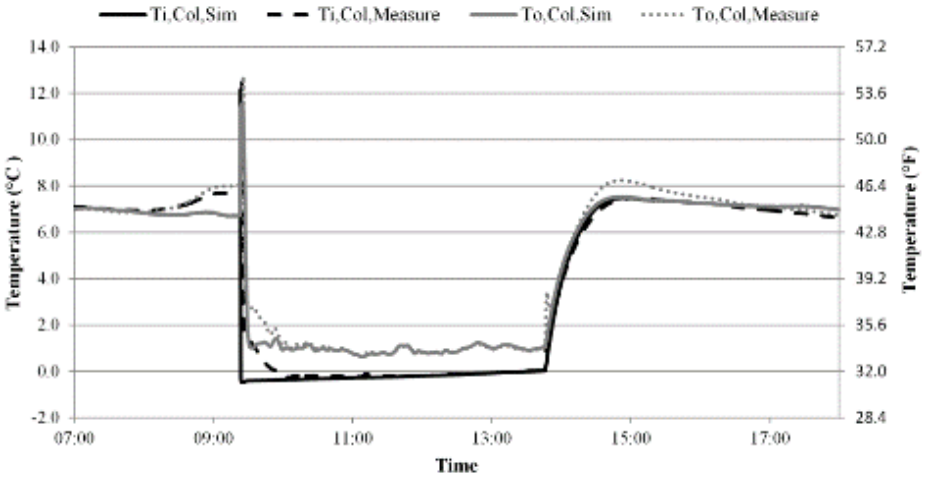

Fig. 2: Comparison of measured and simulated collector temperatures

Fig. 2 compares the measured and simulated temperatures of the solar collectors. In general, both sets of results show good agreement during the day. Larger discrepancies are seen under no flow conditions, which result from difficulties in fully modelling the fluid drain-back feature used in the test bench. The close agreement between measured and simulated inlet collector temperatures during solar loop operations also confirms the ability of the ice tank model to provide accurate predictions of component performance within the system.

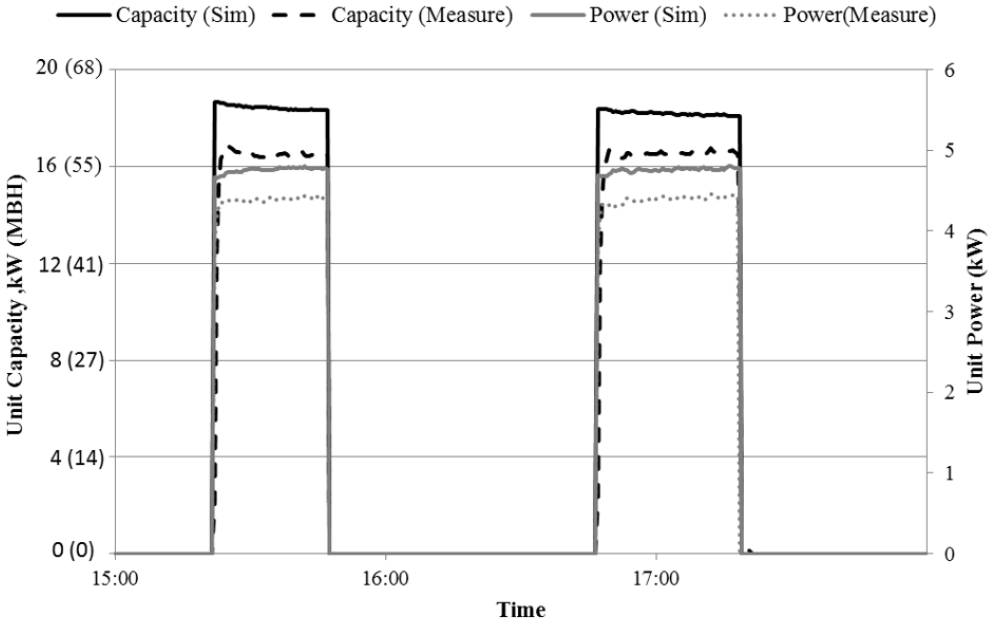

Fig. 3: Comparison of measured and simulated capacity and power input of the heat pump

Fig. 3 shows the comparison of the measured and simulated heat pump capacity and power use. Simulated heating capacities are consistently within 10% of those measured. Discrepancies between the two data sets can be attributed to the fact that simulated performance has been developed based on a provided compressor data sheet, where rating conditions may not be identical to those seen during actual operation. The simulated and measured power values show good agreement, with minimal discrepancies between the two data sets.

1.3 System modelling for nZEBs

The overall objective of the research is to develop a system that is capable of delivering significant energy use reductions in Canadian homes. The developed simulation model is based on the component models described above, and has been modified in accordance to the solar loops in the concept. Wherever appropriate, parameters and sizing were kept the same as in the test bench model. A complete description of system modelling can be found in Tamasauskas et al. (2015).

Tab. 1: Key housing characteristics

	Montreal	Toronto	Vancouver
Roof RSI	8.93 m^2°C/W (R51)	8.93 m^2°C/W (R51)	8.93 m^2°C/W (R51)
Wall RSI	5.46 m^2°C/W (R31)	5.46 m^2°C/W (R31)	4.48 m^2°C/W (R25)
Basement Wall RSI	4.95 m^2°C/W (R28)	4.95 m^2°C/W (R28)	4.95 m^2°C/W (R28)
Basement Slab RSI	2.58 m^2°C/W (R15)	2.58 m^2°C/W (R15)	1.86 m^2°C/W (R11)
Window U-Value	1.35 W/m^2°C	1.35 W/m^2°C	1.35 W/m^2°C
Infiltration	0.75 ACH @ 50Pa	0.60 ACH @ 50Pa	1.0 ACH @ 50Pa
Annual Heat Demand	39 kWh/m^2	36 kWh/m^2	32 kWh/m^2
Peak Heat Load	31 W/m^2	26 W/m^2	22 W/m^2

The investigated system has been initially developed for use in nearly and net-zero energy buildings.

In order to assess potential of the system, housing models were developed for three distinct regions in Canada (Montreal, Toronto, and Vancouver). Tab. 1 summarizes housing characteristics by region.
Further details on the development of each housing model can be found in Kegel et al. (2012). The system model comprises several main components, including solar collectors, an ice tank, a warm water tank, and a heat pump. Tab. 2 contains details on the component models. The heating system considered for all regions are electrical baseboards, the cooling system is a split system of a rated EER of 3.45, the mechanical ventilation has a heat recovery of 84% efficiency and the DHW is prepared by and conventional electrically heated tank. The daily DHW draw has been set to 233 l/day.

Tab. 2: System modelling component details

System Component	TRNSYS Type	Notes
Flat Plate Solar Collector	Type 539	SRCC performance, 27 m^2, slope 40°, azimuth 0°, flow 60 $kg/(h \cdot m^2)$
Heat Pump	Type 919	Same as test bench. Rated COP 4.0
Warm Water Tank	Type 538	Multi-nodal. Volume 1.5 m^3
Ice Tank	Type 214 (Custom)	Volume 5.0 m^3

Further details regarding system parameters and models can be found in Tamasauskas et al. (2015).

1.4 System performance in nZEB housing

The proposed system was simulated in TRNSYS for each selected region using a time step of approximately 5 minutes. Tab. 3 compares the energy use of the base case and solar heat pump systems for each region.

Tab. 3: Energy use of solar heat pump system by region and SPF

	Montreal		Toronto		Vancouver	
	Base	Ice Slurry HP	Base	Ice Slurry HP	Base	Ice Slurry HP
Heat + DHW [kWh]	13,042	4,494	12,099	4,211	11,010	4,157
Cool [kWh]	819	1,591	768	1,406	586	1,124
Fans+Pumps [kWh]	1,222	1,370	1,222	1,352	1,222	1,296
Total Mech. [kWh]	15,082	7,455	14,089	6,968	12,818	6,578
SPF Heating & DHW	1	2.69	1	2.65	1	2.47
SPF Cooling	1	2.07	1	2.24	1	2.28
SPF System	1	2.53	1	2.55	1	2.43

An analysis of the results highlights the strong energy savings potential of the solar heat pump system in all three regions. Total energy savings for the mechanical system (heating, cooling, DHW and distribution) range from a maximum of 51% in Montreal and Toronto to a minimum of 49% in Vancouver. A closer examination reveals the true strength of the system lies in reducing the energy used for heating and DHW, with peak energy savings of up to 66% in Montreal and Toronto, and 62% in Vancouver. Implementation of the new cooling system results in an increase in cooling energy use relative to the base case, primarily due to the energy intensive nature of the ice generation process. Despite this increase, the separation of cooling use and production has important implications for peak demand reductions, and could potentially result in utility cost savings compared to the base case in regions where time of use rates are in effect. The system layout in cooling also allows for preheating of DHW whenever possible. Future work will further examine the demand shifting aspect of the design, in addition to reducing cooling energy use through new charging cycles and more advanced controls.
In order to more fully assess system performance, a seasonal performance factor (SPF) was calculated for each region and mode of operation, which is also contained in system SPFs are summarized in Tab. 3.

The solar heat pump system offers a significant improvement in SPF for all three regions in comparison to a base case of electrical heating and DHW (SPF=1). SPFs in heating mode are higher for Montreal and Toronto, primarily due to the greater abundance of solar radiation (and resulting collector gains).
Fig. 4 compares the energy use of the base case and ice-based systems with fully sized ground-source heat pump systems in Montreal and Toronto. While this comparison is dependent on a number of factors, including solar collector area and storage tank volumes, it is clear that the proposed concept offers energy savings equal or greater than a typical ground source system. This is particularly significant, as it suggests there is a strong potential for the system, especially in areas where it may be difficult to install a vertical ground source system due to space constraints or soil composition.

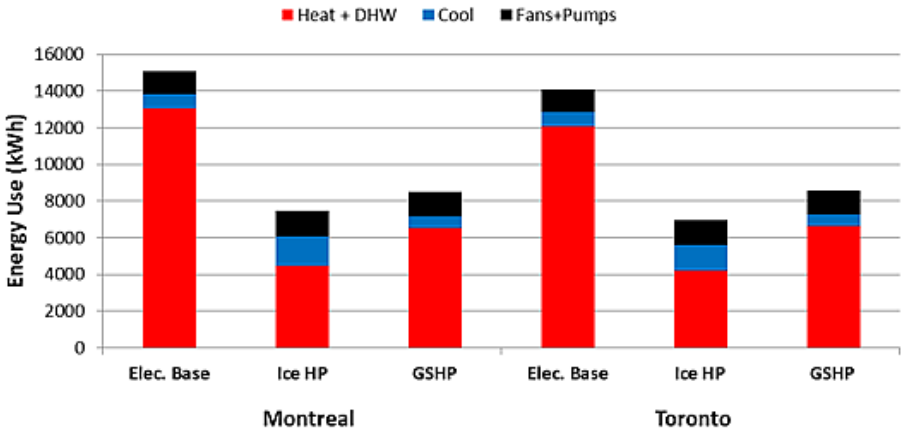

Fig. 4: Comparison of measured and simulated heat pump capacity and electrical power input

1.5 Experimental low energy house in Canada

In the province of Québec (Eastern Canada), more than 75% of new houses still adopt electrical baseboards as main heating systems. For houses with 2.5 inhabitants, the annual average electrical energy consumption is of 26,700 kWh (Statistics Canada, 2013). As residential energy consumption for heating still constitutes a significant component of the total energy demand, reducing it presents a major challenge.
The 2006 Equilibrium Initiative lead by Canada Mortgage and Housing Corporation and the Canadian Solar Building Network brought together the private and public sectors to develop homes “producing as much energy as they consume on an annual basis”.

1.5.1 System description

The experimental low energy house, known as EcoTerra home, is a rural single-family home of 234 m^2 (including a 90 m^2 basement), two-storey, factory built wood-framed modular detached home located in Eastman, Québec, designed by the Macintosh School of Architecture and engineered by the Concordia University research team (Minea et al., 2009; Doiron et al., 2011). The site’s daily average winter (December to March) and summer (June to September) temperatures are -8.6 °C and 15.6 °C, respectively. The annual normal (1971-2000) heating degree days (18 °C basis) is 5,151 Kd, while the total normal cooling degree days (18 °C basis) is about 100. The average daily irradiance at 30° from horizontal varies from 2.1 h in November to 5.4 h in July (ASHRAE 2005). Fig. 5 depicts the schematics of the building technology of the house. Approximately 30% of the south façade area of the house are glazed with triple-pane, argon-filled, low-emissivity windows. A south facing roof-mounted 57.2 m^2 building integrated photovoltaic/thermal system (BIPV/T) converts solar energy into electricity (maximum 2.86 kW_{el}) and heat (maximum 12 kW_{th} at 236 l/s air flow). It consists of 21 UniSolar, amorphous-silicon, 136 W modules fastened to a sloped (30.3˚) metal roof. Outdoor air is drawn under the PV cells by the variable speed fan F1. The PV system is coupled to the grid so that any surplus electricity generated is sent via an inverter to the grid.

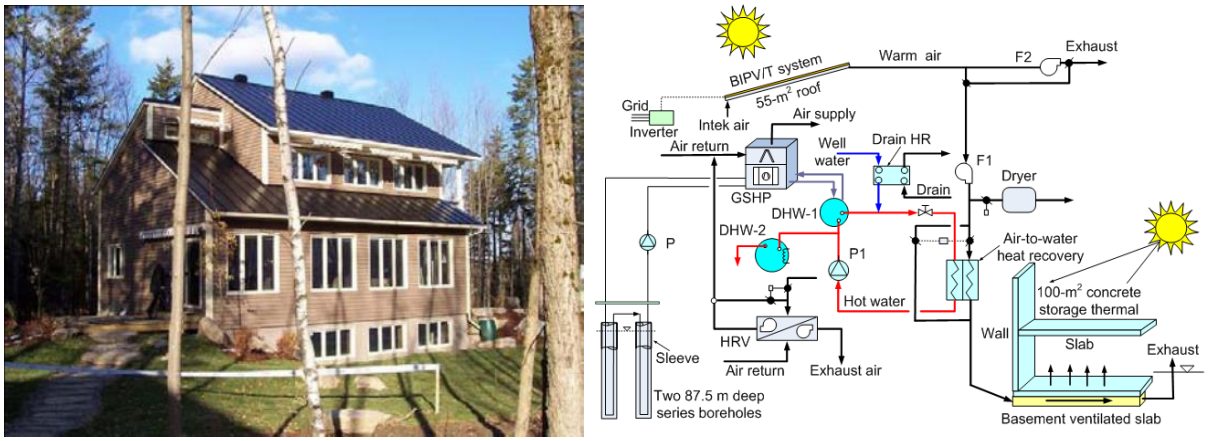

Fig. 5: Configuration of EcoTerra houss HVAC integrated system (Candanedo et al. 2008; Minea et al. 2009; Minea 2013). BIPV/T: building integrated photovoltaic/thermal; BP - brine pump; DHR - drain heat recovery; DHW - domestic hot water; DSH - desuperheater; GSHP - ground-source heat pump; HR-HEX - heat recovery heat exchanger; HRV - heat recovery ventilator; F - fan and WP - water pump.

The home draws power only as needed and excess power is fed back to the utility grid. The outdoor air is heated in the process by absorbing a portion of the solar energy that irradiates on the BIPV/T system.
Depending on the exiting temperature and heating demand, the solar-heated air can be used for drying clothes by circulating warm air through the clothes dryer, for preheating domestic hot water via an air-to-water heat exchanger (except in the winter), and for actively heating the thermal mass of a ventilated concrete slab in the basement. The cold water coming from a well is first heated by a drain-to-water heat recovery (HR) system, prior entering the preheating DHW storage tank. The preheated water is stored within a domestic hot water (DHW) tank where it is further heated by the heat pump's desuperheater (DSH). A second back-up electrical DHW tank then rises the hot water temperature up to 60 °C prior to supplying the consumers. The thermal energy stored is passively released from the top surface of the slab into the living space. Finally, a heat recovery ventilator (HRV) recovers heat from the outgoing, stale household air and uses it to preheat the incoming, fresh outdoor air. During the air-conditioning season, the HRV removes the heat from the incoming air and transfers it to the intake air.

1.5.2 Energy performance

Power generation

During a sunny day of a typical winter week (ref.: February 11-17), it was possible, generally around noon, to transfer about 1 kW of excess electrical power to the grid.

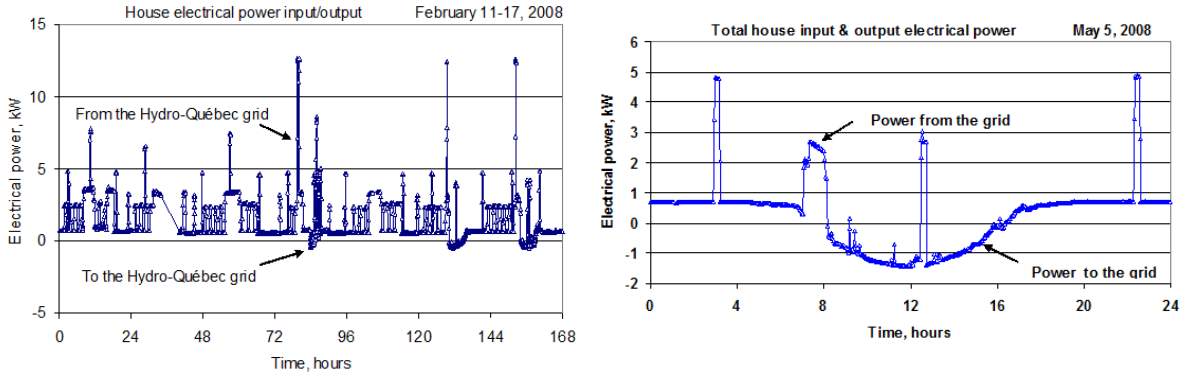

Fig. 6: Generation from the BIPV/T for a typical winter week in February (left) and in May (right)

During warmer spring days (e.g. May, 5), the electrical power in a sunny summer week (e.g. July 7-13), the gross electrical power generated daily by the BIPV/T system exceeded 2.2 kW (Minea, 2013).

Ground-source heat pump

During a typical winter week (February 11-17), the ground-source heat pump extracted 6.35 kW thermal power from the ground with COP varying between 4 (maximum) and 3 (minimum) at the beginning and the end of each running cycle respectively.

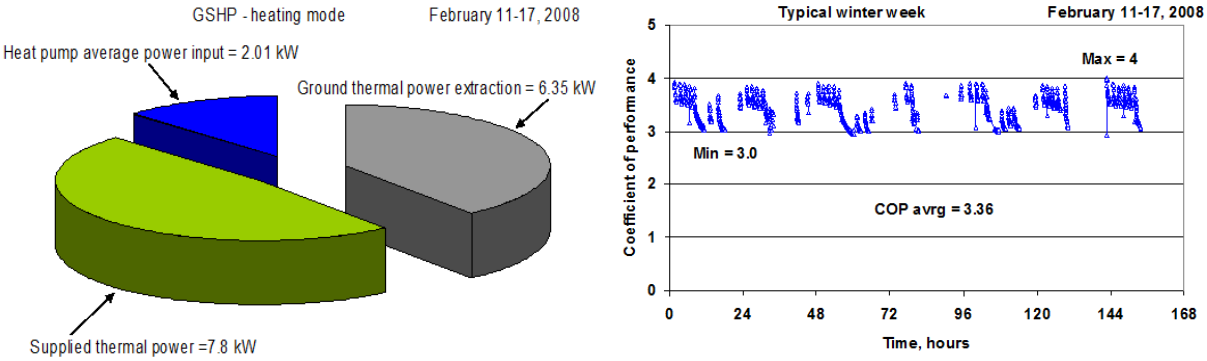

Fig. 7: Performance values of the ground-source heat pump during a typical winter week in February

Heat recovery ventilator

During the same typical cold winter week (February 11-17), the indoor air entered the heat recovery ventilator at around 22 °C prior to being exhausted. The heat recovered heated the outdoor fresh air from entering temperatures as low as -15 °C up to 15-20 °C prior to entering the GSHP. The overall energy efficiency of HRV, based on these measured temperatures, varied around 85%.

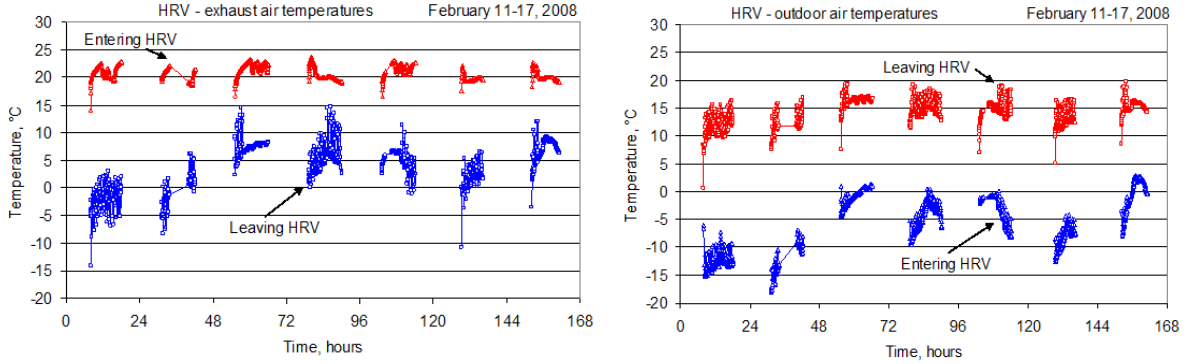

Fig. 8: Temperature at the ventilation heat recovery for a typical winter week in February

1.5.3 Multi-year behaviour of the ground heat exchanger

Between November 2007 and March 2012, the ground-source heat pump has operated in both heating and cooling modes. The house has been unoccupied until September 2009, then occupied by a family of three or, occasionally, four people. The lowest outdoor dry temperature (-35.1 °C) was recorded on January 16th, 2009 during the winter #2 (Tab. 4) (Environment Canada, http://ec.gc.ca).

Tab. 4: Outdoor weather conditions during five consecutive winters (Minea, 2013)

Winter (house status)	Dry temperature [°C]			Relative Humidity [%]		
	Min	Avg.	Max	Min	Avg.	Max
#1 2007-2008 (unoccupied)	-32.0	-5.8	14.2	26.6	76.3	100
#2 2008-2009 (unoccupied)	-35.1	-6.9	19.7	34.0	74.6	100
#3 2009-2010 (unoccupied first 8 months)	-28.0	-4.3	18.0	13.0	83.4	100
#1 2010-2011 (occupied)	-31.0	-6.0	15.0	20.0	83.6	100
#1 2011-2012 (occupied)	-26.0	-3.3	20.0	21.0	79.3	100

During the winter heating mode, the ground-source heat pump has intermittently run according to the house indoor thermostat setting, i.e. 16 °C during the night and 20 °C at daytime. Tab. 5 shows the average operating parameters of the ground-source heat pump during the occupied time.

Tab. 5: Average operating parameters of the ground-source heat pump

Winter	Brine entering heat pump		Saturated parameters			
	Temperature	Flow rate	Evaporating		Condensing	
	°C	kg/s	MPa (abs)	°C	MPa (abs)	°C
#3	5.0	0.536	0.770	-1.76	2.3	37.4
#4	4.6	0.536	0.756	-1.56	2.3	37.1
#5	5.4	0.536	0.770	-1.76	2.3	37.0

The house net energy consumptions during the last three winters, when it was partially or completely occupied as well as the heat pump energy consumption, have slightly decreased because of a more efficient indoor climate control by the owners.

Tab. 6: Electrical energy consumption during three consecutive winters (Minea, 2013)

Winter	House		Heat Pump	Heat Pump vs. House
	kWh	kWh/m²	kWh	%
#3	6,398	27.8	2,055	32.1
#4	5,963	25.9	1,856	31.1
#5	4,948	21.5	1,612	32.5

Ground thermal behaviour

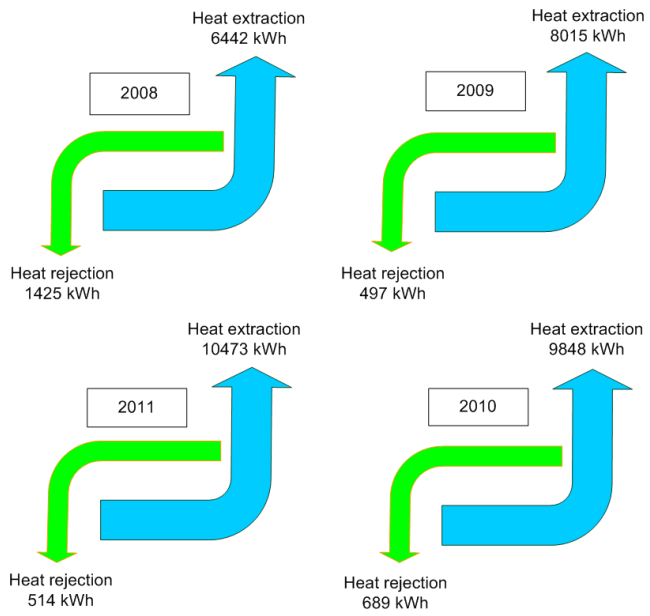

The geothermal system provided heating in the winter and cooling in the summer. The energy transferred to the ground in summer was stored and partially available to be extracted in the winter. During the years when the house has been unoccupied (2008), partially occupied (2009) or fully occupied (2010 and 2011), the heat pump has extracted from the ground 14 to 20 times more heat energy in the heating modes than it has rejected in the cooling modes (Minea, 2013).

At the beginning of the last heating cycle of each heating season, the brine entered the heat pump evaporator at temperatures of only 2 °C lower compared to the brine temperatures entering the heat pump at the beginning of each first heating cycle.

During the cooling dominated summer seasons, the ground has completely recovered its thermal capacity, since at the beginning of next heating season, the brine entered the heat pump at the same temperature, i.e. around 8.3 °C. Looking over the entire 5-year period, at the beginning of the first heating cycle (November 9, 2007), the brine entered the heat pump at 7.5 °C, and, approximately four years later (October 1, 2011), it entered the heat pump at a slightly higher temperature (about 8.8 °C).

On the other hand, at the end of the last heating cycle of the winter #1 (May 31, 2008), the brine entered the heat pump at 4.5 °C, while at the end of the last heating cycle of the winter #4 (April 26, 2011), i.e. approximately three years later, it entered the heat pump at 5 °C.

These experimental results prove that the ground has completely recovered its initial thermal capacity after three and four years of operation, respectively. During these periods, the ground has not been excessively cooled down and thus, no freezing phenomenon occurred. This performance validates the correct design of the vertical closed-loop heat exchanger that, among other factors, accounted for summer ground thermal storage and actual groundwater movement.

1.5.4 Outlook of House Multi-Year Energy Consumption

In the eastern Canada cold climate, the average annual consumption of conventional houses with electrical heating baseboards ranges around 26,700 kWh/a (NRCAN, 2010). As could be seen in Tab. 7 and Fig. 9, the annual net electrical energy consumption (i.e. the electrical energy supplied by the grid minus the electrical energy produced by the photovoltaic system) of the occupied low-energy house between 2010 and 2014 was in average 58% lower compared to the average consumption of conventional houses.

Tab. 7: House net annual electrical energy consumptions

Year	House status	Annual net electrical energy consumption (kWh/a)	Energy consumption reduction vs 26,700 kWh/a (%)
2010	Occupied	11,077	58.5
2011	Occupied	11,993	55.0
2012	Occupied	11,015	58.7
2013	Occupied	10,950	59.0
2014	Occupied	11,110	58.4

It can be also noted that the house net annual specific electrical energy consumption (vs. the total area) of the occupied house varied from 51.2 kWh/m² in 2011 to 47.5 kWh/m² in 2014, of which the ground-source heat pump (compressor, fan and brine circulating pump) as the main heating and cooling device, consumed about 20% each year. The house specific energy consumptions were between 29 and 31% lower compared to the target for heating and cooling of a low energy house located in the Canadian cold climate.

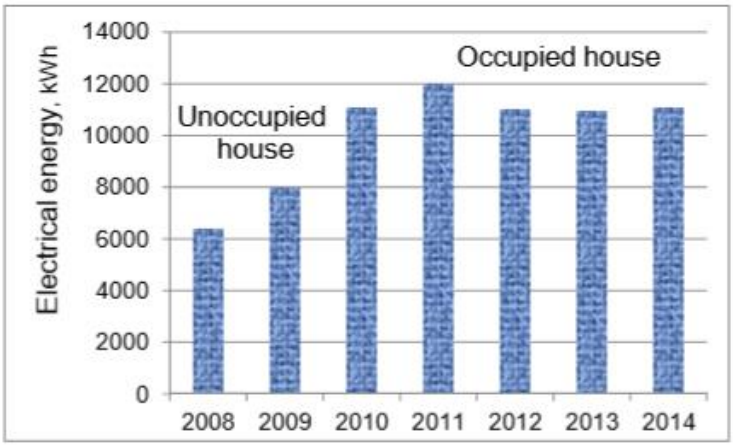

Fig. 9: House net annual electrical energy consumption

2 nZEB technology developments in Japan

In the frame of Task 3 technology evaluations were accomplished within the Japanese Annex 40 projects.

2.1 Experimental evaluation study of HVAC system

The energy requirements for air-conditioning correspond to approximately 40% of the total energy consumption of commercial buildings. To achieve a net Zero Energy Building (ZEB), the reduction of energy consumption for air-conditioning is essential. To reduce the consumption of energy for air-conditioning, the temperature and humidity individual control (THIC) system is a very effective means. The THIC system consists of a humidity controllable outer air processing unit (heat pump (HP) desiccant) and a sensible capacity enhanced variable refrigerant flow (VRF) which has been installed for a demonstration test.

2.1.1 Composition of the THIC System

The THIC system consisted of the humidity controllable outer-air processing unit (HP desiccant), and sensible capacity enhanced VRF. These two mechanisms are appropriately operated by the controller to simultaneously maintain the comfort of the room and save energy. The direct expansion VRF system consumes less energy for heat transfer compared to the central type air conditioner. Moreover, the VRF can avoid heat loss from the connection piping in cooling operation. So, the VRF system is more suitable for significantly reducing energy consumption.

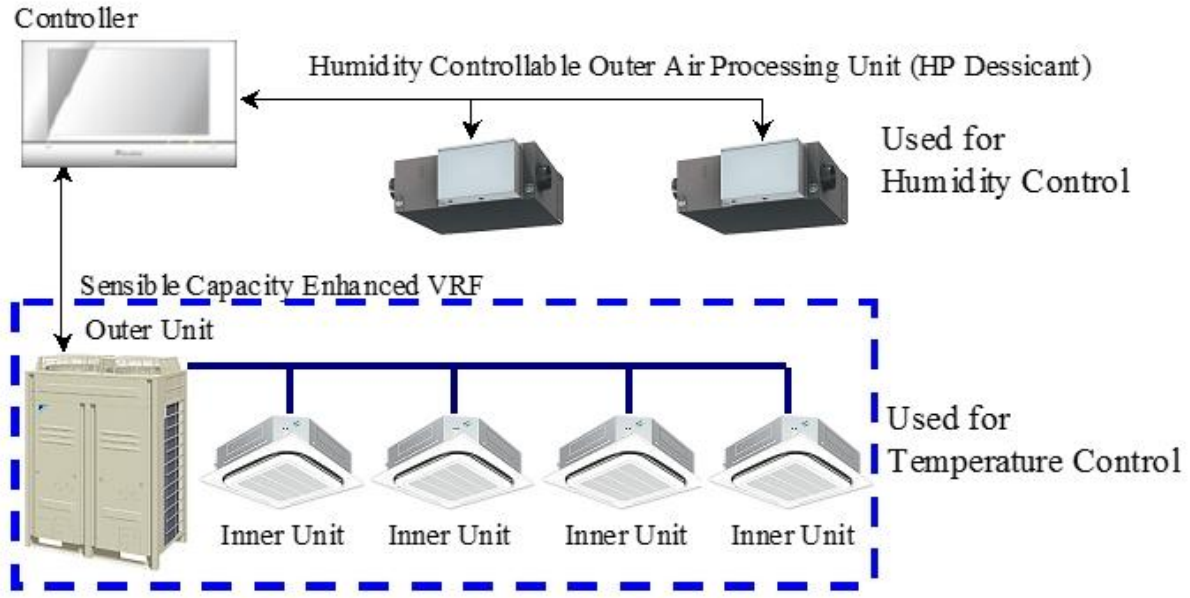

Fig. 10: Composition of the Temperature and Humidity Individual Control (THIC) system

2.1.2 Features of HP Desiccant

To achieve a drastic reduction of energy consumption, an efficient humidity control mechanism is needed. In the THIC system, the humidity controllable outer-air processing unit (HP desiccant) is adopted.

The most important feature of HP desiccant is using the Hybrid Desica Element (HDE), which is a heat exchanger, covered with desiccant material as shown in Figure 2.2. By using HDE, the heat needed for desorption can be supplied directly on to the desiccant materials, and so the required temperature for desorption becomes as low as 40 °C to 50 °C.

By lowering the required temperature for desorption, a heat pump can be used for the desorption process. A heat pump can transfer the heat from the adsorption process to the desorption process, and that drastically improves the efficiency of HP desiccant.

In HP desiccant, two HDEs are operated in batch processing (alternately adsorbing and desorbing the desiccant material).
The HP desiccant with especially high efficiency is used for the THIC system. The optimization of the heat exchanger path arrangement equalizes temperature of the HDE's surface, and improves efficiency.

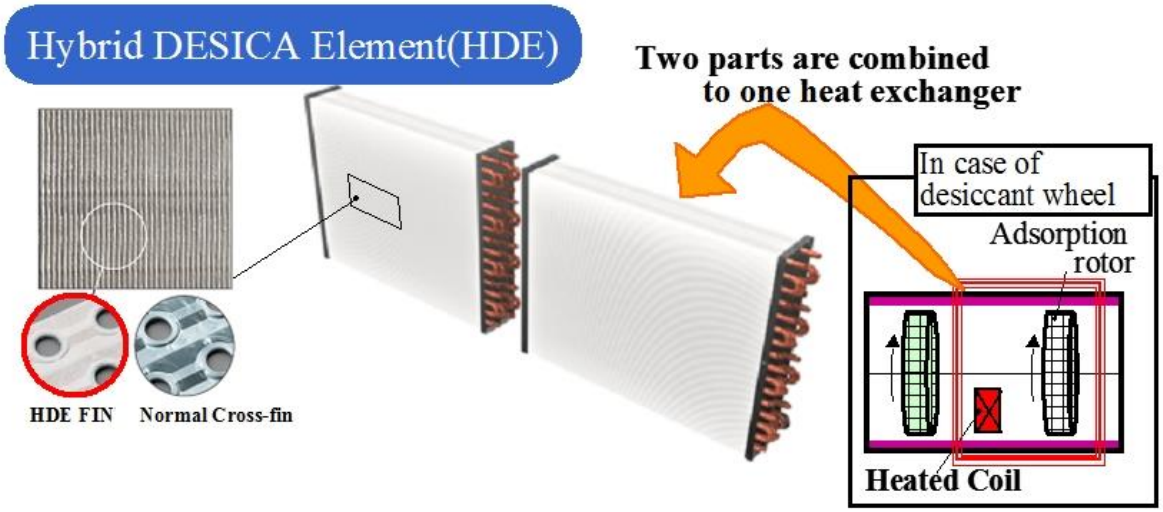

Fig. 11: Hybrid DESICA element

Features of the sensible capacity enhanced VRF

To raise the efficiency of the heat pump, one of the most suitable ways is to reduce the pressure difference between the condensing temperature and the evaporative temperature. In the case of the cooling operation, when the air-conditioning load is low, the evaporative temperature can be raised. In the case that the ambient air temperature is low, the condensing temperature can be lowered.
However, the improvement of efficiency by the reduction of the pressure difference has not been common in the conventional VRF.
One of the reasons that prohibit the reduction of pressure difference is the necessity of the dehumidifying capacity. In the case that the cooling load is small, VRF can be operated with the higher evaporative temperature to fulfill the sensible heat load. But, that makes the latent heat capacity of VRF low at the same time as shown in Fig. 12, and that may make the room air too damp.

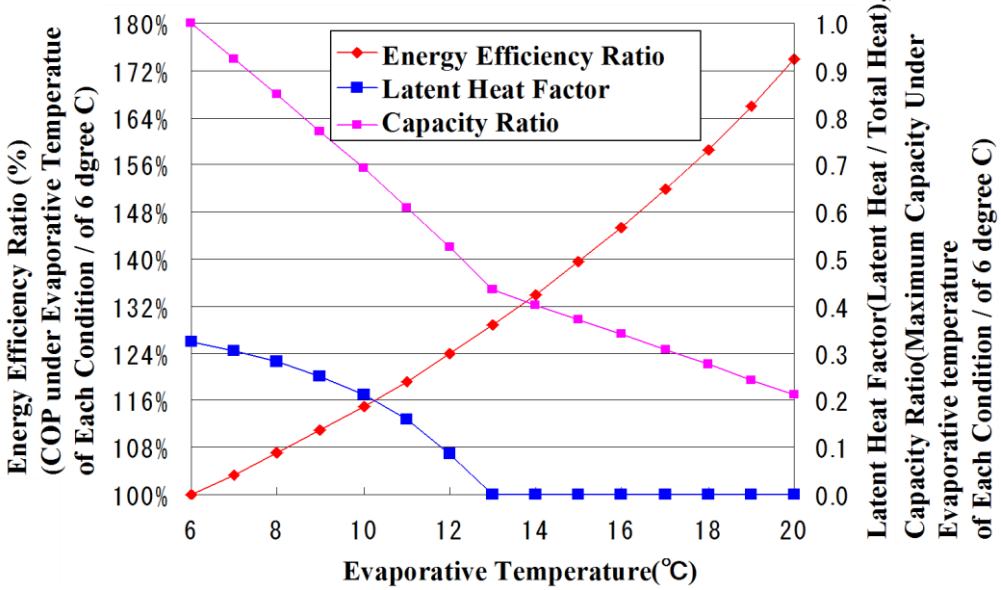

Fig. 12: Evaporative Temperature's Effect to the VRF system

In the THIC system, the latent heat load is treated by HP desiccant. So, the VRF can be operated at higher evaporative temperatures according to the sensible heat load.
The other reason is the limitation of the compressors' operation. A new scroll compressor was developed which is far more tolerant for the operation with the small pressure difference operation, which makes it possible to drastically reduce the pressure difference.
In this way, the sensible capacity enhanced VRF for the THIC system can be operated in smaller pressure difference, and that improves the efficiency under the condition of lower ambient temperature and smaller sensible heat load drastically as shown in Fig. 13.

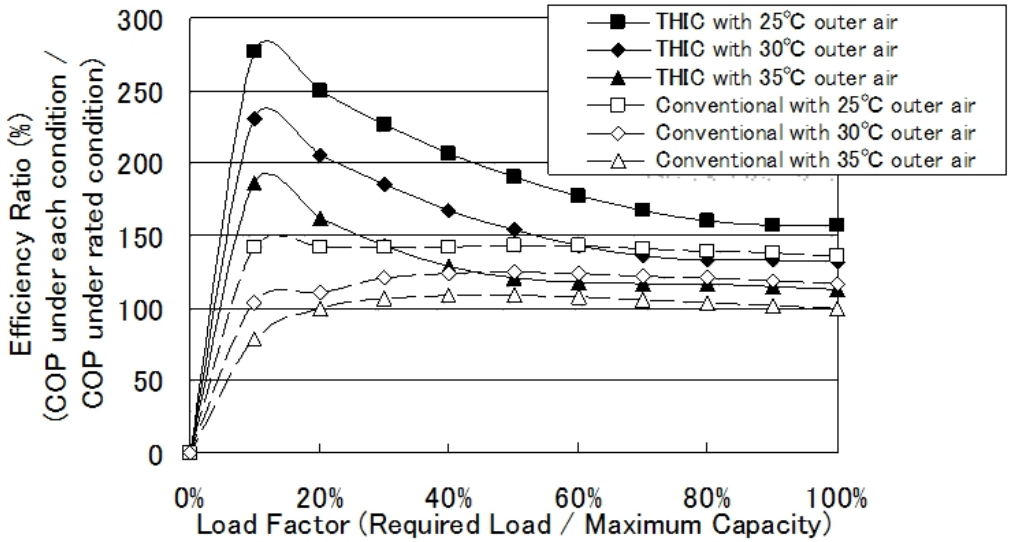

Fig. 13: Comparison of VRF Efficiency

2.1.3 Result of Demonstration Test

The test site was an office in Nagoya University. One room separated into two was used for the comparison of the conventional system and the THIC system as shown in Fig. 14.

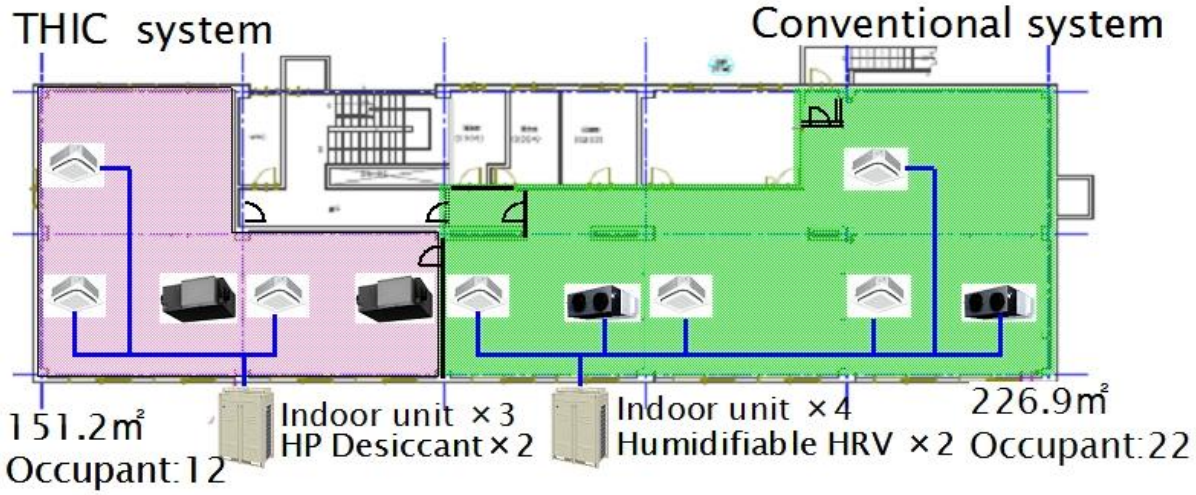

Fig. 14: Outline of Field Test Site

For the eastern area of the office, a combined system of conventional VRF and humidifiable ventilation heat recovery (HRV) was installed as a conventional system. For the western area, a combined system of HP desiccant and sensible capacity enhanced VRF was installed as a THIC system. It was not possible to make the size of both areas even. So, the evaluation hereafter is according to the value divided by the area size.

2.1.4 Result of the Summer Test

The summer test was carried out from June to September. To evaluate the comfort level and energy saving, the temperature & humidity of the room and the energy consumption were measured.

Inner Room Condition

Fig. 15 shows the comparison of the inner room conditions of conventional and THIC systems, respectively.
When the set temperature is 28 °C, the conventional system cannot provide adequate dehumidification capacity. On the contrary, the THIC system can control the inner room condition around the edge of the target condition.

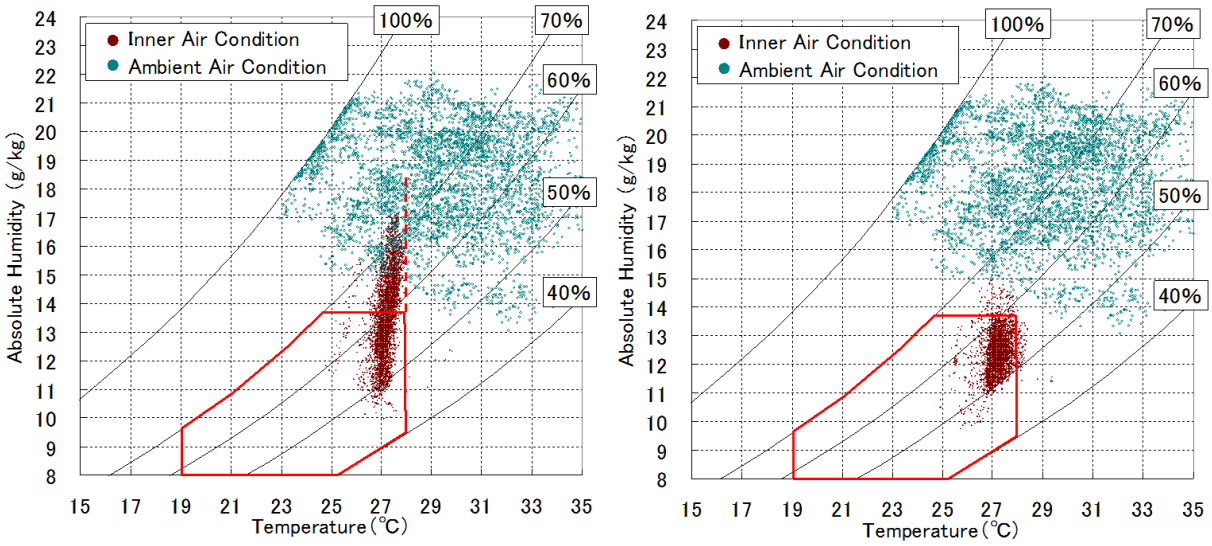

Fig. 15: Inner Air Condition (Set temperature is 28 °C)

In Japan, it was common to set the target temperature to 26 °C. But, after the March 11, 2011 disaster, it became common to set it to 28 °C to correspond with the lack of electricity. However, this result shows that the conventional air conditioning system, without humidity control function, cannot maintain a comfortable air condition in humid summers like in Japan, if the set temperature is 28 °C.

Energy Consumption

Fig. 16 shows the comparison of the integrated energy consumption of the test period.

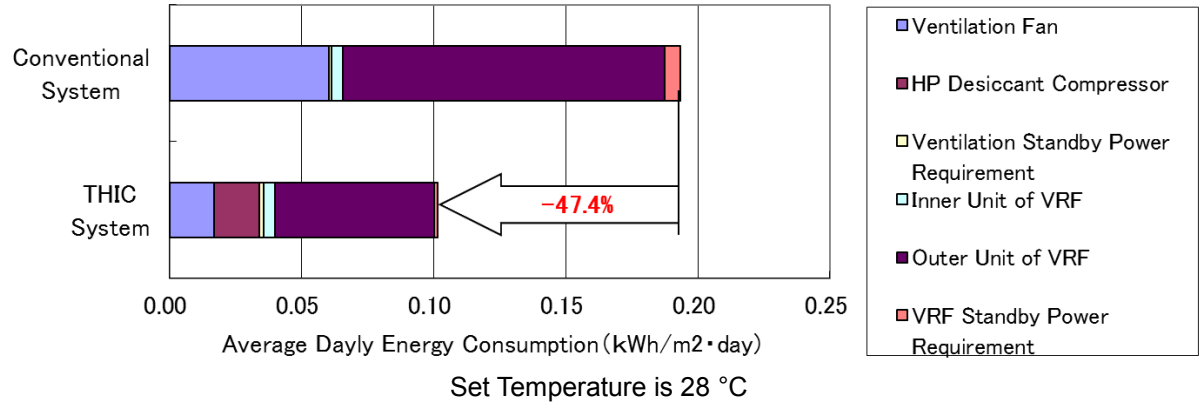

Fig. 16: Daily Energy Consumption

The energy conservation effect of the THIC system in summer goes up to almost 50%.

2.1.5 Result of the Winter Test

The winter test is carried out from December to February, also by measuring the temperature and the humidity of the room and energy consumption.

Inner Room Condition

Fig. 17 shows the comparison of the inner room conditions of the conventional and THIC systems, respectively.
Different from the results of the summer test, under the effect of humidifiable HRV, both the conventional and THIC system can control the inner air to the target condition.

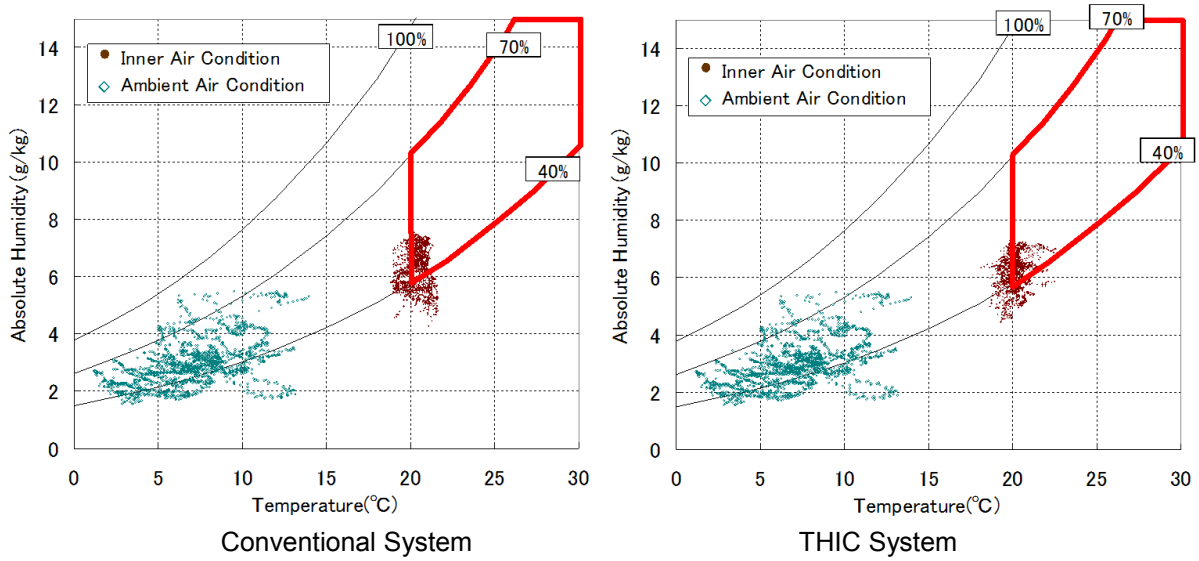

Fig. 17: Inner air condition (Set temperature is 20 °C)

Energy Consumption

Fig. 18 shows the comparison of the integrated energy consumption of the test period.

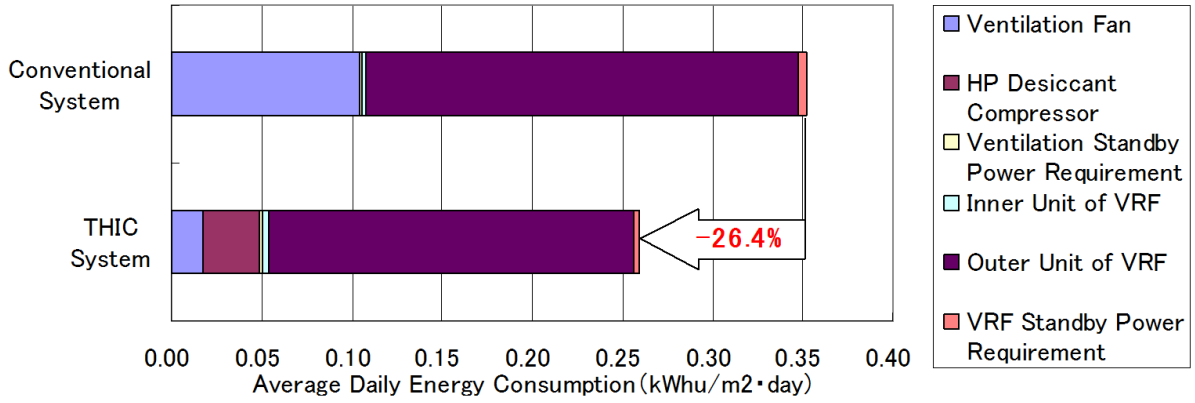

Fig. 18: Average Daily Energy Consumption

The energy conservation effect of the THIC system in summer goes up to almost 30%.

2.2 Annual evaluation using simulation

As the sensible capacity enhanced VRF is characterized by its high efficiency at low load factors and low ambient temperature conditions like spring and autumn, the difference between the conventional system and the THIC system is assumed to be higher in annual operation. The efficiency of the THIC system in an annual operation was evaluated by simulation. The simulation model was established using the data of the demonstration test. The evaluation was conducted on the assumption that the system is installed in a highly insulated building.
The annual effect for energy conservation of the THIC system is calculated by this simulation. The calculation condition is shown in Tab. 8.

Tab. 8: Condition of simulation comparison

System	Building	In Room Heat Generation	HVAC System	Set Indoor Air Condition	
				Cooling	Heating
Conventional	Highly Insulated	10 W/m²	Conventional VRF + Humidifiable HRV	26 °C, 50%	22 °C, 40%
THIC			Sensible Capacity Enhanced VRF + HPDesiccant	28 °C, 60%	20 °C, 40%

As a result, about 74% of the energy consumption can be reduced.

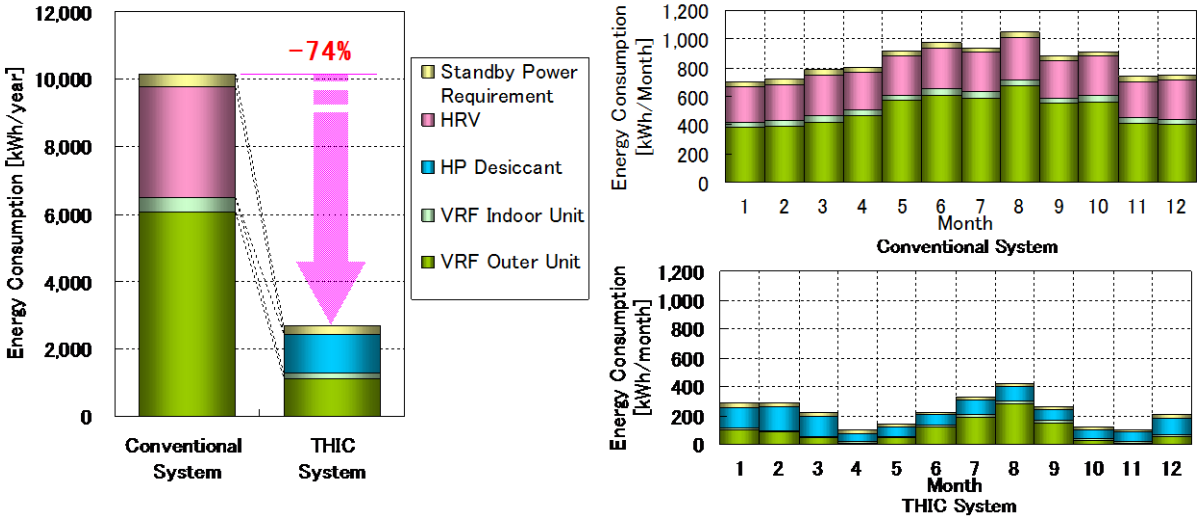

Fig. 19: Evaluation of the total energy savings by simulation

Fig. 19 shows that the energy consumption of the spring and autumn is drastically reduced.

2.2.1 Conclusion

The THIC system consists of a humidity controllable outer-air processing unit (heat pump desiccant) and a sensible capacity enhanced VRF. Demonstration test results showed that the THIC system can reduce energy consumption by approximately 50% in midsummer, and 30% in midwinter. The data also made it possible to develop a simulation to calculate the THIC system's energy consumption. The simulation showed that the THIC system can reduce the energy consumption by 74% in the case that the system is installed in highly insulated buildings and operated throughout the year.
The developed THIC system can maintain a comfortable inner air condition and drastically reduce the energy consumption at the same time.
This excellent result is derived from the 3 points shown below:

- The reduction of air-conditioning loads by individual control of temperature and humidity
- The development of the HP desiccant for efficient humidity control
- The development of the sensible capacity enhanced VRF for efficient temperature control, especially in spring or autumn.

By the installation of this THIC system, the ZEB will be realized comparatively easy in the case of two or three storey buildings. Moreover, it will also achieve a great amount of energy savings in high-rise buildings as well.

2.3 Heat Recovery Heat Pump for Multi-Purpose Use

The multi-function heat-recovery heat pump allows space cooling, space heating, hot water supply and chilled water storage. In summer, this heat pump can realize electricity peak shift utilising chilled water, which is produced and stored in night-time. Furthermore, it produces hot water utilising waste heat from the space cooling operation for space heating or DHW purpose.

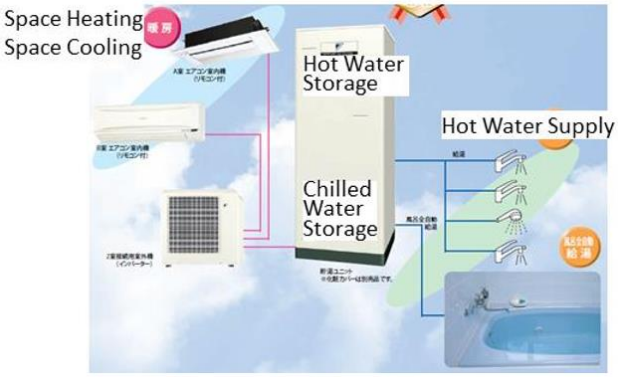

Fig. 20: Layout of the heat recovery heat pump for multi-purpose use

Cold storage operation

In summer season, chilled water storage operation at night-time allows to save chilled water with a temperature of 5 °C with night time cheap electricity price.

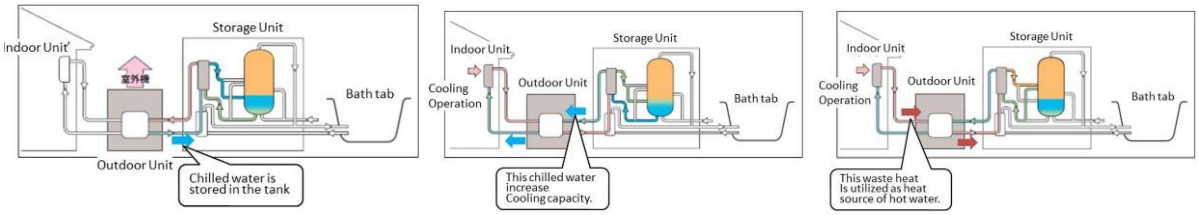

Fig. 21: Operation modes for cooling – night-time storage of cold (left) and daytime use of stored cooling energy (middle) - and heat recovery for DHW operation (right)

Eco cool operation

The at night-time stored chilled water increase cooling capacity without additional electricity. As a result, the stored chilled water allows decreasing electricity consumption at daytime cooling operation by 40%. The blue line in Fig. 22 (left) of daily electricity profile indicates electricity consumption through the day at eco cooling operation where the decrease of electricity consumption decrease compared to general operation can be seen.

Heat recovery operation

In summer, the waste heat of cooling operation is utilised as heat source for producing hot water with a temperature of 50 °C. Since waste heat is effectively used, no electricity is dedicated to use for producing hot water.

Fig. 22: Peak shaving by cold storage and typical installation in Japan

2.4 Development of Performance Evaluation Technology

Performance of solar thermal system has been tested under the outdoor weather condition both for a collector itself and for the total system. In order to perform the test under stable conditions, an environmental chamber was built. The purpose of this study is to develop and verify the procedure and the technical method for testing the performance of solar thermal systems at indoor environmental chamber.

2.4.1 Outline of Indoor Test System

For the indoor environmental chamber, an artificial solar simulator has been built. The solar simulator consists of 24 lamps with a maximum intensity of 1000 W/m² at collector surface with a distance of 5 m from the lamps.
The lamps can be controlled continuously for three different ranges of intensity:

- 500-1000 W/m²
- 300-499 W/m²
- 200-299 W/m²

For the environmental chamber, also a brine-chiller, air-handling unit and a humidifier were installed. The temperature of the chamber is controlled at 20-30 °C with 50-80%rH in summer and 10-25 °C with 30-80%rH in winter.

2.4.2 Field Test Setup

The heat collection performance of the solar collectors has been measured under the actual solar irradiation condition at Soka-city, Saitama-prefecture. Field measurement data is compared to the results of indoor test to verify the validation of indoor test.

2.4.3 Indoor Testing

Collector Performance Test

This test is conducted for evaluating the performance of the collector itself based on JIS A4112. The inlet temperature of the heating medium to the solar collector is controlled by a temperature control unit, which includes a buffer tank and a pump. The inlet temperature can be controlled from -10 to 80 °C. A fan unit is located at the side of solar collector and wind velocity on the surface of the collector is controlled in the range of 2-4 m/s.

Collector System Test

This test is conducted to evaluate the performance of the solar collector system which consists of two or more collectors and a thermal storage tank. The solar simulator installed for the indoor test has a capacity to cover only one collector. Therefore, in this test the second or more collectors are simulated by an electric heater, of which the output is determined by substituting the medium inlet temperature and flow rate of the second collector and the solar irradiation intensity on the surface of the first collector to collector performance curve tested by collector performance test.

Standard DHW load test

This test is conducted to evaluate the performance of DHW systems under the standard solar irradiation and domestic hot water (DHW) load condition. The output of the artificial solar simulator is automatically controlled according to the programmed solar irradiation profile, which simulates the solar irradiation profile on clear sky day. In this test the modified M1 mode is used as standard DHW load profile. The modified M1 mode is a detailed DHW load profile during one day based on the field measurements at a real residence. This mode assumed a family of four and total hot water consumption is 450 liter per day.

2.4.4 Results of Indoor Test

Collector Performance Test

The collector was set to an angle of 15°. The ambient temperature was fixed at 20 °C. The mean flow rate is 2.4 kg/min, because the standard flow rate of solar collector is 1-1.2 kg/min/m². Some collectors use an ethylene-glycol solution as heat collection medium. However, in this test water is used as heat transfer medium to shorten time to set-up tests of several types of collectors. Tab. 9 shows the specification of the different collectors.

Tab. 9: Specification of collectors

Manufacture		A	B	C	D
Type		Flat plate	Vacuum tube	Flat plate	Flat plate
Collector gross area		2.09 m²	2.28 m²	2.09 m²	2 m²
Coefficient	b0	0.711	0.561	0.6975	0.776
	b1	4.609	0.837	4.795	5.440

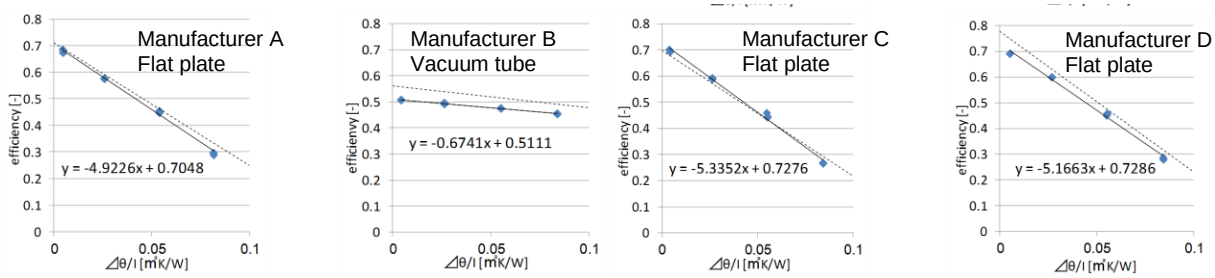

Fig. 23: Results of collector performance test

Fig. 23 shows the results of the indoor performance tests of the collector itself. Type A, C and D are flat plate collectors, while type B is a vacuum tube collector. Solid lines show the results of indoor test and dotted lines is performance which were submitted by manufactures. Results of performance test of these collectors shows good agreement with performance of manufacturer test. However, for the vacuum collector (Type B), there is disagreement between the two tests.

Collector System Test

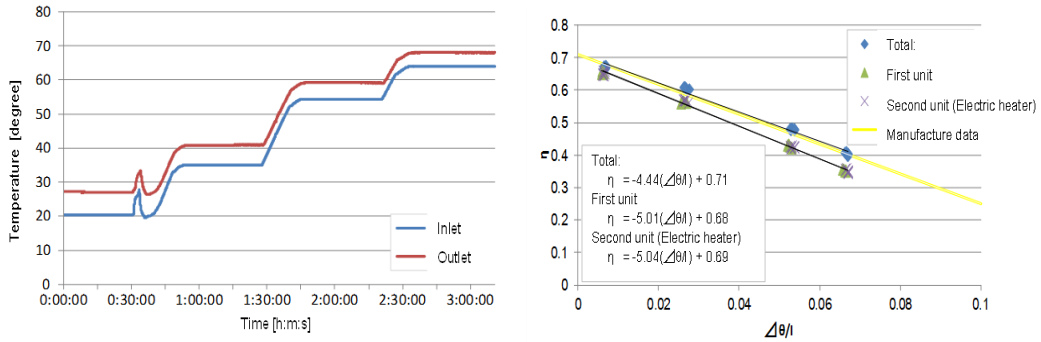

Fig. 24: Inlet and outlet temperature of collector system test (left), collector efficiency of first and second unit of collector system test (right)

Fig. 24 (left) shows the medium inlet temperature to the first unit of the collector and outlet temperature of electric heater which simulates second unit of the collectors. The control of the heater was carried out well according to change of the inlet temperature. Fig. 24 (right) shows collector efficiency of first and second unit (simulated by heater). From Fig. 24, it can be seen that the collector efficiency of first and second unit show good agreement. However, the efficiency of first unit is slightly lower than that of collector performance test.

2.4.5 Conclusion

The tests have been carried out in an environmental chamber. In this chamber an artificial solar simulator and an HVAC system to control the temperature and humidity of the chamber is installed. In this chamber three kinds of test have been conducted: a collector performance test, a collector system test and a standard DHW load test.

More tests of the collector systems will be conducted to establish the collector performance test and collector system test with reasonable accuracy. Especially, there is some difference between the indoor test and manufacturer data for vacuum tube collector. From these results, there are many suggestions about the items that should be investigated, for example the definition of the effective surface area of vacuum tube collector, spectrum distribution of artificial solar simulator, and so on. In addition, standard DHW load tests will be conducted.

The aim of the study is the establishment of solar thermal system test with reasonable accuracy and reproducibility. It results in wider spread of solar thermal systems and it will play an as important role as photovoltaic systems.

3 Multifunctional heat pump system in Switzerland

3.1 Background of the project

Thermal insulations of new buildings in Switzerland are defined by U-values of about 0.2 W/(m²K) adapted to the rather cold climate conditions. However, the internal loads are getting higher due to the increasing use of electric equipment. Thus, in summer operation an increasing risk of an overheating of the buildings exists, especially in office buildings. Therefore, several free-cooling applications have established to keep the energy use for cooling on a low level. By direct usage of the ambient air or the ground for heat dissipation, free cooling creates a possibility to cover the cooling needs by just using energy for the circulation pumps. However, each free-cooling method also has its particular limitations. Cooling based on a night-time radiation and convection of an activated building envelope surface has not been used often as passive cooling option, yet, although there are potentials in moderate climate conditions with moderate night-time outdoor temperatures. The operation gets even more beneficial with the option to use the same surface also for heating purposes like space heating in winter or DHW production in summer. Nevertheless, the properties of the surface may be different for the space heating and space cooling operation, since in space heating mode, losses to the ambiance shall be reduced as far as possible, while high losses to the ambiance are favourable in the space cooling mode.
Therefore, the objective of the project AKTIVA is the investigation of the properties of an outer surface for space heating and cooling mode, which could be represented as solar absorbers or collectors, as well as the integration into a system.

3.2 Lab-test results of unglazed absorber

Lab testing has been performed at the Energy Research Lab (ERL) of the Institute of Energy in Building of the University of Applied Sciences Northwestern Switzerland in Muttenz. Fig. 25 shows the installed absorbers on the roof of the lab.
Three unglazed solar absorbers with different degree of selective coating with long-wave emission coefficients of the infrared radiation of ε_{IR}=0.15 (selective coating), ε_{IR} =0.3 (faint selective) and ε_{IR} = 0.9 (non-selective) have been installed on the roof of the ERL. Tests have been performed at different weather conditions and with different inclination angles.

Fig. 25: Installed absorbers on the roof of the Energy Research Lab

Fig. 26 shows the test results on Sept. 23-24, 2013 at constant absorber inlet temperature of 25 °C, which had good solar irradiation conditions during the day followed by a clear sky in the beginning of the night. As expected the selective absorber reaches the highest capacity for space heating operation during daytime of about 600 W/m^2_{abs} at maximum due to reduced radiation losses by the selective coating. The non-selective absorber only reaches about 500 W/m^2_{abs}, thus for the space heating operation, the selective absorber has advantages of higher heating capacity values.

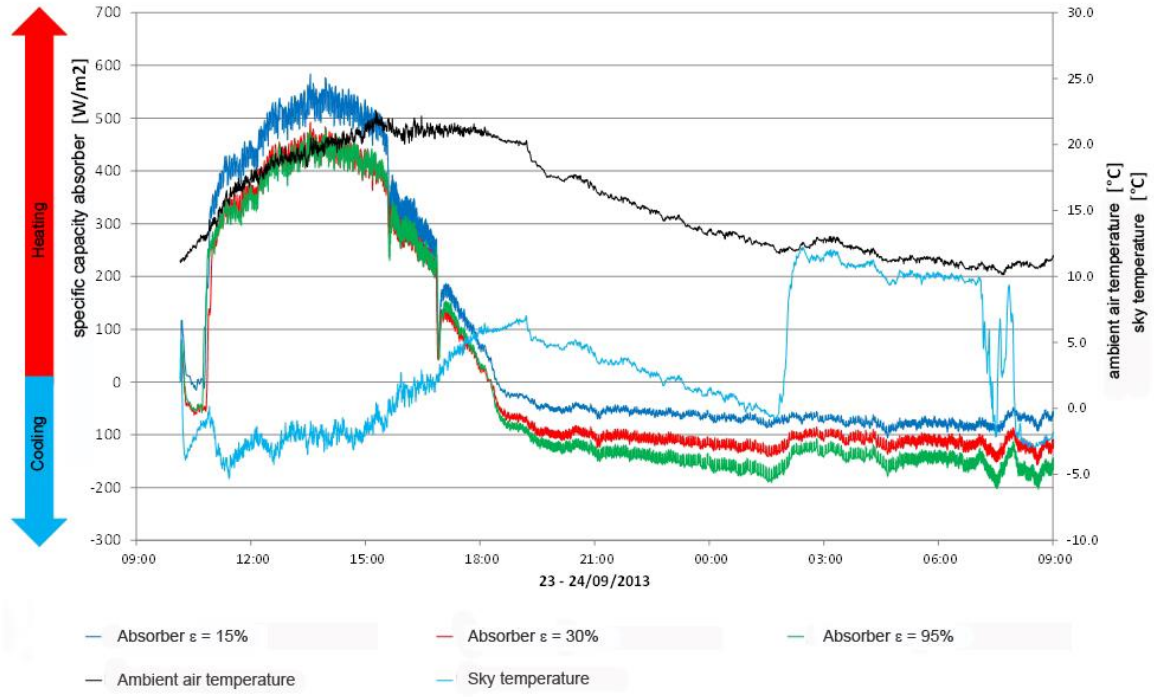

Fig. 26: Measurement results at good solar irradiation at daytime and clear sky at night-time of the three absorbers with different degree of selective coating

In clear nights, though, the (fictive) sky temperature, which has been recalculated by longwave radiation measurements with a pyrgeometer, is significantly lower than the ambient air temperature, in the first night-time hours by about 15 K. Therefore, even if the absorber temperature is in the range of the ambient temperature, the absorber can reject heat by radiation to the night sky depending on the emissivity of the surface.
In the space cooling operation, the favourable property of the absorber is hence a high emission coefficient of the non-selective characteristic, which is opposite to the space heating mode. The good radiative characteristics to the night sky of the non-selective absorber results in a cooling capacity of -200 W/m^2_{abs}, while the capacity of selective absorber is below this value at a cooling capacity of -100 W/m^2_{abs}.
However, at about 2 a.m., clouds come up, which is illustrated in Fig. 26 by the instantaneous rise of the sky temperature to almost the level of the ambient air temperature. Consequently, the cooling capacity of the three absorber are approaching each other and the selectivity is of minor importance, since the radiation exchange with the sky is now limited by the reflexion of the clouds, expressed by a higher sky temperature. The decrease of the cooling capacity of the three collectors is most prevalent for the non-selective collector, while the more selective collectors are hardly affected by the rising sky temperature.

3.3 Component modelling and system integration

Based on the modelling of the dynamic collector test according to EN 12975 (2011) a model of the solar absorber has been implemented in Matlab-Simulink and has been validated using the measurements of the test rig. The model considers the influence of direct and diffuse irradiation as well as convection and radiation due to the ambient and sky temperature.

3.3.1 Validation of the simulation model

In order to compare the measured values with the simulated values, several measurement series were used. The measured values were read into the simulation to simulate the collector model with the same inlet and boundary conditions as in the measurement. For the validation the outlet temperatures of the absorber were compared to the test rig measurements. Absorber parameters were taken of standard test results which were existent for the solar absorber.

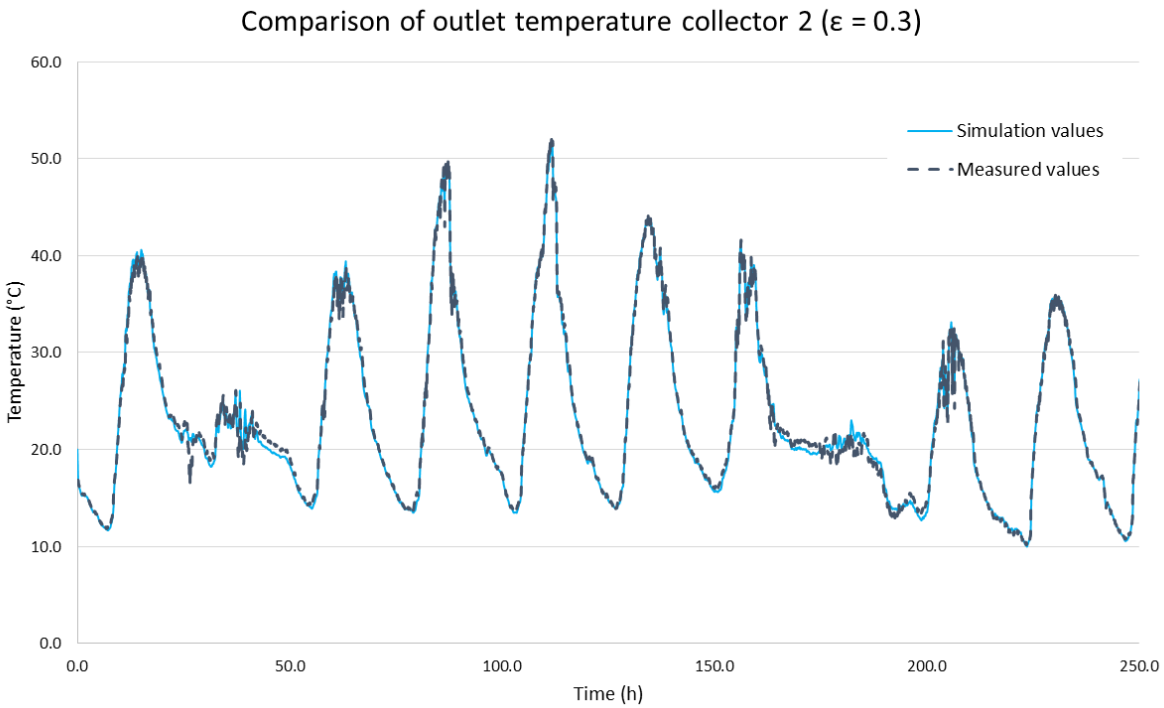

Fig. 27: Comparison of measured outlet temperature of absorber 2 (ε =0.3) to simulated values

As seen in Fig. 27 the outlet temperature of the absorber simulation corresponds well to the measured data. Furthermore, the dynamics of the simulated absorber fits well to the real operation. The simulation of the other absorbers (ε = 0.15 and ε = 0.9, not included as figures) shows a good agreement of the simulation with the measured values, too. Summarising the absorber model is valid to be used for the system simulations.

3.3.2 System integration

After validation, the absorber model was integrated into a system model to determine key figures of the system. Fig. 28 shows the principle of the system integration of the absorber model into a system in order to demonstrate the different operation modes. The system is built-up of a heat pump, a storage tank as well as building zones that are assumed to be equipped with thermally-activated building systems (TABS) which are used as emission system for the space heating and cooling mode.
Therefore, all the chosen components of the system integration can be used for multifunctional operation both in space heating and space cooling. With the integration it is possible to realize following operation modes:

- Space heating operation in wintertime with the absorber as heat source
- Direct space heating operation with the absorber at favourable solar irradiation
- Simultaneous operation of the heat pump for heating and cooling
- Cooling operation in summer with heat pump for additional cooling
- Free-cooling operation in summer by night-time heat rejection with the absorber

By the TABS the flow temperature can be limited to a maximum of 29 °C during heating mode. With sufficient solar radiation and therefore high temperatures at the absorber outlet, the solar heat can be directly circulated through the thermally activated building systems by a heat exchanger. The storage serves as source storage and is used as heat source of the heat pump during winter operation.
During summer operation, the absorber area can be directly linked to the thermally-activated building systems. In this operation the building structure can be recooled by the TABS during night-time in order to have enough capacity of the concrete to remove the space cooling load of the office zones of the next day.

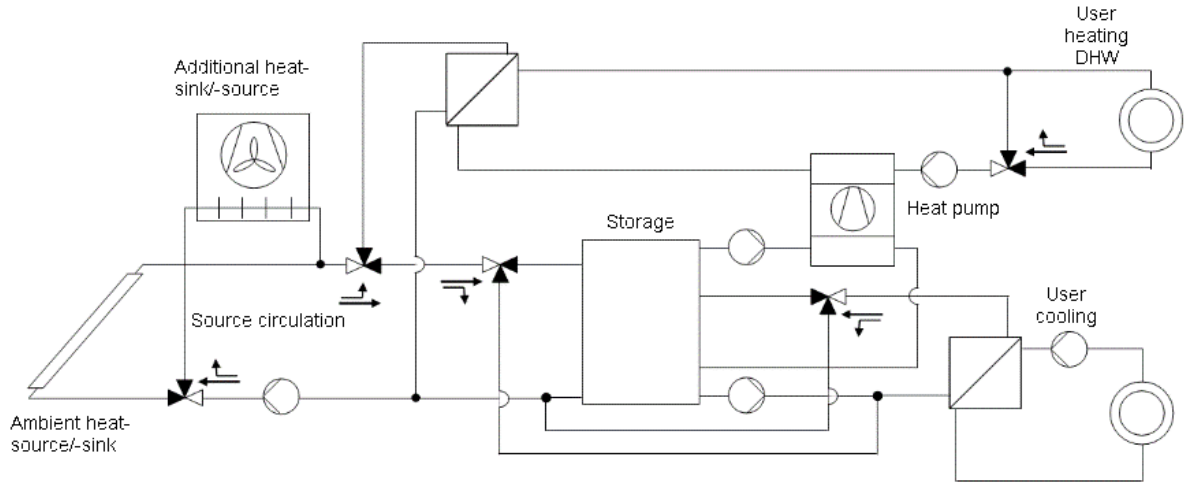

Fig. 28: Principle of system integration of multifunctional components

As alternative, it is also possible to additionally integrate the source storage as storage for the cooling energy in summer operation. By the additional storage it is possible to enhance the free-cooling fractions at favourable night-time conditions when the recooling of the TABS are already terminated before the end of the night.
In adverse night-time weather conditions and thereby limited ambient potential for the recooling of the TABS during summer operation, the heat pump can be operated as back-up chiller to provide additional cooling energy.

3.4 Simulation results

Both the space heating and the space cooling operation were investigated by system simulations. Simulations have been performed for two room zones in north and south orientation with single office use according to the Swiss standard SIA 2024 (2006) for the weather data of Zurich Meteoschweiz average year according to the Swiss standard SIA 2028 (2010). As extreme weather for the space cooling mode a warm summer of Lugano warm year in southern Switzerland according to SIA 2028, which already has Mediterranean climate has been used. The room zones are equipped with TABS in the middle of the 30 cm concrete ceiling and a pipe distance of 0.2 m.
The design of the absorber is 0.33 m^2_{abs}/m^2_{ERA}, where the index “abs” denotes the absorber aperture area and the index ERA denotes the energy reference area. This corresponds to a three-storey office building with entirely covered roof area by the absorber. The tested absorber types can be directly used as roof material. The storage design corresponds to 5 l/m^2_{ERA}.
Simulations have been performed for different surface properties of the absorber. For the evaluation of the different properties simulations for extreme combinations of the emission coefficient of 0.1 (selective) and 0.9 (non-selective) and the inclination angles of 5° (flat roof) and 90° (façade integration) have been accomplished.

3.4.1 Heating operation

Fig. 29 shows the system integration in space heating operation by the heat pump with the absorber as only heat source. The heating operation in winter was evaluated from October to March.
At higher solar irradiation, also a direct solar heating is considered. Direct solar heating is activated, if the storage temperatures are higher than the necessary flow temperatures for the thermally activated building systems. Fig. 30 shows the overall seasonal performance factor with and without direct solar heating. Without direct solar heating seasonal performance factors are in the range between 3.94 at adverse properties of the absorber for the heating mode, and 4.35 for favourable properties (high inclination, selective coating).

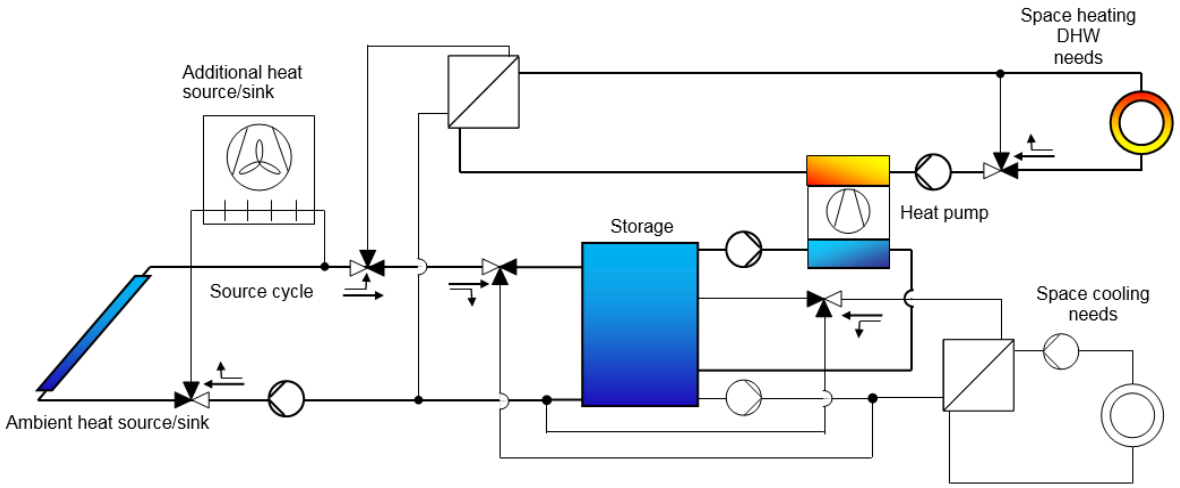

Fig. 29: Principle of system integration in space heating mode with the heat pump and absorber heat source

These values are in the range of ground-coupled heat pumps. Recalculated to the heat source fraction, a degree of coverage of the solar energy is in the range of 75-80%.
With the direct solar heating option, the SPF increases up to about 5 at favourable absorber properties for the space heating model, which makes up a difference of 0.7 to the SPF without direct solar heating.
Since the direct solar heating option has a higher dependence on temperature levels than the required supply temperature for the TABS, it is clear that good properties of the absorber are needed to reach these required higher temperatures. Thus, the difference decreases with adverse properties of the absorber to 0.25. Thus, it depends on absorber properties, if the extra hydronic expense for a direct solar heating option seems justified.

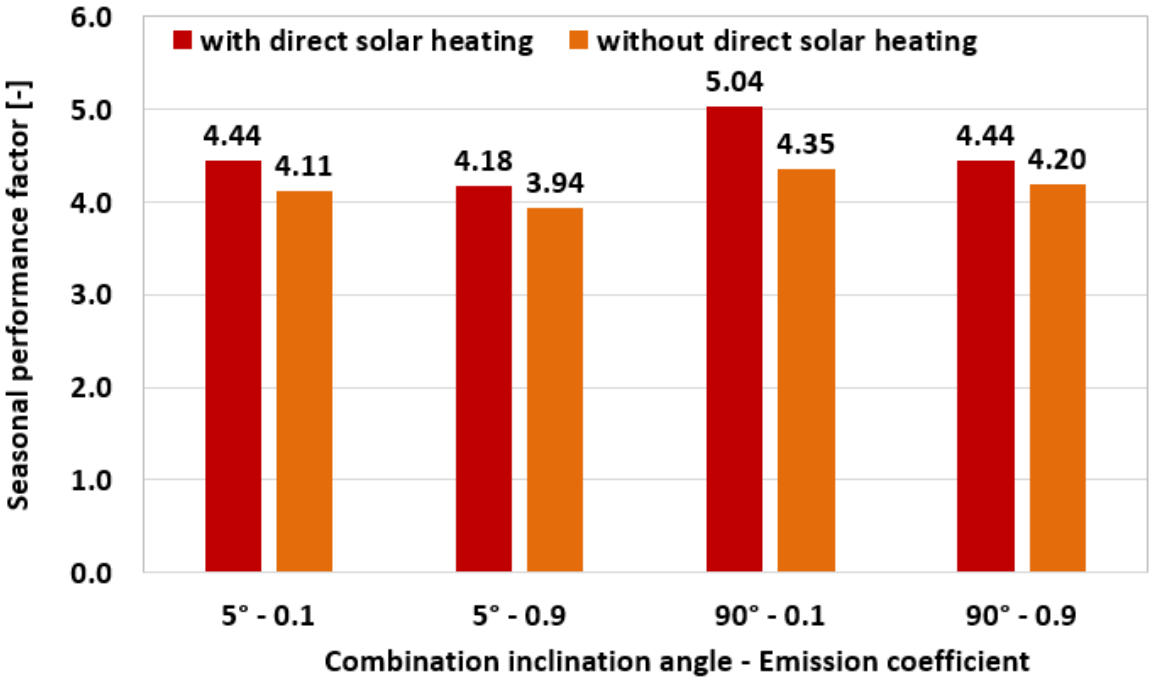

Fig. 30: Overall seasonal performance factor with and without direct solar heating

3.4.2 Discussion of simulation results for space heating operation

From the performed simulations the following statements can be made for the space heating operation:

- Absorbers designed for cooling operation can serve as only heat source for locations in the Swiss middleland during normal winters with ambient temperatures down to -10 °C.
- The seasonal performance factors of the heat pump without solar direct heating reaches values around SPF_h = 4 depending on the absorber properties. With good absorber properties higher values as an SPF_h = 4 are possible.
- Due to the use of the absorber near the ambient temperature, the heat losses to the ambiance are lower than at higher temperatures of the absorber, so the incidence angle has a similar influence as the selectivity if the absorber is used as heat source.
- A further increase of the seasonal performance factor is possible with higher shares of direct solar heating.
- Since direct solar heating depends on the temperature level, a selective absorber has advantages and reaches higher direct solar fractions.
- The specific absorber yields increase at increasing heating load, since with a rising heating load the absorber tends to work on lower temperature levels, which reduces the heat losses to the ambiance. However, direct solar fractions decrease, since temperature high enough for the direct solar operation are less often reached.

3.4.3 Cooling operation

Fig. 31 show the integration for the free-cooling mode with integrated cold storage. As for the direct solar space heating operation, the integration of the source storage of 5 l/m²$_{ERA}$ as cold storage has been evaluated separately.

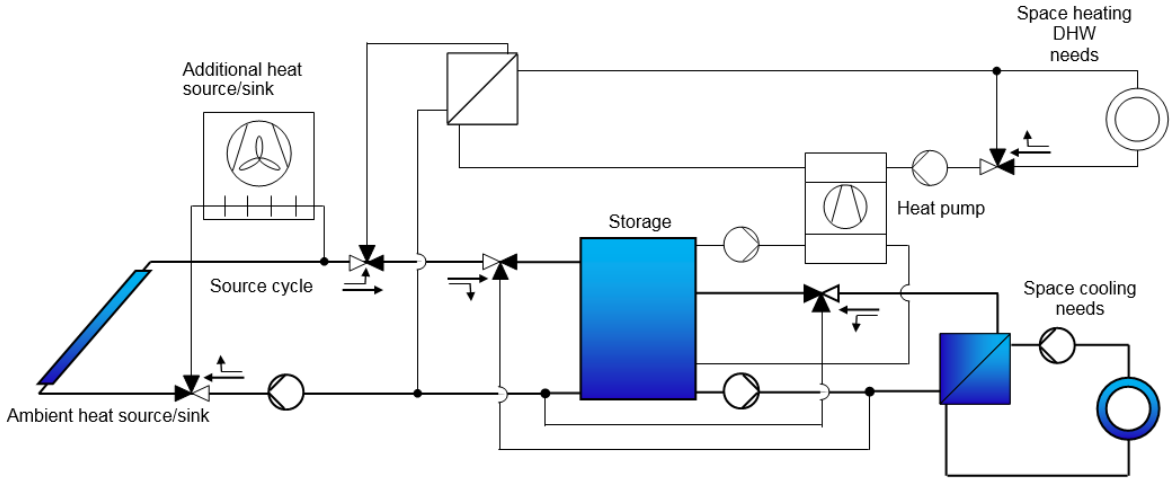

Fig. 31: Principle of system integration in space cooling mode for free-cooling operation with the absorber and integrated source storage as cold storage

The storage can be charged, if cooling loads of the room zone are lower than the free-cooling potential by night-time cooling. The degree of coverage in free cooling operation for the different absorber properties is depicted in Fig. 32 with and without storage integration. In moderate summer climate of Zurich Meteoschweiz, high degree of coverage of above 90% for good absorber properties, i.e. high emission coefficient of the non-selective absorber and low inclination for better view factor to the sky.

For rather adverse properties, still above 80% of the cooling needs can be covered by free-cooling. For these properties, the inclination angle is no longer of importance, since the radiative fraction is low due to the low emission coefficient of 0.1. In general, the properties are of minor importance in moderate climate, since the convective fraction of the heat rejection is still high due to relatively low ambient nighttime temperatures. In Zurich Meteoschweiz, for instance, 85% of the night-time hours are below 15 °C.

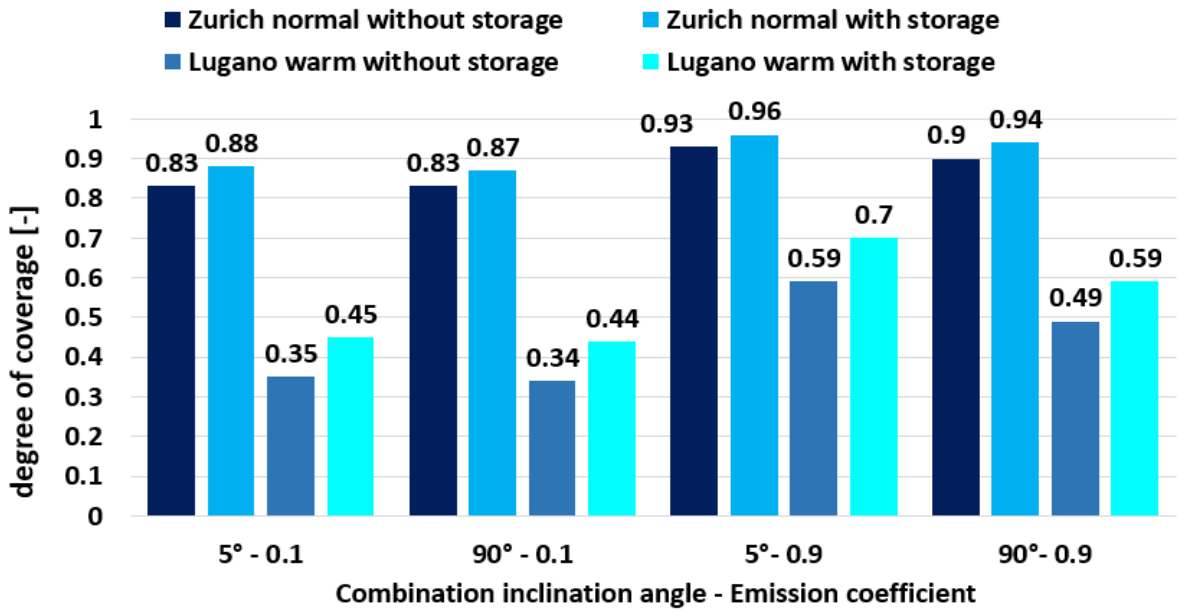

Fig. 32: Comparison of the degree of coverage in cooling mode with and without integration of a storage for Zurich Meteoschweiz normal year and Lugano warm year

Regarding the storage integration, the increase of the degree of coverage is limited to about 3% with good properties, and about 5% for rather adverse properties in moderate climate.
As comparison, additionally the extreme summer climate of Lugano warm year is included in the Fig. 32, as well. The degree of coverage notably decreases to about 60% with good absorber properties and to about 35% with rather adverse. Thus, the radiative fraction is more important than in moderate summer climate, since the potential for convective heat rejection is limited. Due to the more restricted potential for free cooling in warm summer nights, the storage integrations yields a higher increase of the degree of coverage, since nights with adverse weather conditions can be supplied by buffered cooling energy from the storage. Thus, the increase of degree of coverage with integrated storage is in the range of 10%.

3.4.4 Discussion of simulation results for cooling operation

From the performed simulations the following statement can be made for the space cooling operation:

- At cooling operation, buildings with one to two stories with an activated roof area can reach covering parts up to over 90% at moderate ambient conditions during a normal summer at the Swiss middleland.
- The selectivity of the area is not critical at moderate ambient conditions because of convection potential. Due to a higher operating temperature of the surface, the missing emission of highly selective absorbers are compensated through a higher fraction by convection, so the absorbers still reach a good cooling power. The higher additional cooling part reduces the performance factor.
- A brief designing or warm ambient temperatures interfere a heat dissipation through convection, so the emission as well as the emissivity are the crucial values. In this case, only non-selective absorbers with good emissivity reach high coverage ratios. Furthermore, the coverage ratios increase notable due to lower additional cooling.
- An integration of a storage can increase the coverage ratio at free-cooling operation. The rise is the higher, the lower the degree of coverage without storage respectively the less favourable the ambient conditions.

3.5 Conclusions

Based on test rig measurements of absorbers with different surface properties a simulation model of the absorber has been developed and validated. The model has been integrated in a system configuration suitable for multifunctional operation in space heating and cooling mode in order to evaluate the key characteristics of degree of coverage and seasonal performance factors for the operation modes.

In space heating operation for buildings up to three storeys, i.e. an absorber size of 0.33 m^2_{abs}/m^2_{ERA}, seasonal performance factors of the heat pump operation with the only source energy of the solar absorber reaches values in the range of 4 without direct solar heating, which corresponds to typical values of ground-source heat pumps. With direct solar heating SPF of up to 5 are reached in the simulation. Selective properties are of minor importance for the absorber operation as heat source, since the absorber operation temperature is close to the ambient air temperature, and thus, losses to the ambiance are low. However, in order to increase direct solar heating, which may significantly improve the SPF of the space heating operation, selective properties are essential in order to reach the necessary temperature level.

In space cooling operation, high degrees of coverage in the range of 80% to above 90% are reached. In moderate climate also the non-selective properties are not so predominant, since there is still potential for heat rejection by convection. In extreme summer climate, though, with higher night-time temperatures, the radiation fractions and thereby the impact of the non-selective properties are more important.

Summarising, both in space heating and space cooling operation high performance values are achieved with the absorber as only heat source and sink, respectively. However, based on the prevailing load situation, optimization potentials exist regarding the properties of the absorber.

4 Integrated heat pump developments at ORNL

The U.S. Department of Energy's (DOE) Building Technologies Office (DOE-BTO) has a long term target to maximize the energy efficiency of the US building stock by year 2030. Maximizing building energy efficiency is an essential facilitating step to enable market uptake of NZEBs including net zero energy homes (NZEH). To achieve the vision of a building stock with maximized energy efficiency, a deep reduction of the energy used by the energy service equipment of -50% or more compared to today's best common practice is required. One promising approach to achieve this is to produce a single piece of equipment that provides multiple services. ORNL developed a general concept design for such an appliance, called the integrated heat pump (IHP) (Murphy et al. 2007a, b).

4.1 Integrated heat pump development

The energy service needs of an NZEB include space heating and cooling (SH/SC), water heating (WH), ventilation (V), and possibly dedicated dehumidification (DH) and humidification (H) as well, depending on the requirements of the specific location. These requirements differ in significant ways from those for non-NZEB. In some locations such as the Gulf Coast area, additional to SH/SC and WH loads, DH will almost certainly be required during the shoulder and cooling seasons.

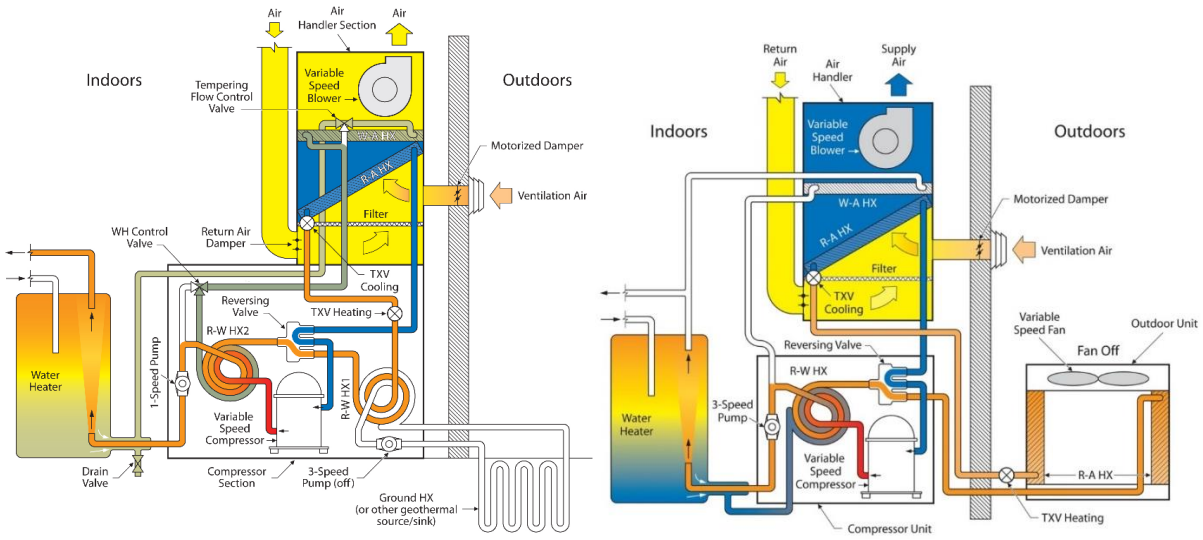

Fig. 33: Concept of the ground-source (left, dedicated dehumidification and water heating mode depicted) and air-source integrated heat pump (IHP) (right, dedicated space cooling and water heating mode)

As noted above, one promising approach to efficiently meeting these needs is with an IHP – a single system based on variable-capacity or variable-speed (VS) heat pumping technology. The energy benefits of an IHP stem from the ability to utilise otherwise wasted energy; for example, heat rejected by the SC operation can be used for WH. Significant energy savings are possible from the higher efficiency operation of the components, the load matching capability of the VS equipment (providing heat exchanger unloading benefits), outdoor-source heat pump water heating, and waste heat recovery in the combined SC and WH mode.
With the greater energy savings the cost of the more energy-efficient components required for the IHP can be recovered more quickly than if they were applied to individual pieces of equipment to meet each individual energy service need. An IHP can be designed to use either outdoor air or geothermal resources as the environmental energy source/sink. The principle of the ground-source and air-source integrated heat pump development is depicted in Fig. 33.

4.2 IHP Variants and Developments

There are two primary versions of the IHP, a geothermal or ground-source (GS-IHP) and air-source (AS-IHP).The principles shown in Fig. 33 have been evaluated with lab-test results of real components, which were implemented in components models in TRNSYS system simulation software and annual performance simulations were accomplish for five different climatic locations across the USA. Results confirmed substantial energy saving potentials with the IHP fulfilling the target to increase energy efficiency by more than 50% vs. standard technology of minimum efficiency requirements. Saving potentials were evaluated to

- 52%-65% for the ground-source integrated heat pump
- 47%-67% for the air-source integrated heat pump

Details on the investigations are contained in Appendix A.1.
In the following, ORNL activities have focused on development of four different embodiments of the IHP. One is an electric GS-IHP and the other three are AS-IHPs (two electrically-driven and one natural gas engine driven).

4.3 Ground source integrated heat pump (GS-IHP)

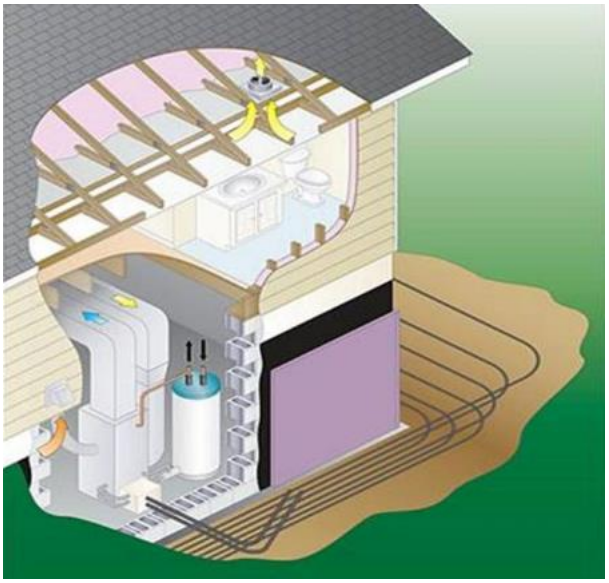

Fig. 34: GS-IHP conceptual installation

The GS-IHP system uses a variable-speed (VS) compressor, VS indoor blower (for SH/SC distribution), and VS pumps for ground heat exchanger (GHX) fluid circulation, and for hot water circulation. A 190 l WH tank is included. The prototype system development is a 7 kW nominal design. The testing residence is a well insulated 240 m² house, located in a range of climate zones.
In early 2008 the industrial partner Climate Master, Inc (CM) and ORNL began a series of GS-IHP system design iterations resulting in two generations of GS-IHP for lab and field testing. ORNL used the detailed lab measurements of refrigerant and source/sink conditions to calibrate the heat pump design model (HPDM) (Rice (1991); Rice et al. (2005)) which was incorported into the TRNSYS simulation model for estimation of annual performance and energy savings potential. The process is documented by Rice et al. (2013) and Baxter et al. (2013) and shortly summarized in this subsection.
The HPDM was calibrated in each of the four operating modes: SH, SC, SC + WH, and dedicated WH using the publicly available optimization program GenOpt (Wetter, 2009). Results of the HPDM are in good agreement with the lab-testing results, namely in a range of 5% of the capacity, in the range of 2% for the compressor power and in the range of 4% for the COP.
Further modelling steps were undertaken to model as well a baseline system in order to compare the results to the state-of-the-art and the modelling of the ground-source heat exchanger (GHX).
For the comparison a baseline system was defined, corresponding to standard equipment with minimum efficiency requirement.
With the modelled systems of the ground-source heat exchanger and the IHP system simulations for the 7 kW prototype were performed for five climate zones, resulting in energy saving potentials between 40-60% depending on operation mode and climate zone. Details on the modelling and simulations results are including in Appendix A.2. Based on the simulations, a field test was performed.

4.3.1 Field tests of GS-IHP

The home was split into four zones, upstairs, downstairs living space, master bedroom, and basement, which were all controlled to same set points of 21.7 °C for heating and 24.4 °C for cooling. Fig. 35 shows the test site for GS-IHP (left) and GHX layout (right).

Fig. 35: GS-IHP test site (left) and GHX layout (right)

The GHX had a total of 796 m of high density polyethylene (HDPE) pipe placed around the foundation of two of the basement walls in addition to two utility trenches and a rain garden in the backyard.

During the cooling season, the unit can operate in three of the four modes: SC, SC+WH, or WH. If there are coincident space cooling and water heating demands, the unit will run in the SC+WH mode. If there is only a demand for water heating, the unit will run in WH mode. During the heating season, the unit only operates in two of the four modes: SH and WH. There is no combined space heating and water heating mode, so the unit gives water heating priority unless the indoor space temperature falls by a pre-set number of degrees below the heating set point.

The 1st generation prototype was monitored for the 2011 year (January through December) with details summarized in Baxter et al. (2013). Several technical issues were encountered during the year that resulted in frequent interruption of GS-IHP operation. While this limited the extent of the collected performance data, what was available provided valuable information to CM, enabling them to develop a much improved 2nd generation prototype.

Tab. 10: Projected 2nd generation GS-IHP prototype energy savings vs. baseline for House 2 in 2012

Operation mode		GS-IHP	Baseline Equipment	Percent Savings Over Baseline
Space Cooling	COP	6.77	3.38	
	Delivered [kWh]	5202	5202	
	Consumed [kWh]	768	1539	50.1 %
Space Heating	COP	5.19	2.68	
	Delivered [kWh]	8765	8765	
	Consumed [kWh]	1690	3265	48.2 %
Resistance heat		29	127	
Water Heating	COP	3.79	0.89	
	Delivered [kWh]	2313	2313	
	Consumed [kWh]	610	2605	76.6 %
Resistance heat		0	2605	
Total	**Consumed [kWh]**	**3177**	**7519**	**57.8 %**

The 2nd generation prototype was installed at the test site on May 7, 2012 with the help of CM personnel. Monitoring of the 2nd generation system took place from June 2012 through January 2013. Tab. 1 give performance data of the 2nd generation prototype for the different operation modes compared to the baseline system. Since an entire year's worth of data was not able to be collected during the project, approximations were made for months where data was not available, so that the annual performance could be estimated.

The first step in this process was to fit a sinusoidal wave to the daily average outdoor air temperature (OAT) and daily average entering water temperature (EWT) data. These waveforms were then used to generate average monthly OATs and EWTs for the months without data. The load in each mode was then estimated by plotting the monthly delivered output in [kWh] against the average OAT for the month. A linear fit was applied and, along with the estimated OAT, a delivered load was estimated for months without data. Similarly, the COPs for each mode were estimated by plotting the existing data against the average EWT for each month. Details are given in Appendix A.2.

4.4 Electric air-source integrated heat pump

For the electric driven AS-IHP, two different system prototypes have been developed. One of them is a single compressor or combined system, and the other is a two-box system.

4.4.1 Single compressor or combined system

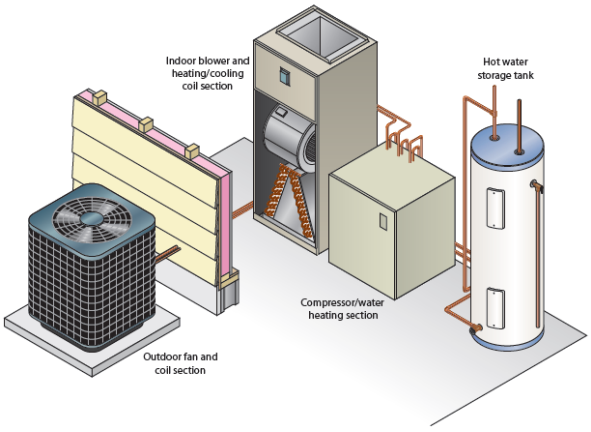

Fig. 36: AS-IHP conceptual design

A nominal 10.6 kW design cooling size was selected for development. ORNL and manufacturer team members engaged in an iterative process of prototype analyses/design, lab testing, and re-design based on lab results. Three generations of prototypes were developed leading to field testing. The design uses VS compressor, blower, and fan. Dual electronic expansion valves (EEVs) are used to provide a wide range of refrigerant flow control. A double-walled concentric tube heat exchanger (HX) was used for WH operation with tube-and-fin HXs for the indoor and outdoor coils for the first prototype design. Subsequent prototypes used compact HX designs for all three HXs.

Expected WH modes of operation included dedicated WH using the outdoor coil as the heat source and combined space cooling (SC) and WH, both of which employed the full condensing (FC) output for WH. Another WH mode used desuperheating (DS) during SC or SH operation. A pump capable of at least two-speed operation was required to meet both FC and DS water flow requirements.

One technical challenge for the AS-IHP system development was refrigerant charge management. This challenge is greater for air-source systems than for ground-source units, because outdoor air coils have much larger internal volume than water-to-refrigerant HXs of similar capacity. To deal with this issue, the manufacturer developed a proprietary design to manage charge between operating modes.

Another design challenge is in WH operation. VS compressors typically can operate at maximum condensing temperatures only above a certain speed, with limits on condensing temperature dropping linearly below this speed. This constraint limits the minimum compressor speed for dedicated WH. In addition, to reach maximum output water temperatures above about 50 °C (122 °F) while staying within the compressor operating envelope, higher speeds with output capacity of 10.5 kW (3 tons) or more are required. As such, a pump capable of providing ~1.14 m^3/h (5 gal/m) or higher flow is required. Operation in DS-only mode can also provide temperatures above 50°C (122°F).

Following a similar process as that used for the GS-IHP system analyses, results of the prototype lab tests were used to calibrate the variable-speed research version of the DOE/ORNL heat pump design model (HPDM).

In turn, system performance maps generated by the HPDM were used in the TRNSYS/HPDM (T/H) simulation model for estimation of annual performance and energy savings potential. The process is documented in Rice et al. (2014a) and summarized in this subsection.

ORNL used the detailed lab measurements over a wide range of refrigerant, outdoor and indoor air temperature, and entering DHW temperature conditions to calibrate the HPDM in each of the operating modes utilising the GenOpt program (Wetter, 2009).
Once this process was completed, we used the HPDM to generate performance maps (i.e., tables) of capacities, powers, and mass flow rates for each mode as a function of all relevant independent variables, e.g., compressor speed, indoor and outdoor temperature and RH, and entering water temperature (EWT) from the DHW loop. The DS operation was modeled in TRNSYS as a fixed HX effectiveness based on the laboratory test data.
Annual performance analyses were conducted with the T/H model using the same house, climate locations, control set points, and daily DHW use profile and quantity as for the GS-IHP analyses described earlier. For winter operation, thermostat control priority was given to SH with WH limited to DS (and back-up electric elements as needed) until the SH heating load was satisfied. This approach provides better control of the indoor space temperature in the winter season than with WH priority control. Dedicated WH (using the outdoor coil as a source) is limited to operation above a specified cut-off ambient, when no SH call is active, and in shoulder months when the ambient is below a specified cut-off. In SC mode, DS WH operation is used first when a WH call is active, until a prescribed water draw is reached, when the unit will switch to combined SC+WH operation with FC output.
Simulation results for the 2nd prototype configuration are shown in Tab. 11 for each location.

Tab. 11: Energy use and savings predictions for AS-IHP Lab Prototype 2 Design

Operation		ASIHP	Baseline Equipment	Percent Savings Over Baseline
Space Cooling	Consumption [kWh] Atlanta	905	1566	42.2 %
Space Heating		1359	2314	41.2 %
Water Heating		987	3293	70.0 %
Ventilation		189	189	
Total		3440	7361	53.3 %
Space Cooling	Consumption [kWh] **Houston**	1480	2498	40.7 %
Space Heating		598	1062	43.6 %
Water Heating		664	2728	75.7 %
Ventilation		189	189	
Total		**2931**	**6476**	**54.7 %**
Space Cooling	Consumption [kWh] **Phoenix**	2320	3395	31.7 %
Space Heating		398	724	45.0 %
Water Heating		665	2392	72.2 %
Ventilation		189	189	
Total		**3572**	**6700**	**46.7 %**
Space Cooling	Consumption [kWh] **San Francisco**	11	21	44.8 %
Space Heating		703	1304	46.1 %
Water Heating		1123	3676	69.4 %
Ventilation		189	189	
Total		**2030**	**5189**	**60.9 %**
Space Cooling	Consumption [kWh] **Chicago**	340	623	45.5 %
Space Heating		3974	6287	36.8 %
Water Heating		1545	4110	62.4 %
Ventilation		189	189	
Total		**6048**	**11209**	**46.0 %**

The entries in red show the portion of the total energy use for that mode that was from resistance heat. Total HVAC/WH energy savings relative to the all-electric baseline unit averaged 52%, ranging from 46-47% in the cold and hot locations to >60% in the mild marine climate. The predicted average space conditioning savings are 42% with average WH savings of 70%.

4.4.2 Field test of AS-IHP

Cooling season summary

Before the field testing started work was done to set up the test house occupancy simulation. The water draw schedule used at the site is based on the latest Building America water draw generator http://www1.eere.energy.gov/buildings/residential/ba_analysis_spreadsheets.html. Latent, sensible and various building loads are based on the Building America House Simulation Protocols (Hendron and Engbrecht, 2010).

Fig. 37: Field test site in Knoxville, TN

Occupancy simulation is accomplished via scheduled operation of small space heaters (to simulate sensible heat), and humidifiers (to simulate latent heat). DHW loads (dishwasher, clothes washer, showers, sinks, etc.) are simulated by operating solenoid controlled water valves according to the programmed schedule. Temperature control set points of 49.0 °C (120 °F) for WH and 24.4 °C (76 °F) for space cooling were implemented in the system controls prior to starting data monitoring in May.
Fig. 37 shows pictures of the field test site. The primary operating modes experienced during this period were SC only (Dedicated SC), SC + desuperheater (DS) WH (SC+DS) and SC + FC WH (SC+WH)
Fig. 38 illustrates the SC and WH monthly average COPs for each mode and average for the entire month for May through September 2014. The average monthly SC COP has ranged from about 5.0 to 5.35 each month, while the monthly WH COP has ranged from 3.23-4.75 (ignoring electric element power usage). There was a small amount of backup WH electric element energy consumption during the summer, but this was due to control system issues (e.g. control computer failing to reboot properly, etc.). No element usage would be expected in the summer period under the hot water use profile in effect at the test house.

Tab. 12: Cooling seasonal average COPs

Mode	Energy delivered [kWh]	Energy use [kWh]	Average COP
SC	7416	1444	5.14
WH (no element)	1014	231	4.39
Total/average	8430	1675	5.03

Heating season

Heating season field monitoring began in October 2014 and continued through May 2015. Temperature control set points of 49 °C (120°F) for water heating and 21.7 °C (71 °F) for space heating were implemented in the system controls prior to starting data monitoring in October. System performance data are currently under analysis and review by the manufacturing partner and by ORNL and are not available for reporting at this point. A full annual performance report is expected by late Fall 2015.

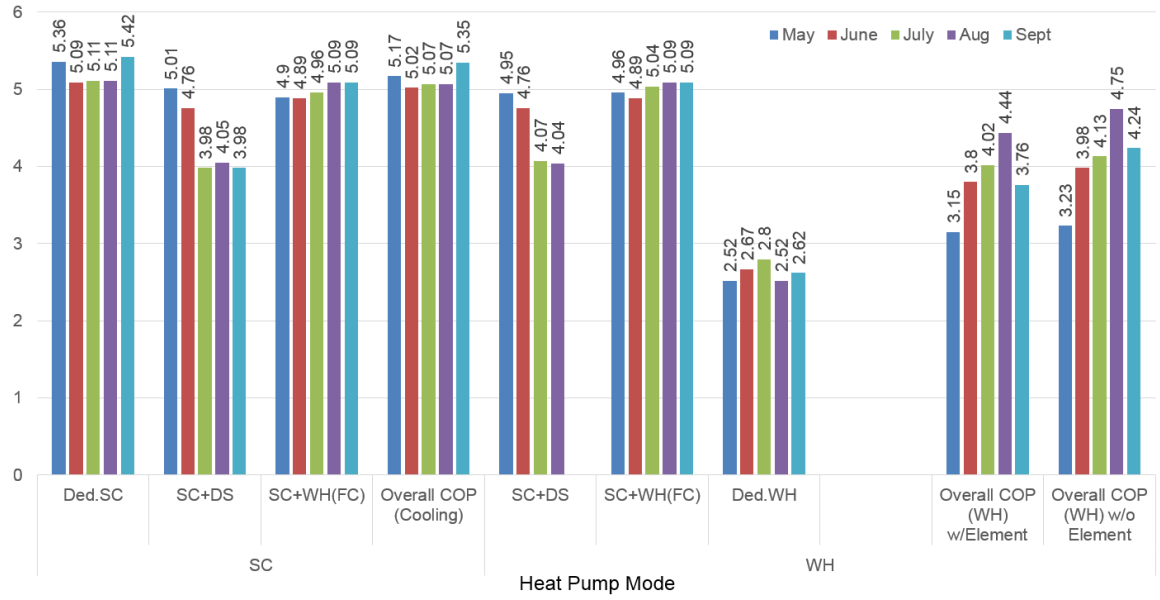

Fig. 38: Field test results of the AS-IHP Prototype 2 in Knoxville in cooling season

4.4.3 Two-box air-source integrated heat pump (AS-IHP) system

ORNL has been engaged in a 2nd AS-IHP system development effort with another manufacturer partner (Lennox Industries). This embodiment of the concept is a two-unit or "two-box" system based on a central high-efficiency ASHP coupled with a prototype water heating/ dehumidification (WH-DH) module (see Fig. 39 (left)).

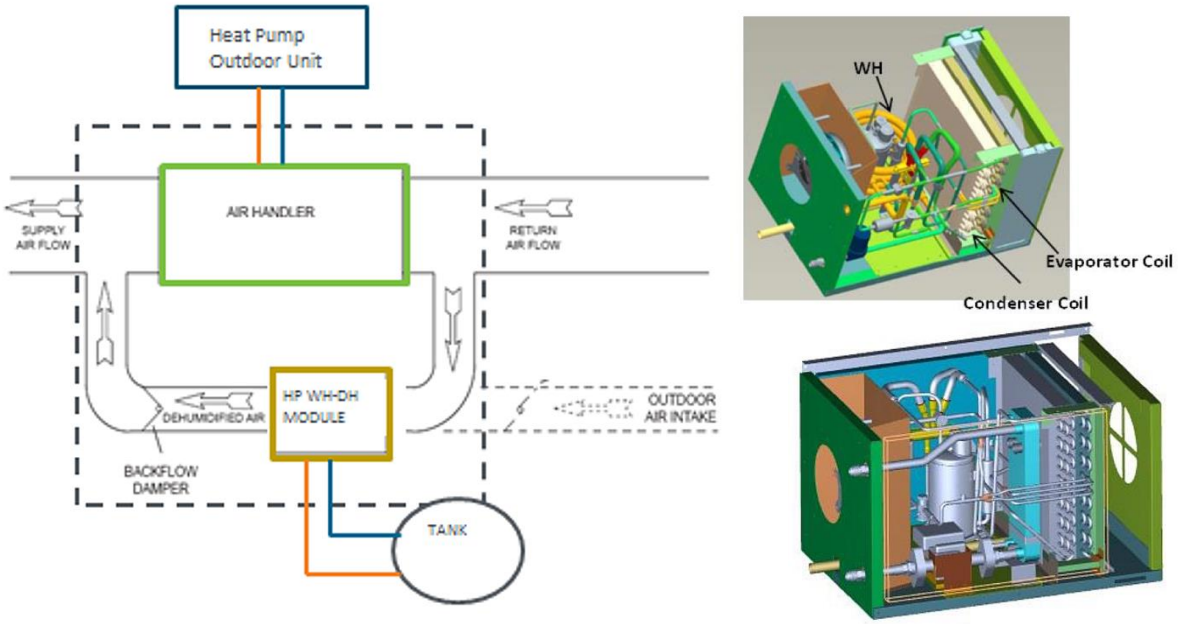

Fig. 39: Concept of the two-box AS-IHP (left) and prototypes of the WH-DH module (right)

The WH-DH module can be integrated with the ASHP unit by a parallel secondary duct loop around the central air handler, receiving a portion of the central return air, when the secondary (WH-DH) blower is operating and returning this air to the supply air stream. It also has an optional connection to an outdoor air intake to provide a means for conditioning and circulating ventilation air through the central duct system. A dedicated space DH cycle addresses humidity control and integration of heat pump WH is expedient, since the small vapour compression components can perform double-duty. This integrated yet independent operation of the WH-DH unit provides dehumidification of the central return and ventilation air as well as a central heat source for the WH mode.

The independent operation is especially useful in the shoulder months which often require dedicated DH, along with WH, but little or no SC or SH.
Another significant advantage is that this IHP approach can be relatively easily applied to retrofit/upgrade applications as well as new constructions, utilising standard electric water heaters and a wide range of multi-capacity and variable speed ASHPs.
In retrofit applications, even if the tank is remote from the heat pump indoor section, the WH-DH unit can be located at the WH tank and the system will still retain most or all of the IHP advantages. Details of the development are given in Rice et al. (2014b) and summarised here.

WH-DH module field test prototype design summary

The design of the WH-DH module is based on US Patent 8,689,574 B2 (US Patent Office 2014). Fig. 39 (right) shows a computer aided design (CAD) drawing of the system concept. Performance goals for the WH-DH unit are to meet or exceed US EnergyStar performance levels (http://www.energystar.gov/) for WH and DH modes of operation.
For the DH mode, the Energy Factor (EF_d) requirement for EnergyStar rating is >1.85 l/kWh for units with water removal capacity of < 35.5 l/d (< 75 pints/d or < 9.375 gal/d). For WH, an EF ≥ 2.0 (W/W) is required for EnergyStar designation. The remaining design goal was to provide water heating capacity of ~2 kW, about twice that for existing EnergyStar HPWH products.

Tab. 13: Energy Use and Savings Predictions for AS-IHP with Prototype 1 WH-DH Unit Configuration. Values in bracket and italic refer to resistance heat.

Operation		ASIHP	Baseline Equipment	Reduction from Base
Space Cooling	Con-sumption [kWh] **Atlanta**	1059	1741	39.2 %
Space Heating		1965 *(31)*	2311 *(18)*	15.0 %
Water Heating		1553 *(488)*	3380 *(3380)*	54.1 %
Dehumidification		299	319	6.2 %
Ventilation Fan		202	189	-6.9 %
Total		5079	7941	36.0 %
Space Cooling	Con-sumption [kWh] **Houston**	1975	3035	34.9 %
Space Heating		906 *(3)*	995 *(0)*	9.0 %
Water Heating		1169 *(246)*	2813 *(2813)*	58.5 %
Dehumidification		1035	1154	10.3 %
Ventilation Fan		179	189	5.6 %
Total		5264	8187	35.7 %
Space Cooling	Con-sumption [kWh] **Chicago**	402	740	45.6 %
Space Heating		4915 *(669)*	6214 *(916)*	20.9 %
Water Heating		2122 *(906)*	4218 *(4218)*	49.7 %
Dehumidification		154	154	0.0 %
Ventilation Fan		169	189	10.5 %
Total		7762	11514	32.6 %

Two generations of lab prototypes were assembled by Lennox and tested at ORNL and at Lennox facilities. The initial prototype used an R-410A rotary compressor with a cooling capacity of ~2 kW (~7000 Btu/h) and 2.8 cooling COP (9.5 Wh/Btu EER) ratings.
Separate condensers were used for each operating mode -- a 3.5 kW (1-ton) fluted tube-in-tube double-walled water-to-refrigerant heat exchanger (HX) and a three-row fin-and-tube air-to-refrigerant HX, in combination with a common two-row fin-and-tube evaporator. The 1st generation module was tested extensively at ORNL in FY2013 in both the WH and DH modes.

Cooling season summary

Before the field testing started work was done to set up the test house occupancy simulation. The water draw schedule used at the site is based on the latest Building America water draw generator http://www1.eere.energy.gov/buildings/residential/ba_analysis_spreadsheets.html.

Latent, sensible and various building loads are based on the Building America House Simulation Protocols (Hendron and Engbrecht, 2010).
A 2nd generation WH-DH prototype was then built and tested by Lennox in 2014. It used the same compressor and DH mode condenser as the first unit. A brazed-plate water-to-refrigerant HX replaced the tube-in-tube design to provide a lighter weight, more compact and easily insulated design. Larger air duct inlet and outlet duct collars were implemented to reduce the static pressure drop in the unit and improve its airflow capability.
DH mode tests of the 2nd generation prototype have shown about a 7% improved DH EF relative to that for the first prototype - ~2.15 l/kWh vs. ~2 l/kWh. We believe this was due to the improved evaporator refrigerant flow distribution and more uniform airflow over the evaporator and condenser from the larger inlet/outlet ducts. WH mode test results showed an EF of ~2.05, thus slightly exceeding the WH performance goal for the project.

Two-box AS-IHP field test system plans.

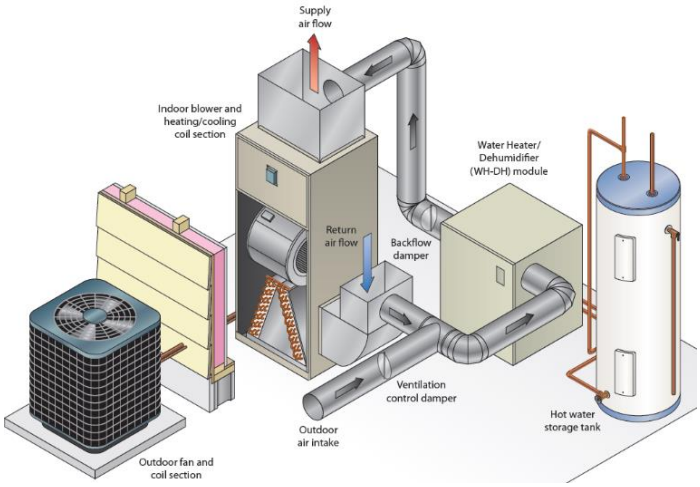

Fig. 40: Two-box AS-IHP field test system arrangement

The field test design is generally based on the prototype 2 architecture implementing its operating mode efficiency improvements. Fig. 40 provides a CAD schematic of the general layout of the field test prototype WH-DH design.
A field test of two-box system began in July 2015 in the test house pictured in Fig. 37. An artist's concept of the system arrangement is given in Fig. 40. The ASHP for the field test system will be a new VS ASHP product recently lauched by Lennox with nominal 10.5 kW (~3-ton) cooling design capacity. These ASHPs have rated seasonal cooling and heating COPs > 5.8 (> 20 SEER) and > 2.9 (> 10 HSPF), respectively. This is at least 8-10% higher than the rated performance of the two-speed ASHP used for the annual performance analyses summarized in Tab. 13 above. Given the higher efficiencies of the VS ASHP and the current WH-DH prototype, we are reasonably confident that the field test system should reach or exceed the 40% annual energy savings project target (average over a range of U.S. climates).
The Lennox VS ASHP can be coupled to a Solar photovoltaic (PV) system (Lennox SunSource®, Lennox 2013a, b). Rice et al. (2014b) investigated how many 275 W_p DC solar modules would be needed to offset the annual electrical AS-IHP system energy requirement for each city included in Tab. 13. Annual generation output of the PV modules was estimated with the method reported by Dobos (2013). For Atlanta and Houston 13 modules and 15 modules, respectively, should be adequate to supply the annual electric power needs of the AS-IHP system. For Chicago, the maximum of 16 solar modules would still leave a shortfall of 2157 kWh. At the time this report is being put together, the rated power of the PV modules has increased to 300 W_p. Use of this PV option is currently not included in the field test plans.

4.4.4 Gas engine driven AS-IHP

Gas Engine-Driven Heat Pumps (GHP) can be an attractive economic choice in parts of the US where the typical engine fuels such as natural gas, propane or liquefied petroleum gas (LPG), can be less expensive than electricity (Mahderekal et al., 2012). Compared to conventional fuel-fired furnace heating systems they are projected to reduce fuel consumption for space heating by 35% and for water heating by 80% (Vineyard, 2014). They also significantly reduce summer cooling electric peak demand compared to electric air-conditioning (AC) systems. A GHP can be a more attractive climate control system than conventional single-speed electric heat pumps for a number of reasons, e.g.:

- Variable speed (VS) operation: Typically, the GHP can cycle at minimum speed and modulate between a minimum and maximum speed to match the required load. As a result, the part load efficiency of such a system will be high. Its seasonal operational cost and cycling losses will be lower than those of a single speed system with an on–off control system.
- Engine heat recovery: The engine's waste heat can be recovered to significantly augment SH capacity in winter and to provide DHW heating year-round. Thus, the system's efficiency will be increased.
- As noted already, GHPs rely on natural gas or LPG fuels as the primary energy source. In many regions of the US, these fuels are less costly than electricity for a typical overall HP COP and efficiency of the engine leading to energy cost savings for the building owner.
- By including a generator with the engine, a GHP can produce its own power to run the electric auxiliaries (fans, pumps, etc.). This resource can also be used to generate extra power to charge a battery and provide backup power for essential building needs (refrigerator, lights, etc.) in the event of an electric grid outage. The battery can be used to start the engine, so the GHP could effectively operate independently of the electric grid, if necessary (Intellichoice Energy, 2014).

ORNL and partners Southwest Gas Corp (SWG, a gas utility company) and Intellichoice Energy (engineering consultancy company), and Marathon Engine Systems (engine and system manufacturer) have been collaborating toward development of a multi-function (or IHP type) gas engine driven heat pump (Vineyard, 2014). The system design was based on the needs of the SWG market located in the southwest US (Las Vegas, Phoenix, Tucson).

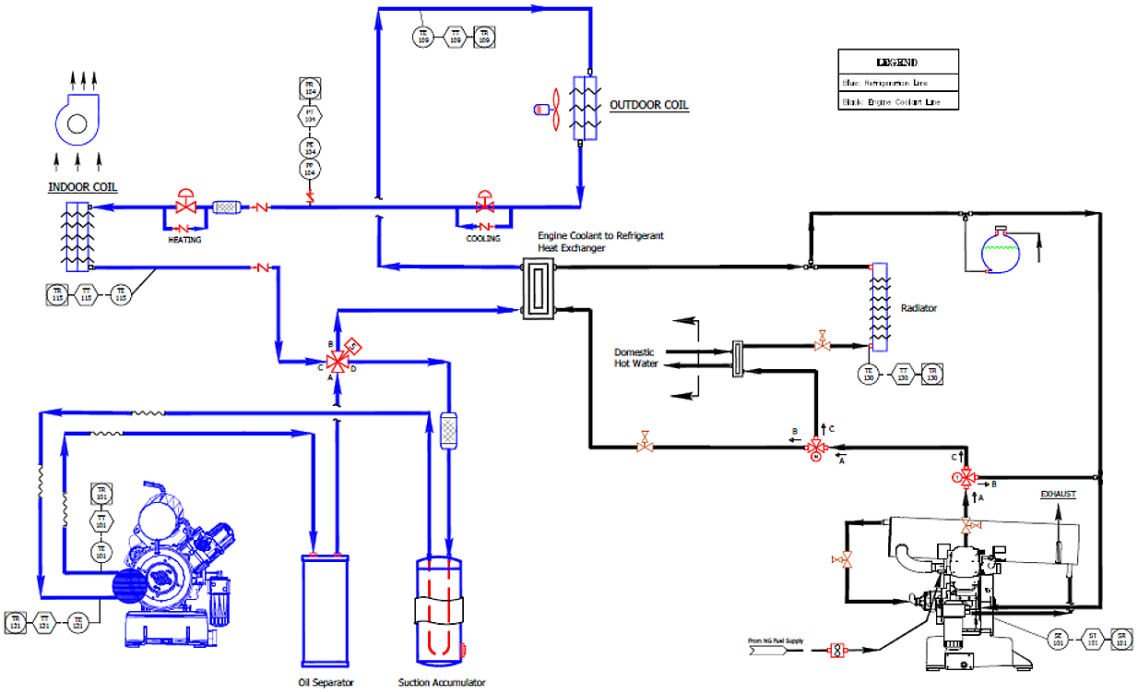

Fig. 41: Gas-engine AS-IHP schematic: space cooling mode operation shown, blue lines signify to refrigerant and black lines engine coolant flow

This area is a part of the hot-dry climate zone of the US and characterized by very long, very hot summers, but also experiences very cold winters in parts of the area due to elevation. Fig. 41 is a schematic of the system. The engine coolant to refrigerant heat exchanger component (approximately in the centre of the schematic) is used during winter SH operation to boost the compressor suction pressure and augment SH capacity. DHW heating is provided by heat recovery from the engine coolant via the heat exchanger component in the centre right-hand side of the schematic.

Initial, Alpha, prototype

Similarly, as for the electric IHP system projects, the gas engine IHP team worked through a number of iterations of prototype design, fabrication and lab testing as well as field testing.

Fig. 42: Development steps of the Gas-engine AS-IHP: Alpha (1st generation) prototype – lab test set up (left), Alpha prototype at field test site in Las Vegas area (middle) and Beta prototype field test unit (right).

Fig. 42 left is a photo of the first generation, or Alpha, prototype as set up for testing at ORNL. Summary cooling and heating lab test results are given in Fig. 43.

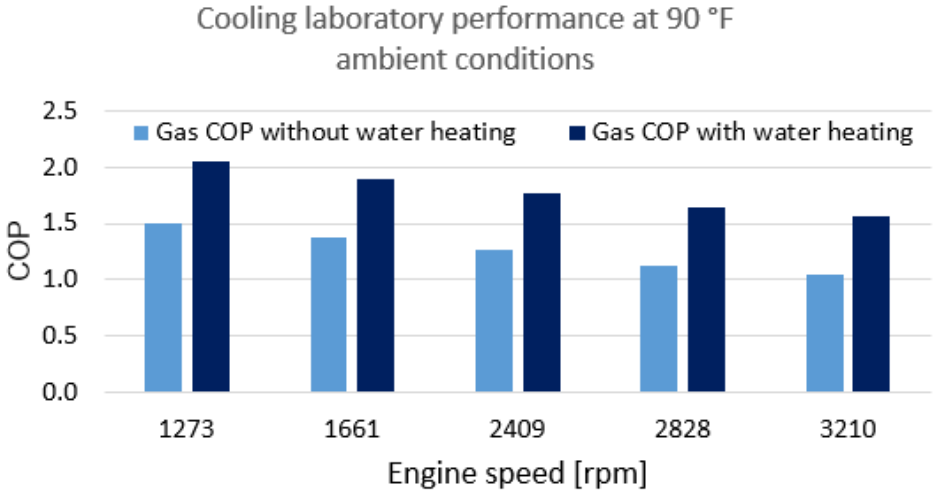

	Performance target	Test results
Cooling capacity @ 35°C, kW	12.3-18.2	14.4
Cooling COP (gas) @ 35°C	1.3	1.28
Heating capacity, kW @ 8.3°C	14.7-22.0	21.1
Heating COP (gas) @ 8.3°C	1.5	1.48
DHW supply, m^3/d	0.225	>0.225
DHW supply temperature, °C	60	~60
Ancillary electric loads, kW	0.75-1.0	~0.95

Fig. 43: Alpha 1 Cooling COP with and without WH vs. Engine speed (based on gas consumption) (upper diagram) and Alpha prototype lab test summary results vs. project goals; engine rpm ~2400 (lower table)

In December 2012, 20 of the Alpha protoypes were installed in occupied homes in the SWG service area. They were monitored through June 2014 (Vineyard, 2014; SWG, 2014).
Fig. 42 middle shows a photo of one of the systems in Las Vegas. Summary energy cost results for the 2012 test year (for eight systems in the Las Vegas area) are presented in Fig. 44.

Site #	2012 baseline energy costs	2013 Alpha prototype energy costs	Savings, %
1	$3,083	$2,877	6.7
2	$3,061	$2,660	13.1
3	$2,356	$2,068	12.2
4	$1,569	$1,442	8.0
5	$3,163	$2,760	12.7
6	$3,237	$2,819	12.9
7	$3,379	$2,798	17.2
8	$3,680	$3,375	8.3

NOTE – savings expected to be greater in colder locales with greater winter gas usage for space heating.

Item	Cost for 1000 units
Controls (engine/system)	$1,000
Recuperator	$ 600
Compressor	$ 500
Insulation	$ 200
Radiator/fan	$ 450
Drive assembly	$ 250
Outdoor coil	$ 800
Cabinet	$1,300
Alternator/generator	$ 500
Refrigerant circuit, w/parts	$1,100
Engine	$2,300
Total	**$9,000**

Fig. 44: Alpha 1 Cooling COP with and without WH vs. Engine speed (based on gas consumption) (left) and Alpha prototype lab test summary results vs. project goals; engine rpm ~2400 (right)

Fig. 45 presents results of a survey of homeowners who hosted the Alpha prototype field test systems. In terms of system operation and indoor comfort, most responses were either favourable or very favourable. By a small majority, most residents also felt that the DHW performance was improved compared to the baseline gas WH systems they replaced.

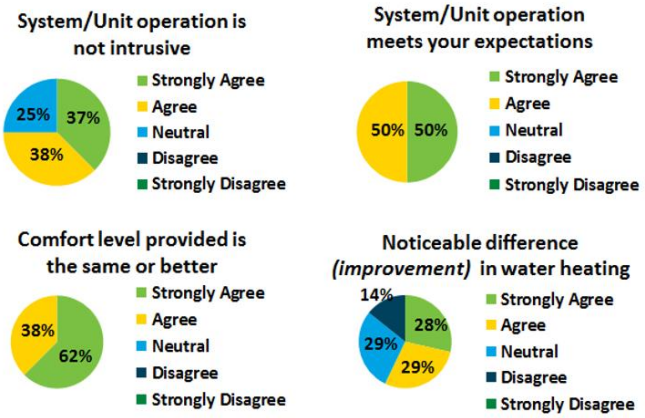

Location	Years for 4.1 AC COP (14 SEER)	Years for 5.3 AC COP (18 SEER)
Elko, NV	3.9	3.7
Las Vegas, NV	7.3	8.9
Phoenix, AZ	7.5	11.7
New York, NY	3.6	3.9
Chicago, IL	4.0	4.1
National average	**5.3**	**5.8**

[1]Assumes target system cost for 1,000 units of $9,000 is met

Fig. 45: Alpha prototype homeowner survey results (left: Vineyard, 2014) and simple payback[1] vs. baseline gas furnace, gas water heater, and electric AC (cooling seasonal COPs of 4.1 and 5.3) (right)

Beta prototype

Based on the Alpha prototype performance results, the team proceeded to development of a next, Beta, generation system. In July 2014 the Beta prototypes were installed at the Las Vegas area field test sites (see photo of one unit in Fig. 42 right). The major differences between the Beta and Alpha prototypes were that the outdoor coil size increased on the Beta and the fan motor size went from a 0.56 kW electric to 0.25 kW electric motor. The engine operating speeds were also changed. The Alpha I prototype low speed was 1800 rpm and the high speed was 3400 rpm.

For the Beta prototype the low speed was increased to 2350 rpm while the high speed setting stayed the same. During peak cooling or heating demands during the 2013 test period, the Alpha unit could not maintain indoor temperature on low speed. For cooling months the indoor temperature would rise and the engine RPM would increase to 3400 RPM. This generally resulted in longer run times when compared to the Beta unit operation in the 2014 summer.

For instance during the particularly hot week of July 21, 2014 with site average temperatures ranging from 38.3 to 45.0 °C (and peak temperatures from 46.1 to 55 °C), most of the Beta units generally operated at 2350 RPM (low speed) for over 80% of the time (SWG, 2014).

Tab. 14 indicates the Beta units in the 2014 summer ran 35% less time on average than did the Alpha units during the same time period in 2013. In addition to the Beta operating hours being lower than Alpha hours, the overall fuel use by the Beta units averaged ~20% less than that of the Alpha units.

Tab. 14: Beta vs. Alpha propane (LPG) prototype field test unit performance

Month	Beta unit runtime, hours (2014)	Alpha unit runtime, hours (2013)	Beta unit propane usage		Alpha unit propane usage	
			Liters	Liters/h	Liters	Liters/h
August	202	353	328.5	1.62	454.6	1.29
September	222	211	355.5	1.60	271.7	1.29
October	52	218	81.9	1.58	280.7	1.29
November	49	25	74.8	1.52	32.2	1.29
Total or avg.	525	807	840.7	1.60	1039.2	1.29

While the Alphas had lower fuel use/h (due to the lower speed operation), the Beta units ran less time to achieve the same comfort level results.
A customer/homeowner survey was also conducted for the Beta prototypes. Overall results indicated the installation, service, and operation of the Beta units met customer expectations. However, a noise issue came up with the Beta units that had not been apparent at the Alpha unit field test sites. Beta unit cabinet enhancements and improvements in the field installation process made a significant improvement in the overall unit vibration and sound pressure levels as compared to the Alpha prototypes.
However, the overall noise reduction made it possible for some of the field test site home-owners to now hear a low level sound wave frequency (less than 90 Hz). The same engine parts were used in both the Alpha and the Beta units. Detailed sound analyses revealed that there are three sources of noise: combustion noise, combustion induced mechanical noise and mechanical noise. The induced and mechanical noise concerns have been addressed effectively. Engine combustion (exhaust) noise has also been reduced sufficiently by the current muffler design (Mahderekal, 2015).

Beta prototype with power generation capability

Low cost (~$500) DC generators, rated for 2400 Watts, were installed on the prototype for internal (to the unit) and external electric power supply. Fig. 46 right shows the generator installation. A DC to AC transformer was included to convert the 24 Volt DC generator output to the 120 Volt AC output needed by the unit fans and external electric loads.

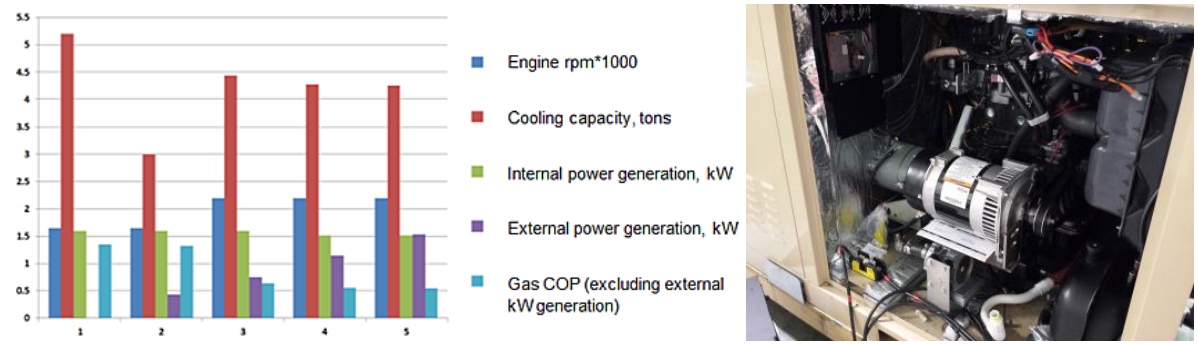

Fig. 46: Lab test results for prototype with low-cost generator (left) at 35 °C (95 °F) – x-axis indicates test number engine rpm ~2400 and Beta prototype with AC generator (right)

Short term (three day long) testing was performed in order to investigate the performance of the unit with low cost power generation. The ambient temperature was set at 35 ºC and indoor temperature was set to 26.7 ºC with relative humidity of 51%. Fig. 46 summarizes the performance of the system at different conditions.
The internal power generator consistently produced about 1.5 kW for the indoor and outdoor fans. At 1600 rpm and zero external power extraction, the cooling capacity was 18.2 kW (5.2 tons). With extraction of 0.4 kW for external loads, however, the cooling capacity fell to 10.6 kW (3 tons). Further increases in external electric load at 1600 rpm resulted in engine stall.

At 2200 rpm the system could produce much more external power, but at lower efficiency. Up to 1.6 kW of external power could be produced without significant loss of cooling capacity. This is enough power to run essential household appliances during emergency grid power loss. The tests revealed that the natural gas to electricity generation efficiency of the unit is between 12-20% (not including hot water production). This suggests that, for most efficient overall operation, grid electricity should be used for the indoor and outdoor fans whenever available and only switch to the generators when grid power is lost.
Due to the low electric generation efficiency with the initial DC generators, it was decided to modify the design and use a single 5000 Watt AC generator as shown in Fig. 46 right. A control/operation strategy to use grid electricity for the unit indoor and outdoor fans whenever available was adopted. During grid outage situations, the unit controller will increase the engine speed and keep it constant and turn on the AC generator. The generator will produce approximately 1.6 kW AC power for indoor and outdoor fans and other electricity needs of the heat pump system. It will also produce approximately 1-2 kW of additional electric power for emergency external needs such as lighting, refrigerator, etc.
It is expected that average electricity demand from the generator will be in the range of 2-3 kW (40 to 60% of rated output) in which the 5 kW generator efficiency is fairly high (~70%).
Laboratory test performance results for the latest Beta prototype are summarized in Tab. 15. Field testing of this version began in June 2015 and a final report is expected after the 2015/2016 heating season.

Tab. 15: Beta prototype cooling mode lab test results

OD temp [°C]	Engine [rpm]	SC Capacity [kW]	WH Capacity [kW]	Fuel use [kW]	OD Fan [W]	ID Fan [W]	Gas COP		System COP (with fan power from grid)	
							w/o WH	w/ WH	w/o WH	w/ WH
35.0	1400	5.8	2.0	3.4	442	885	1.69	2.29	1.22	1.65
35.0	1800	8.8	3.7	5.0	442	885	1.77	2.51	1.40	1.99
35.0	2200	10.9	0.0	6.8	442	885	1.61	1.61	1.34	1.34
35.0	3100	14.6	9.1	11.7	442	885	1.25	2.02	1.12	1.82
35.0	3400	16.3	10.5	13.3	442	885	1.23	2.02	1.11	1.83
40.6	3400	13.3	11.1	14.1	442	885	0.95	1.74	0.86	1.59
40.6	3000	13.7	0.0	11.5	442	885	1.19	1.19	1.07	1.07
40.6	2800	12.1	8.8	10.1	442	885	1.20	2.07	1.06	1.83
40.6	2200	11.0	7.3	6.7	442	885	1.64	2.73	1.37	2.28
46.1	2200	7.0	6.6	7.5	442	885	0.94	1.83	0.80	1.55
46.1	2800	9.8	11.2	11.5	442	885	0.85	1.82	0.76	1.64
46.1	3400	13.3	12.5	15.6	442	885	0.85	1.66	0.79	1.53
51.7	3039	10.0	10.1	14.7	442	885	0.68	1.37	0.63	1.26

5 Net Zero Energy Residential Test Facility at NIST

In 2009, the National Institute of Standards and Technology (NIST) received American Recovery and Reinvestment Act funding for the construction of a Net Zero Energy Residential Test Facility (NZERTF) on the NIST Campus in Gaithersburg, Maryland. The facility was to be constructed as a typical residence for a family of four that could achieve net zero site energy use on an annual basis. Net zero energy use was to be accomplished through the combination of low energy loads due to a high performance enclosure, efficient mechanical systems, and low energy fixtures and appliances in combination with site-generated energy using roof-mounted solar panels. Following the demonstration of net zero site energy use, the facility is to be used by NIST's Energy and Environment Division as a research laboratory to test and measure residential energy technologies, indoor environmental quality, materials, and other aspects of sustainable performance in a realistic context. Fig. 47 shows the NZERTF.

Fig. 47: Net Zero Residential Testing Facility (NZERTF) on the NIST campus

5.1 Building characteristics

The NZERTF is a unique building, built like a residence, yet it is truly a laboratory. Among the NZERTF's unique features is access to three separate ground source heat exchangers, a radiant basement floor heating system, a solar thermal hot water system with variable solar collector area and storage capacity, a 10.2 kW_p (DC) photovoltaic system, a heat recovery ventilation system, and various means of interfacing the smart grid with smart appliances. The facility also incorporates three different means of distributing conditioned air throughout the house – a sealed sheet-metal duct air distribution system; a high-velocity ducted air distribution system; and provisions to incorporate a mini-split heat pump system. The NZERTF uses a smart meter to measure the energy imported and exported to the electric grid. Fig. 48 left shows the floor plan of the first floor and garage and Fig. 48 right of the second floor.

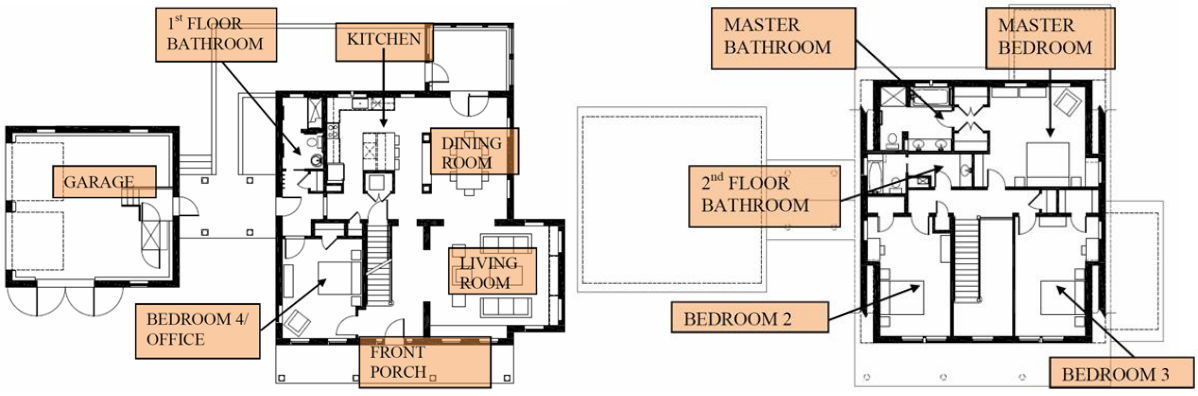

Fig. 48: Floor plan of the Net Zero Energy Residential Testing Facility (NZERTF), first floor and garage (left) and second floor (right)

5.2 Technical concept

The heating and air-conditioning system used for the first year in NZERTF consisted of an air-source heat pump system that incorporates a dedicated dehumidification cycle. The air distribution duct system was designed for less than 125 Pa external static pressure drop at the air handler with supply and return duct airflow rates of 2039°m^3/h with all registers fully open. The dedicated dehumidification cycle is provided by control algorithms that manage a hot gas bypass arrangement along with an additional indoor air heat exchanger that reheats the dehumidified air. The outdoor unit incorporates a two-speed scroll compressor with two modulated hot gas valves on the compressor discharge that send hot gas through a third pipe to the indoor reheat heat exchanger during active dehumidification. A supply air temperature sensor provides the control signal used to proportionally modulate the flow of hot refrigerant gas to maintain a pre-set supply temperature during dedicated dehumidification. The indoor air handler unit contains a variable speed indoor fan. At the Air-Conditioning, Heating, and Refrigeration Institute (AHRI) rating conditions (AHRI, 2008), the cooling capacity is 7.60 kW and the A-Test EER (COP) is 3.82. In the heating mode at AHRI rating conditions, the unit has a heating capacity of 7.80 kW. The unit has a seasonal energy efficiency ratio (SEER) of 4.63 and a heating seasonal performance factor (HSPF Region IV) of 2.65.

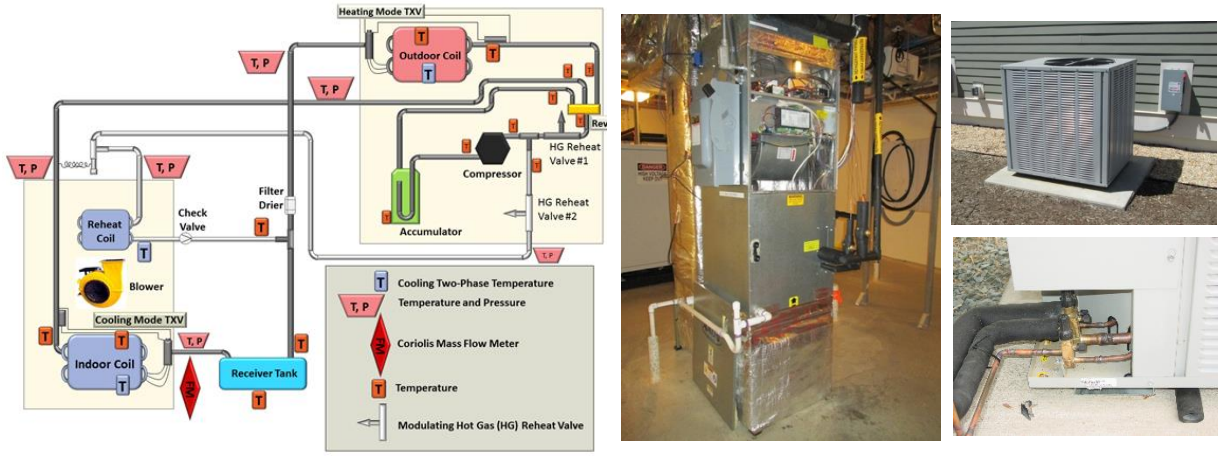

Fig. 49: Building Technology for the first operation year of the NZERTF: schematic (left), indoor unit (middle) and outdoor unit (right above) with reheat piping (right below)

5.2.1 Thermal and electric load profiles

In order to have reproducible use pattern for the equipment testing, artificial thermal load to emulate occupancy have been used in the NZERTF. Despite the very energy-efficient design of the HVAC systems, lighting and appliances, life-style of the occupants has been assumed similar to families living in a conventional house. Therefore, user profiles according to the U.S. Department of Energy Building America program were implemented, see Fig. 50 left. Based on survey data reported in Hendron and Engbrecht (2010), it was decided that the virtual family will consist of 2 adults, 1 child in middle school age (14) and 1 child in elementary school age (8). For every weekday, a daily schedule has been made based on working routine and school attendance of each family member, see Fig. 50, which is given in Appendix A.3.

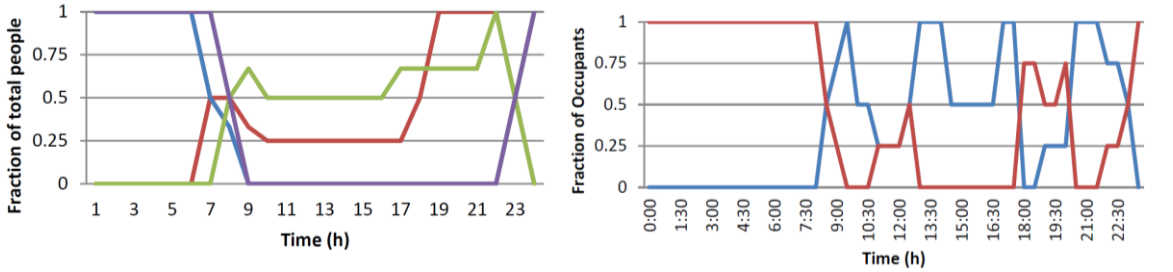

Fig. 50: Building America profile (left) and NZERTF occupancy profile for Saturdays (right)

Sensible and latent loads

Emulating human occupancy, like in NZERTF, requires accounting for the sensible and latent loads generated by the presence and activities of the occupants themselves. So, the sensible loads have been simulated by resistive heaters placed in the bedrooms, kitchen and living room areas. Each heater represents a member of the family of 70 W. The emulation of the latent heat of each person has been done according to Monteith (1972), respecting the occupants schedule and emulating a cooking schedule depending on the presence of the family by an ultrasonic humidifier shown in Fig. 51 left. The total daily moisture generation of each person is shown in Tab. 16.

Tab. 16: Total daily moisture generated by cooking events and the NZERTF occupants

Days	Daily Moisture from Cooking (liters/gallons)	Daily Moisture from People (liters/gallons)	Total Daily Moisture Cooking + People (liters/gallons)
Sunday	0.99 / 0.26	5.83 / 1.54	6.83 / 1.80
Monday	0.74 / 0.20	3.87 / 1.02	4.61 / 1.22
Tuesday	0.74 / 0.20	4.0 / 1.06	4.74 / 1.25
Wednesday	0.74 / 0.20	3.87 / 1.02	4.61 / 1.22
Thursday	0.74 / 0.20	4.0 / 1.06	4.74 / 1.25
Friday	0.74 / 0.20	3.87 / 1.02	4.61 / 1.22
Saturday	0.99 / 0.26	5.63 / 1.49	6.22 / 1.75

* The numbers are calculations used for target set-points and do not reflect the measurement accuracy

Fig. 51: Latent load generators (left) and sensible load generators (right) of the occupancy emulation installed in the NZERTF

Plug loads

All plug loads are automated according to a schedule. The mechanism to control all plug loads, except the cycle-based loads, have a start-time and an end-time. In time-based control, the data acquisition/controller unit start a load based on its start-time and turns it off when the end-time is reached, which ressembles a criteria-based controller, which, however, terminates with a reached criterion. For safety purposes, a timeout criterion is also applied to these loads, which terminates their use, if a certain elapsed time is reached. Plug loads, which are difficult or unsafe to automate, are emulated with resistive loads. All plug loads, including standby, that are rated less than 200 W are emulated with resistant heating boxes, and plug loads larger than 200 W are emulated with heating elements connected to a relay-box as depicted in Fig. 52.

Fig. 52: The heating elements for plug loads with larger than 200 W power requirement and their relay-boxes (left) and a relay-box, wiring diagram, and a toaster plugged into it (right)

5.3 Data acquisition

Sensors were installed throughout the facility to monitor the ambient conditions as well as the performance of each particular subsystem in the house. Fig. 53 left shows a schematic that describes the sensor system in the facility. The data acquisition system is installed in the garage to separate its heat load from the house, and three PVC conduits installed between the garage and the main house carry signal wire between the two locations. Two of the conduits terminate in the basement of the house, while the third terminates in the floor in the closet of Bedroom 2. Electrically-shielded flexible conduit installed within the walls during construction carry the signal extension wires to each room of the house. These extension wires carry four pairs of conductors to each location; some contain Type T thermocouple wires while others contain wire for other analogue signals. Thermocouple and analogue signal plug panels are installed in the walls of each room of the facility as shown in Fig. 53 right, and wires are routed to devices within the room through chases to minimize tripping hazards.
Separate instrumentation systems were installed to measure the performance of the PV system, the wind speed and direction on the roof, and the electrical usage within the house. These systems used RS-232 or RS-485 serial connections to communicate their data to the main data acquisition system.

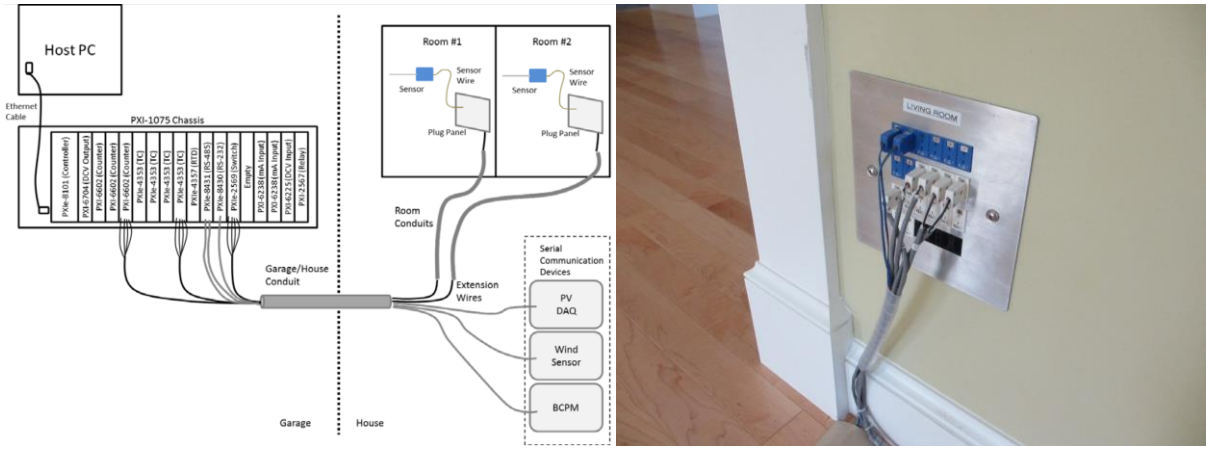

Fig. 53: General schematic of the whole house monitoring system (left) and typical room plug panel (right)

5.4 NZERTF electrical systems

The facility is equipped with two distinct electrical systems. One system consists of the circuits that would typically be in a home (“house circuits”) while the second set of circuits is used to power any instrumentation that would not typically be in a home (e.g., air sampling pumps used for short-term monitoring of indoor air quality). Each main circuit panel has a maximum current rating of 200 A, and each circuit within the panels is monitored. Receptacles using instrumentation power can be distinguished from the normal house circuits by the label “RP BB” on their faces.
The primary purpose of the electrical monitoring system is to determine whether the NZERTF ultimately produces more electricity than it consumes. It is also used to measure the electrical consumption of the various subsystems within the house and to control some occupant-driven loads, such as lights and the virtual occupants’ sensible heat.
The NZERTF’s electrical monitoring system measures electrical power and energy from two perspectives; the electricity imported into (or exported from) the house and the electricity as it is distributed throughout the house. These perspectives, of course, are interrelated. Namely, the electrical energy imported/exported depends on the relative quantities of the electricity generated by the photovoltaic system and the electricity consumed by the loads within the house.

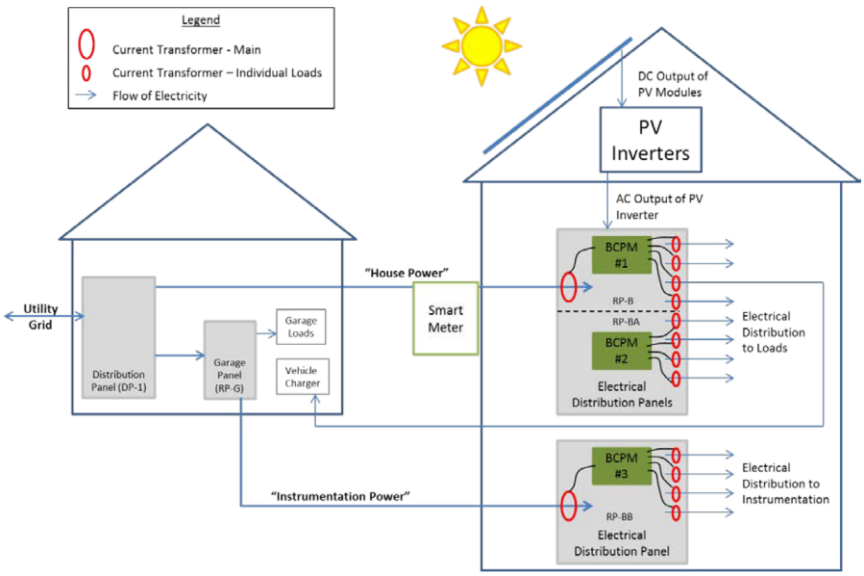

Fig. 54: NZERTF electrical monitoring system schematic

Physically, the electrical wiring for the site is divided into branches for House Power, Instrumentation Power, and Garage Power. Circuits on the House Power branch (electrical panels RP-B and RP-BA in the basement) are those that are typically found within a residence, such as appliances, lights, water heaters, TVs, etc. These are the circuits that will determine whether the house operates in a net-zero fashion.

The Garage Power branch (RP-G) feeds the equipment in the garage, such as the data acquisition equipment and the garage's heating and cooling system. The Instrumentation Power branch (panel RP-BB in the basement) is a subset of the Garage Power branch that is sent inside the house to power any instrumentation necessary to monitor the performance of the house or simulate activities of occupants. An electrical panel situated in the garage serves as the main distribution panel, with a single circuit from that panel feeding a separate electrical panel in the basement of the house (RP-BB). While this electricity is not counted against the net-zero energy tally for the house, the thermal load of the equipment powered on this branch must still be considered. While most of the equipment in the garage is powered by Garage Power, there are several receptacles in the garage that are fed from House Power. These are intended to provide electricity for a (future) vehicle charging station.

Tab. 17 demonstrate the expanded uncertainty of the daily energy totals for the generation, consumption, and imported electricity, and the exported electricity on a typical day, March 15, 2014. The latter value was calculated using a summation of the individual circuits as measured by the BCPM, the main line CTs on the BCPM, and the smart meter. As expected, the uncertainty for the summation of the BCPM circuits is considerably larger than the main line CTs and the smart meter. The agreement for the energy totals between the main line CTs and the smart meter is excellent, and the energy totals using the summation of circuits also matches the other two methods within the uncertainty bounds.

Tab. 17: NZERTF total energy and expanded uncertainty (k=2) of the generation (PV), consumption, imported electricity, and exported electricity for March 15, 2014

	BCPM - Individual Circuits				BCPM - Main CT			Smart Meter		
	Gen.	Cons.	Imp.	Exp.	Cons.	Imp.	Exp.	Cons.	Imp.	Exp.
Energy (kWh)	53.3	38.9	23.9	38.3	39.6	24.6	38.3	39.7	24.6	38.1
Uncert. (kWh)	0.54	0.75	0.53	0.76	0.44	0.29	0.39	0.40	0.25	0.38
Uncert. (%)	1.0	1.9	2.2	2.0	1.1	1.2	1.0	1.0	1.0	1.0

5.5 Payback period

The costs of NZERTF are with $656,398 about 33% higher than the costs of a conventional building (ca. $493,712). The annual energy cost savings is estimated to be $4,526. With the simple buy back approach, the buyback time will be 36 years. With a 30-year-fixed-rate mortgage (most common financing option for a new home purchase) it will take another 29 years after the 30 year mortgage for the savings to offset the costs (calculated with a 20 % down payment).

5.5.1 Life-cycle cost analysis

If the home is financed with a 30-year fixed-rate mortgage with a 20% down payment at 4.375 %, the additional monthly mortgage payment is $650 or $7,800 annually. This means, the extra annual mortgage costs are 72% higher than the energy cost savings of $4,526.
The life-cycle cost methodology, as defined in ASTM Standard Practice E917 (2010), considers all costs related to the house over the selected study period, whether it is construction costs, operating costs, or resale value at the end of the study period. In order to simplify the analysis, initially assume that the homeowner remains in their home or assumes there is no home price appreciation, the higher performing building design will not fetch a higher resale price relative to the Maryland code-compliant design (no resale value), and the maintenance, repair, and replacement costs are comparable between the two building designs. Fig. 55 shows the life-cycle cost analysis for 8 study periods from 1 year to 100 years. For a study period 5 years or less, the homeowner realises net savings in present value life-cycle costs, because the upfront financial incentives are enough to offset the higher down payment and future monthly costs (mortgage payments and energy bill) for the first 5 years. However, by the end of year 6 the homeowner realises net costs, which continue to increase until the mortgage is paid in full after 30 years. At which time the energy cost savings lowers present value net costs until net cost savings is realised in about Year 85. Based on these results, it is better for the homeowner to buy the net zero energy home if the homeowner expects to move sometime in the first 5 years, but is not cost-effective for any longer study periods. In the worst case (30 years study period), the additional present value costs are equivalent to a mark-up of 7.0 % relative to the Maryland code compliant design to get a net zero energy, LEED platinum certified, high-performance house. Fig. 55 shows the net costs to a homeowner exclusively the resale value of the home.

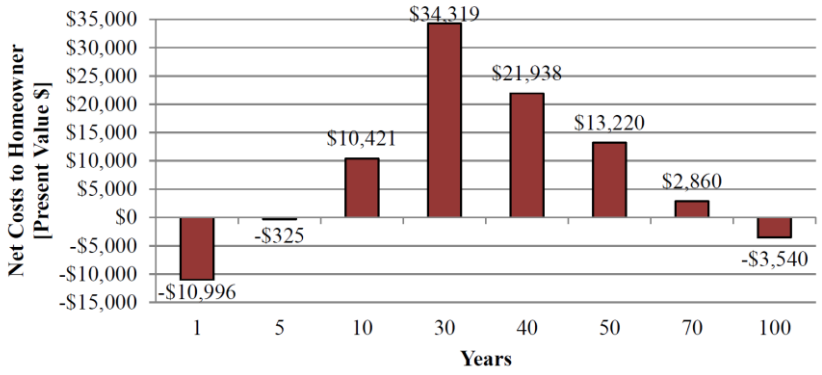

Fig. 55: Net costs to homeowner by study period (no resale value)

Also possible is to take the resale value into account. Fig. 56 shows the cost analysis inclusively the resale value across 8 study periods from 1 year to 100 years. Once the residual value has been included in the life-cycle cost analysis, the net zero energy home becomes more cost-effective over all of the study periods relative to the life-cycle costs without residual value shown in Fig. 55. The homeowner realizes present value net cost savings for both residual value approaches for a 1-year, 5-year, 10-year, and 20-year study period, which includes 56 % of all home ownerships. Using the market approach, the homeowner realises present value costs of $775 over a 25 year study period while the LCC residual value approach leads to net cost savings of $11,230.

The homeowner realises net present value costs for Year 30, Year 40, and Year 50, because the decrease in the discounted value of the residual value is greater than the present value of the energy cost savings.
Although, it is important to note that the net present value costs for either approach across those 3 study periods range from $879 to $9,411, which is equivalent to a 0.2 % to 1.9 % mark-up of the cost of the Maryland code-compliant home ($493,712). So, in the worst case scenario, the homeowner is paying the equivalent of a 2 % mark-up for a net zero energy, LEED platinum certified, high-performance home.

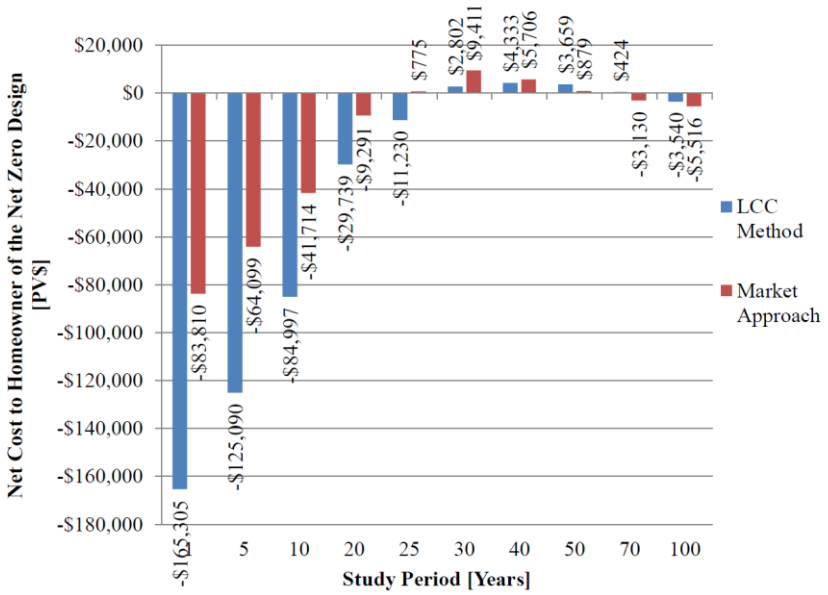

Fig. 56: Net costs to homeowner by study period (including resale value)

5.6 Experiences with the NZERTF

5.6.1 Whole house energy performance summary

The ASHP system was used to provide the space heating/cooling during the first demonstration year. The ground-coupled heat exchangers, high-velocity air distribution system, and basement radiant floor heating system were not utilised. The house was operated as a single zone with constant thermostat set points of 23.8 °C and 21.1 °C during the cooling and heating seasons, respectively. Only two of the four solar thermal collectors in conjunction with the 303 l storage tank were utilised for water heating. The lights, appliances, plug loads, and sensible and latent loads associated with the virtual occupants were operated in accordance with the previously defined schedules. Selected results are presented in units of energy [kWh] and energy per unit floor area [kWh/m^2] of the conditioned space, 387 m^2, which includes the living area (252 m^2) and the basement (135 m^2).

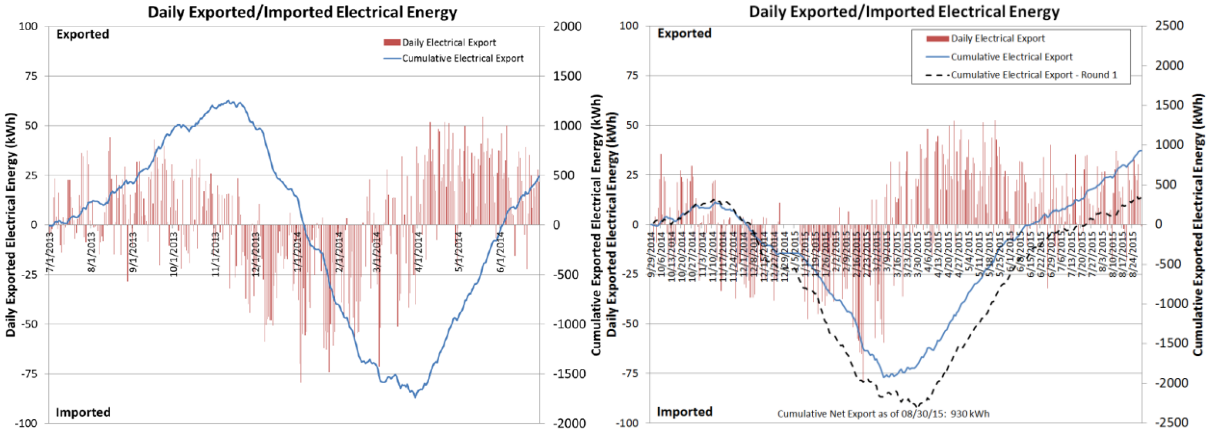

Fig. 57: Electrical energy balance for the first year (Year 1, left) and the second year (Year 2, right)

Fig. 57 left shows the daily and cumulative net electricity use for the first year of operation. A positive value indicates that the house produced more energy than it consumed and represents the quantity of energy exported to the grid.
A negative value indicates that the house imported energy from the grid to meet the energy usage over the 24-hour period. For the 12 months (July 2013-June 2014) the house produced 484 kWh more electrical energy than it consumed.
The energy consumption by end use is tabulated in Tab. A 12 in the Appendix A.5 and displayed graphically in the stacked bar chart in Fig. 58.

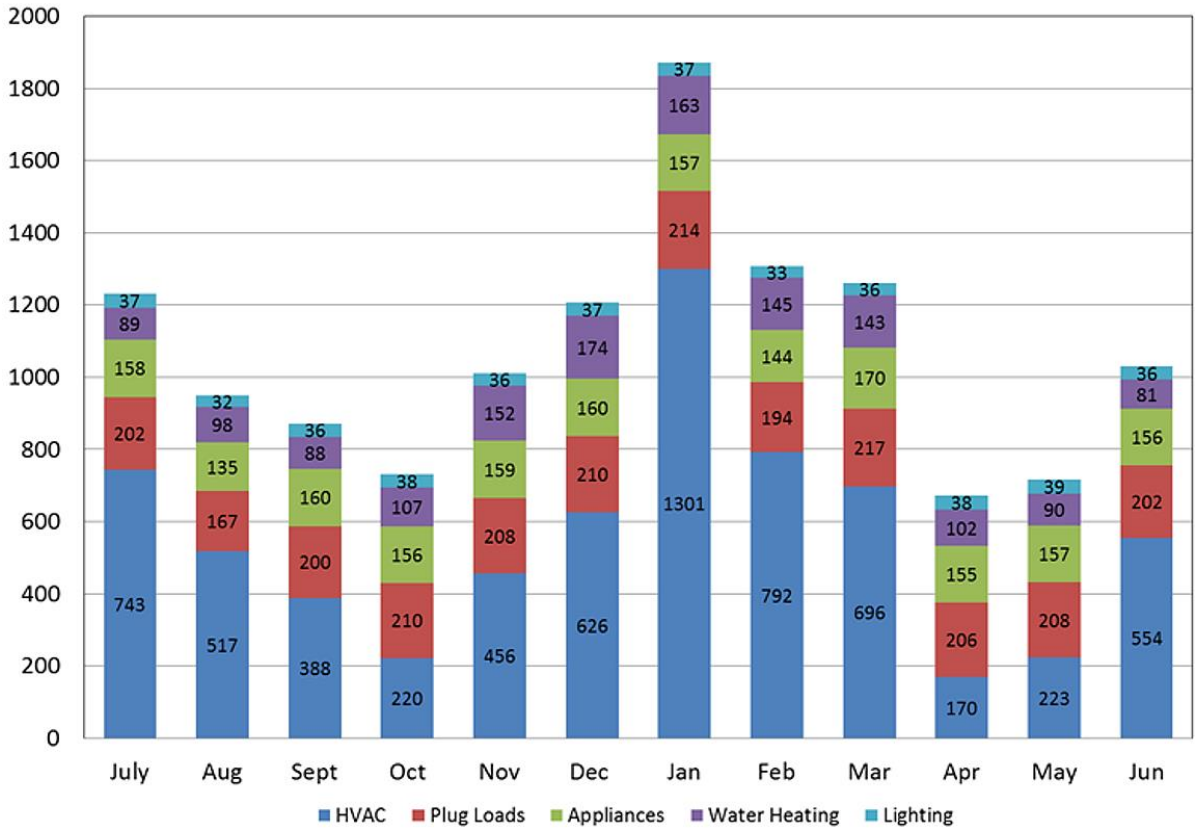

Fig. 58: Energy consumption by end use for the first year of operation

The top five energy end uses for the twelve month interval are:

1) space conditioning (6685 kWh; 17.3 kWh/m^2),
2) plug loads (2440 kWh),
3) appliances (1868 kWh),
4) energy associated with producing hot water (sum of heat pump water heater and the solar thermal circulating pumps) (1432 kWh), and
5) lighting (435 kWh).

The space conditioning energy consumption includes 514 kWh of energy consumed by the heat recovery ventilation (HRV).
The energy usage by each individual appliance is shown in Fig. 59, with the clothes dryer consuming the greatest amount in this category.
The solar photovoltaic (PV) system and associated inverters experienced no malfunctions over the yearlong period converting 16.8 % of the incident solar irradiance into AC electrical energy. As expected, the conversion efficiency of the PV array increases as the average cell temperature decreases, Tab. A 13 in the Appendix A.5. The conversion efficiencies for December, January, February, and March were lower than expected as a result of the 8, 8, 12, and 10 days, respectively, when all or part of the solar array was covered with snow and/or ice for all or part of the daylight period. For all of the winter snow events, the reference cell plane of the array irradiance detector cleared well in advance of the PV array. The monthly conversion efficiencies, from direct to alternating current, of the PV system inverters all exceeded 94.5 %.

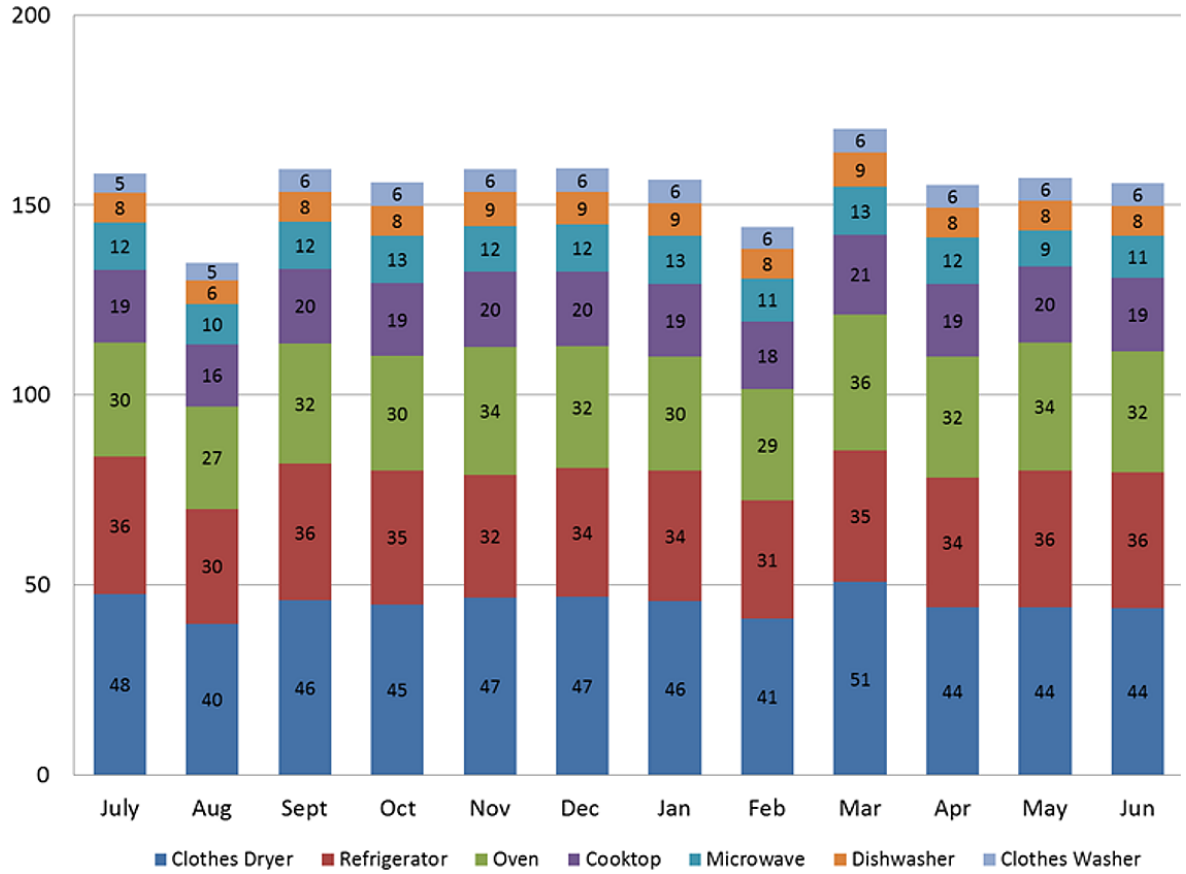

Fig. 59: Energy consumption by appliances

The solar thermal hot water system provided 54% of the energy required to meet the domestic hot water load over the twelve month interval. The solar thermal collectors were totally or partially covered with snow and/or ice during the same time intervals as the photovoltaic array. The two circulating pumps consumed 320 kWh/a.
The solar hot water system malfunctioned for a total of 11 days in late August and early September as a result of an electrical fault in the glycol-circulating pump. The auxiliary heat pump water heater unit malfunctioned for 9 days in November and operated exclusively in the electric resistive mode as a result of a control wire becoming dislodged. Of the total energy consumed by the heat pump water heater unit, 975 kWh (88%) was consumed by the heat pump and controls and 137 kWh (12%) by the auxiliary resistive heating element.

5.6.2 Heat pump energy performance summary

When operated in the cooling mode, the unit operated with a seasonal COP (total thermal load/total electricity consumed) of 3.19 compared to the rated value of 3.82. There are two primary reasons that the measured seasonal cooling COP was less than the rated seasonal cooling COP. The seasonal cooling standby energy was 5.2% of the total heat pump energy consumed and is not taken into account in the rating procedure used to determine rated seasonal cooling COP. The second contributor is the fact that when the heat pump operated in the dedicated dehumidification mode, the COP is significantly less than when operating in its normal mode, as seen in Tab. A 14 in the Appendix A.5. For example, in August 2013 the heat pump operated in the dedicated dehumidification mode approximately 41% of the time during which the measured COP was 0.89. The current rating procedure does not address the degradation in performance that may occur when a heat pump unit operates in a dedicated dehumidification mode during a portion of the cooling season.
In the heating mode, the measured seasonal COP was 2.06 compared to the rated seasonal COP value of 2.65. The seasonal heating standby energy was 3.5% and is not considered in the rating procedure used to determine seasonal heating efficiency.

The resistive heat is energized whenever the heat pump unit is in the defrost mode. The testing/rating procedure does not include the impact of resistive heat during the defrost cycle. The thermostat heating configuration allows the user to prescribe a 1st stage differential, 2nd stage differential, 2nd stage delay time, and 3rd stage differential. The differential temperature is relative to the current set point temperature and the delay time is the maximum amount of time a given stage is allowed to operate before energizing the next higher stage. The cooling and heating mode differentials and delays were selected to maintain comfortable conditions throughout the year and minimize the use of resistive heat during the heating season. In the heating mode, 40 minutes was the maximum time the thermostat would permit the heat pump's compressor to operate in its high speed mode before energising the electric resistance heat. This type of control logic appears to be effective in the cooling mode, but produced unnecessary usage of electric resistance heat in the heating mode.
During the seven months that cooling was required, the sensible to total load ratio varied from 0.58 to 0.78. Currently most high efficiency heat pump systems operate with a sensible to total load ratio of greater than 80 %. The higher latent loads associated with low energy homes will benefit from new technologies and control strategies that better address moisture removal. In the NZERTF enhanced moisture removal was made possible through the use of a heat pump that incorporated a dedicated dehumidification mode.
An analysis was performed to quantify the energy usage associated with the heat pump operation due to additional thermal loads introduced by the heat recovery ventilation (HRV). The HRV has two energy impacts, the fan energy and the increase or decrease in the thermal load resulting from introducing outdoor air into the house. For example, when the outdoor air temperature is lower than the indoor air temperature additional energy will be required to heat the home during the heating season compared to an identical home without an outdoor air ventilation system. During the cooling season, the introduction of outdoor air may increase or decrease the sensible and latent loads, dependent on the outdoor air temperature and moisture content relative to the indoor temperature and relative humidity. Nevertheless, the heat recovery capabilities of the HRV resulted in the provision of reliable ventilation rates with the fan energy required being largely compensated by the energy recovered. During the one-year period, the HRV consumed a total of 514 kWh in fan energy, as shown in Tab. A 12 in the Appendix A.5. It is assumed the fan power required for the balanced ventilation system without an HRV would be equivalent to the ventilation system utilising a HRV. Tab. A 15 in the Appendix A.5 captures the energy impact of the HRV and ventilating to the same degree using a balanced ventilation system without a HRV. The Appendix A.5 give further details on the operation of the building technologies.

5.6.3 Indoor air quality and comfort

Charcoal test kits were deployed to measure indoor radon concentrations in the house following the EPA Protocols for Radon and Radon Decay Product Measurements in Homes (EPA, 1993). These measurements were made in the basement, first floor, and second floor. The average of all samples is below the EPA action level of 4 pCi/L (EPA, 1993).
The building materials for the NZERTF were specified to have low emissions of volatile organic compounds (VOCs), including a prohibition on products with any added formaldehyde. Indoor air samples have been collected to measure the levels of approximately two dozen individual VOCs and formaldehyde in order to determine the impact of the building material specifications. These samples are collected monthly and will be used to determine if the VOC emission rates for the house change over time. Measurements reported in Poppendieck et al. (2014) show that the use of medium density fiberboard and particleboard with no-added formaldehyde resins for cabinetry and other finished products effectively controlled the formaldehyde emissions and kept concentrations below levels in typical new homes. Monitoring of seasonal indoor VOC concentrations in Poppendieck et al. (2014) suggests that building envelope components may be a source for some VOCs, especially aldehydes and alkanes.
Indoor dry bulb temperature, globe temperature, and relative humidity sensors are installed in the kitchen (on top of the counter), living room, master bedroom, bedroom 2, and bedroom 3 and readings are used to calculate thermal comfort parameters.

Indoor dry-bulb temperature only is also measured in the attic, basement, bathrooms, office, dining room, and the entryway, but thermal comfort performance is not determined for these spaces. All measurements are recorded every 1 min.
In order to evaluate thermal comfort in selected rooms, the indoor dry-bulb temperature (T_{in}), globe temperature (T_{globe}), and relative humidity (RH) are measured.
The globe temperature accounts for radiative heat transfer with interior building surfaces, as this is a primary determinant of thermal comfort. The globe temperature measurements require a correction based on the room air speed. The air speed was measured in selected rooms with a hot wire anemometer with the ventilation heat recovery and central air handling unit fan ON to determine this correction. It was assumed that the air speed would remain essentially constant given that the house is unoccupied and access to the house by researchers and visitors is limited. In the rooms where thermal comfort is to be evaluated, the air speed was consistently less than 0.1 m/s. The operative temperature was calculated using Equation 4.5 (Markus and Morris, 1980)

$$T_{globe} = T_{in} + f_g\,(T_{mrt} - T_{in}) \tag{4.5}$$

where f_g is a factor based on globe size and air velocity, and T_{mrt} is the mean radiant temperature. Given that the air velocity was < 0.1 m/s and the globe size is 40 mm, f_g from Markus and Morris (1980) is 0.48.
Equation 4.5 is used to calculate T_{mrt} from the measured T_{globe}. Since these equations are valid for conditions when air movement is less than 0.1 m/s, they are valid both when the air handler fan is running and when it is off.
To evaluate the thermal comfort conditions, the operative temperature (T_{op}) is calculated as follows. From ASHRAE Fundamentals (ASHRAE, 2013), T_{op} is the average of T_{in} and T_{mrt} when the air velocity is < 0.4 m/s and T_{op} < 50 °C.

$$T_{op} = T_{in} + (T_{globe} - T_{in}) / (2f_g) \tag{4.6}$$

Temperature and humidity measurements are used to evaluate thermal comfort using two parameters: the predicted mean vote (PMV) and the predicted percentage of dissatisfied (PPD) (ASHRAE, 2010). Values of PMV between -0.5 and +0.5 and PPD < 10% are considered "comfortable." In the summer, the occupants are assumed to be clothed between 0.36 clo (walking shorts, T-shirt) and 0.57 clo (short-sleeve shirt, trousers), where "clo" is the clothing insulation level. In the winter, the occupants are assumed to be clothed between 0.61 clo (long-sleeve shirt, trousers) and 1.14 clo (suit jacket, vest, long-sleeve shirt, trousers). It was assumed that the activity level of the occupants ranged between 0.7 met (sleeping) and 1.7 met (walking around), where "met" is the metabolic rate (ASHRAE, 2010). Fig. 60 show the results as average monthly values of the two comfort measures.

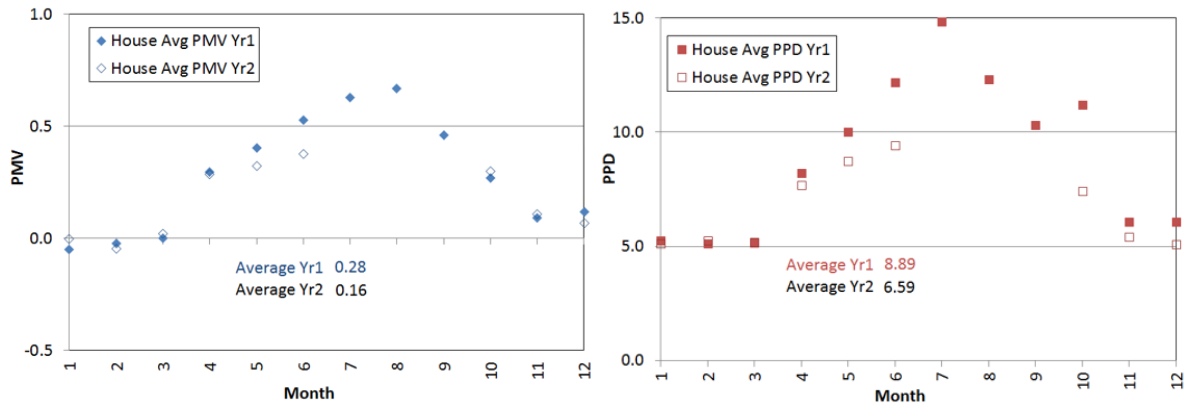

Fig. 60: Thermal comfort evaluation as PMV (left) and PPD (right)

5.6.4 Conclusions

During the first year of operation the residence generated 13,523 kWh of electricity using the 10.2 kW_p solar photovoltaic system. The house consumed 13,039 kWh (33.7 kWh/(m²a)) of electrical site energy while meeting the electrical and comfort needs of a typical U.S. four member family, resulting in a net energy export of 484 kWh.

The solar photovoltaic system converted 16.8% of the incident solar radiation into useful AC electrical energy. The solar thermal hot water system provided 54% of the energy required to meet the domestic hot water load.

The greatest end use of electricity within the residence was for space conditioning, followed by plug loads, and appliances. Ventilating the house to exceed the ASHRAE Standard 62.2-2010 requirement using an heat recovery ventilation (HRV) resulted in 1,965 kWh (5.1 kWh/(m²a)) of energy consumption: 514 kWh to power the HRV fan and an additional 1,451 kWh (3.7 kWh/(m²a)) of energy being used by the heat pump to meet the additional sensible and latent loads. This represents 31.8% of the energy consumed by the heat pump, 15.0% of the total energy consumed by the house, and 14.5% of the energy generated by the photovoltaic system. If the HRV had provided the exact flow rate specified by ASHRAE Standard 62.2-2010 requirement, 137 m³/h versus the measured flow rate of 171 m³/h, and assuming identical fan power in both cases, it is estimated that the total energy impact of the HRV would have been 1,676 kWh (4.3 kWh/(m²a)) or 12.8% of the house's total annual energy consumption.

Among the lessons learned during this one year study was the significant impact that snow and/or ice can have on the output of a photovoltaic system attached to an extremely well-insulated roof. Significant periods of time were needed for the snow/ice cover to melt as a result of the well-insulated roof assembly. It was also observed that a simple control device, such as the heat pump's thermostat, can have a significant impact on the energy needed during the heating season. Despite these challenges, it was shown that net zero can be achieved for a home slightly larger than the average size currently being constructed in the U.S. with all the amenities and features of a modern home.

5.6.5 Further research

The NZERTF has a vast array of features and capabilities that will be utilised in the future. Over 200 future research and development opportunities suggested by 22 organizations are summarized in Domich et. al. (2015). Recommended "research and development opportunities" within this document range from practical tests for assessing the airtightness of building enclosures to dynamic control of the heating, cooling, and ventilation systems taking full advantage of emerging "smart grid" capabilities.

The third year of testing will focus more on indoor environmental quality (IEQ); we will measure temperature and humidity distributions within the space hourly (or more), plus, we will add a small duct, high velocity (SDHV), variable-speed compressor, variable-speed indoor blower heat pump system. A 11 kW cooling capacity, variable-speed, SDHV air-source heat pump has been selected to operate with the existing "big duct" system in a one-day-ON, one-day-OFF alternating scheme. It is hoped that this type of side-by-side comparison under almost identical weather conditions and indoor loads will provide the best comparison. We will measure the instantaneous cooling/heating capacity and COP in addition to the added IEQ measurements mentioned above.

6 Conclusions

In Task 3 of the IEA HPT Annex 40, technology developments for heat pumps in nZEB have been performed. Due to the normally highly efficient building envelopes of nZEB the loads of the building are different from conventional buildings. While the space heating operation may decrease, and additional cooling need due to the risk of summerly overheating may arise. On the other hand, the DHW normally has a larger share of the overall heating needs due to decreasing heating demands. Based on this load situation, heat pumps have advantages to supply different building services even in simultaneous operation with efficiency gains.
Therefore, developments performed under the Annex 40 concentrated on two aspects:

- On the one hand the ability of heat pumps to provide different building services with the same generator led to the development of integrated multifunctional heat pumps. Due to the high integration higher investment in highly efficient components can be justified. Moreover, the integration of dehumidification by separation of latent and sensible load can significantly improve the performance.
- On the other hand, installation of renewable energy on-site offers options to integrate these components with the heat pump, e.g. a solar thermal system could be operated directly for the DHW production, but could also serve as heat source for the heat pump. Especially the integration by a source storage, eventually as ice storage, can be beneficial both for the collector efficiency and as stable heat source of the heat pump.

In the USA the development of integrated heat pumps (IHP) has already begun in 2005 with a conceptional analysis. In the frame of the Annex 40 variants of IHP have been developed and field monitoring has been accomplished. Besides an electric system, which is well suited also for retrofitting, a gas engine driven system with on-board power generation in a beta-prototype has been developed. Performance results of the systems confirm the target value of 50% savings vs. the baseline systems.
In Canada and Switzerland, the integration of solar collectors as heat source for the heat pump has been investigated. Both components and systems, respectively, have been investigated by lab-testing which gave the data basis to model and validate the components. As next step the models have been implemented in a system simulation environment and saving potentials were evaluated, resulting in similar performance values as ground-source heat pumps for the respective boundary conditions. Thus, the integration of heat pump and solar components may hold further development potentials for the application in nZEB, where on-site renewable generation may be installed as a standard system.
Furthermore, in Japan, an optimisation of the air-conditioning operation with VRF systems could be achieve by separating sensible and latent loads. With a dessicant system which was optimised for low regeneration temperatures, temperature for the sensible load could be increased, i.e. pressure difference decreased. The two steps together led to substantial energy saving, which were evaluated to more than 70% compared to conventional operation, which is a big step for the air-conditioning especially in regions with high dehumidification load.
Last but not least the Net Zero Energy Residential Testing Facility (NZERTF) at the NIST campus has been equipped and commissioned in the frame of the Annex 40. The NZERTF has the capability to provide tunable and reproducible load conditions of a typical nZEB as test environment of dedicated NZEB technologies. The first two years of operation have shown a slight positive balance of the test house itself, so the NZEB target could be confirmed. In the first year, the house was operated with an air-to-air heat pump.
The development show that even though heat pumps are already a very energy-efficient technology further development potentials by systems integration and the optimisation of temperature conditions for different applications as well as the integration with other building technology may still yield further efficiency gains.

7 Acknowledgements

IEA HPT Annex 40 is a co-operative research project on heat pump application in nearly Zero Energy Buildings in the framework of the Heat Pumping Technologies (HPT) Technology Collaboration Programme (TCP) of the International Energy Agency (IEA). This report is based on the contributions of all participants in the Annex 40 and the constructive and co-operative discussions during the project as well as the contributed results are highly appreciated.

The support and funding of the IEA HPT Annex 40 by the Swiss Federal Office of Energy (SFOE) is highly appreciated and gratitude is expressed to the programme manager of the SFOE heat pump research Stephan Renz for advice and support in the IEA HPT Annex 40 and the Swiss national contributions.

Abbreviations

AHRI ..... *Air-Conditioning, Heating, and Refrigeration Institute*
ASHP ..... *Air-Source Heat Pump*
BIPV/T ..... *Building Integrated Photovoltaic-Thermal*
BTO ..... *Building Technology Office*
CAD ..... *Computer Aided Design*
COP ..... *Coefficient of Performance*
DH ..... *Dehumidification*, *Dedicated DeHumidification*
DHW ..... *Domestic Hot Water*
DOE ..... *Department of Energy*
DS ..... *Desuperheating*
e.g. ..... *exempli gratia*
EER ..... *Energy Efficiency Ratio*
EEV ..... *Electronic Expansion Valve*
EF ..... *Energy Factor*
ERA ..... *Energy reference Area*
ERL ..... *Energy Research Lab*
EWT ..... *Entering water temperature*
FC ..... *Full condensation*
FY ..... *Fiscal year*
GHG ..... *Greenhouse Gases*
GHP ..... *Gas Engine Driven Heat Pump*
GHX ..... *Ground Heat Exchanger*
GSHP ..... *Ground-Source Heat Pump*
GSHPwDS ..... *Ground-Source Heat Pump with Desuperheating*
HDE ..... *Hybrid Desica Element*
HDPE ..... *High density polyethylene*
HEX ..... *Heat Exchanger*
HP ..... *Heat Pump*
HPDM ..... *Heat Pump Design Model*
HPT ..... *Heat Pump Technologies*
HPWH ..... *Heat pump water heater*
HR ..... *Heat Recovery*
HRV ..... *Heat Recovery Ventilation*, *Heat Recovery Ventilator*
HVAC ..... *Heating Ventilation and Air Conditioning*
HX ..... *Heat Exchanger*
IEA ..... *International Energy Agency*
LCC ..... *Life Cycle Cost*
LEED ..... *Leadership in Energy and Environmental Design*
LPG ..... *Liquified Petroleum Gas*
MRT ..... *Mean Radiant Temperature*
NIST ..... *National Institute of Standards and Technology*
NRCan ..... *National Research Council Canada*
nZEB ..... *nearly Zero Energy Building*
NZEB ..... *Net Zero Energy Building*
NZERTF ..... *Net Zero Energy Residential Test Facility*
NZR ..... *Net-Zero Ready*
OAT ..... *Outside Air Temperature*
OT ..... *Operative Temperature*
PMV ..... *Predicted Mean Vote*
PPD ..... *Predicted Percentage of Dissatisfied*
PV ..... *Photovoltaics*
RH ..... *Relative humidity*

SC ..... *Space Cooling*
SDHV ..... *small duct, high velocity*
SH ..... *Space Heating*
SPF ..... *Seasonal Performance Factor*
ST ..... *Solar Thermal*
T/H ..... *TRNSYS-HPDM*
TABS ..... *Thermally activated building system*
THIC ..... *Temperature and Humidity Individual Control*
VRF ..... *Variable Refrigerant Flow*
VS ..... *Variable Speed*
WH ..... *Water Heating*

Literature

AHRI. 2008. *Standard for Performance Rating of Unitary Air-Conditioning & Air-Source Heat Pump Equipment.* AHRI 210/240. Arlington, VA: Air-Conditioning, Heating, and Refrigeration Institute, Arlington, US

ASHRAE. 2013. *ASHRAE Handbook – Fundamentals*, American Society of Heating, Refrigerating and Air-Conditioning Engineers Inc, Atlanta, US

ASHRAE. 2010. *ASHRAE Standard 55-2010: Thermal Environmental Conditions for Human Occupancy*, American Society of Heating, Refrigerating and Air-Conditioning Engineers Inc, Atlanta, US

ASHRAE. 2005. *Handbook of Fundamentals*. American Society of Heating, Refrigeration and Air-conditioning Engineers Inc, Atlanta, US

ASTM Standard E917-05. 2010. *Measuring Life-Cycle Costs of Buildings and Building Systems*, Annual Book of ASTM Standards, ASTM International, West Conshohocken, PA, 2012, pp. 277-295, US

Baxter, V. D., Rice, C. K., Murphy, R. W., Munk, J. D. M., Ally, M. R., Shen, B., Craddick, W. G., Hern, S. A. 2013. *Ground-Source Integrated Heat Pump (GS-IHP) Development,* ORNL CRADA Final Report NFE-07-01000. May 2013, US

Candanedo, J., Minea, V., Athienitis, A. K. 2008*. Low-energy houses in Canada: national initiatives and achievements*. IEA HPP Annex 32 Workshop, 9th IEA HP Conference Zurich, May 19, 2008, CA

Dobos, Aron P. 2013. *PVWatts Version 1 Technical Reference*, National Renewable Energy Laboratory, Technical Report NREL/TP-6A20-60272, October. 2013, US
URL: http://rredc.nrel.gov/solar/calculators/PVWATTS/version1

Doiron, M., O'Brien, W., Athienitis, A. K. 2011. *Energy Performance, Comfort, and Lessons Learned from a Near Zero Energy Solar House*. ASHRAE Transactions 117(2):585-596, CA

DOE, U.S. Government. 2010. *Uniform Test Methods for Measuring the Energy Consumption of Water Heaters*, Code of Federal Regulations, Title 10, Chapter II, Volume 3, Part 430, Subpart B, Appendix E, US

Domich, P.D., Pettit, B., Fanney, A.H., Healy, W.M., *Research and Development Opportunities for the NIST Net zero Energy Residential Test Facility*, NIST Technical Note 1869 (2015), Accessed Sep-8-2015, http://dx.doi.org/10.6028/NIST.TN.1869, US

EPA. 1993. *Protocols for radon and radon decay product measurements in homes*, U. S. Environmental Protection Agency, Washington D. C.,
http://www.epa.gov/radon/pdfs/homes_protocols.pdf. accessed Aug-14-2015, US

EN 12975:2011. 2011*. Thermal solar systems and components - Solar collectors - Part 1: General requirements*, German version EN 12975-1:2006+A1:2010, EU

Hendron, R. 2008. *Building America Research Benchmark Definition Updated December 19, 2008*. National Renewable Energy Laboratory, US

Hendron, R., Engbrecht, C. 2010. *Building America House Simulation Protocols.* NREL report: TP-550-49426, October 2010, US

Intellichoice Energy. 2014. *Black (Dark) Start Cooling, Heating and Power Generation Demonstration Test on Military Installations Performance and Reliability Report*. Report to U. S. Department of Defense Construction Engineering Research Laboratory. October 2014, US

Kegel, M., Sunye, R., Tamasauskas, J. 2012. *Lifecycle Cost Comparison and Optimisation of Different Heat Pump Systems in the Canadian Climate*. Proceedings of eSim 2012, Halifax, CA.

Klein, S.A. 2010. *TRNSYS 17 – A TRaNsient SYstem Simulation program*. Madison, WI: University of Wisconsin-Madison Solar Energy Laboratory, US

Lennox Industries Inc. 2013a. *SunSource® Home Energy System Product Specifications*, Publication #210664, Sept. US:

Lennox Industries Inc. 2013b. *SunSource® Home Energy System Application and Design Guidelines*, Publication #CORP1312-L2, July 2013, US

Mahderekal, I., Shen, B., Vineyard, E. A. 2012. *System Modeling of Gas Engine Heat Pump*, paper, # 2179 in Proceedings of 2012 International Refrigeration and Air-Conditioning Conference at Purdue, July 16-19, West Lafayette, US

Mahderekal, I., 2015. *Personal communication to Van Baxter*, October 27, 2015, US

Markus, T. A., Morris, E. N. 1980. *Buildings, Climate, and Energy*. Pitman Pub, US

Minea, V., Chen, Y. X., Brendan O., Candanedo, J. 2009. *Economical heating and cooling systems for low energy houses – System assessment and field monitoring,* Canada final report Task 2 & Task 3 of Annex 32, Heat Pump Programme, International Energy Agency, CA

Minea, V. 2013. *Efficient heating and cooling systems for low-energy houses*, Journal of Green Building, Volume 7, Number 4: 16-35, CA

Monteith J. L. 1972. *Latent Heat of Vaporization in Thermal Physiology*. Nature: New biology, vol. 236, no. 64, p. 96, 22-Mar-1972, US

Munk, J. D., Ally, M. R., Baxter, V. D., Gehl, A. 2014. *Measured Space Conditioning and Water Heating Performance of a Ground-Source Integrated Heat Pump in a Residential Application.* Proceedings of the 11th IEA Heat Pump Conference 2014, May 12-16 2014, Montréal, CA.

Murphy, R.W., Baxter, V.D., Rice, C. K., Craddick, W.G. 2007a. *Air-Source Integrated Heat Pump for Near Zero Energy Houses: Technology Status Report*. ORNL/TM-2007/112, July, US

Murphy, R.W., Baxter, V.D., Rice, C. K., Craddick, W.G. 2007b. *Ground-Source Integrated Heat Pump for Near Zero Energy Houses: Technology Status Report*. ORNL/TM-2007/177, December, US

Natural Resources Canada (NRCAN). 2010. *Office of Energy Efficiency*.
URL: http://oee.nrcan.gc.ca/, CA

Orvik, E.B. 2014. *Analysis of the Heating and Cooling System Including Heat Pumps and Chillers at Miljøhuset GK, Oslo.* Project Thesis at the Norwegian University of Science and Technology (NTNU), Dept. of Energy and Process Engineering. EPT-P-2014-25, NO

Orvik, E.B. 2014: *Analysis of the Heating and Cooling System at Miljøhuset GK.* Master Thesis at the Norwegian University of Science and Technology (NTNU), Dept. of Energy and Process Engineering. EPT-M-2014-4, NO

Poppendieck D., Ng L., Schlegel M., Persily A., Hodgson A. 2014. *Long term air quality monitoring in a net zero energy residential test facility designed with specifications for low emitting interior products*, Indoor Air 2014, Hong Kong, US

Rice, C. K., Shen. B., Baxter, V.D., Shrestha, S.A., Uselton, R.B. 2014b. *Development of an Air-Source Heat Pump Integrated with a Water Heating / Dehumidification Module*. Proceedings of the 11th IEA Heat Pump Conference 2014, May 12-16 2014, Montréal (Québec), US

Rice, C. K., Shen, B., Munk, J.D., Ally, M.R., Baxter, V. D. 2014a. *Development of a Variable-Speed Residential Air-Source Integrated Heat Pump*, Proceedings of the 11th IEA Heat Pump Conference 2014, May 12-16 2014, Montréal (Québec), US

Rice, C. K., Baxter, V. D., Hern, S. A., McDowell, T., Munk, J. D., Shen, B. 2013. *Development of a Residential Ground-Source Integrated Heat Pump.* Conference Papers CD for 2013 ASHRAE Semi-Annual Meeting in Dallas, US

Rice, C. K., Jackson, W.L. 2005. DOE/ORNL Heat Pump Design Model on the Web, Mark VII Version. URL: http://www.ornl.gov/~wlj/hpdm/MarkVII.shtml, US

Rice, C. K. 1991. *The ORNL Modulating Heat Pump Design Tool - Mark IV User's Guide*, ORNL/CON-343, US

SIA 2024. 2006. *Standardnutzungsbedingungen für die Energie- und Gebäudetechnik*, Swiss Society of Engineers and Architects, Zurich, CH

SIA 2028. 2010. *Klimadaten für Bauphysik, Energie- und Gebäudetechnik*, Swiss Society of Engineers and Architects, Zurich, CH

SWG. 2014. *PERC III - Residential natural gas heat pump (RGHP) Research & Development Program*. Project report to the Propane Education and Research Council (PERC). Southwest Gas Corporation, December 2014, US

Statistics Canada. 2013. *Energy Use Statistics*. URL: http://www.statcan.gc.ca/pub/11-526-s/2010001/partpartie1-eng.htm, 2011, CA
[Modified 2013; Accessed September 2015]

Tamasauskas, J., Poirier, M., Zmeureanu, R., Sunye, R. 2012a. *Modeling and optimisation of a solar assisted heat pump using ice slurry as a latent storage material*, Solar Energy 86(11):3316-3325, CA

Tamasauskas, J., Poirier, M., Zmeureanu, R., Sunye, R. 2012b. *Development of a mathematical model for the simulation of a non-agitated ice slurry storage tank*. Proceedings of eSim 2012, Halifax, CA.

Tamasauskas, J., Poirier, M., Kegel, M., Sunye, R. 2015. *Development and Validation of a Solar Assisted Heat Pump Using Ice Slurry as a Latent Storage Material.* Science and Technology for the Built Environment 26(6): 837-846, CA

Vineyard, E. A. 2014. *Multi-function fuel-fired heat pump CRADA*. Presentation to 2014 DOE Building Technologies Office Peer Review meeting, April, Washington, DC, US
URL: http://energy.gov/sites/prod/files/2014/10/f18/emt07_vineyard_042414.pdf, US

Wetter, M. 2009. *GenOpt® Generic Optimisation Program User Manual Version 3.0.0*. Lawrence Berkeley National Laboratory Technical Report LBNL-2077E, US

A. Appendix

A.1 Simulation results TRNSYS Simulations of ORNL before field testing

Tab. A 1-Tab. A 3 provide summary results of sub-hourly simulations of the annual performance of a DOE minimum efficiency (2006 efficiency minimums) baseline HVAC/WH/DH system, an AS-IHP, and a GS-IHP for the five locations. Tab. A 2 gives the baseline system results, both for annual energy use and hourly winter and summer maximum peak kW as well as mid-afternoon summer peak kW demand.
The baseline system included a fixed capacity air-source heat pump (ASHP) with a rated seasonal cooling COP of 3.8 (SEER of 13 Btu/Wh) and US Region IV seasonal heating COP of 2.3 (HSPF of 7.73 Btu/Wh), an electric water heater with a rated efficiency or energy factor (EF) of 0.90, a 19 l/d (5 gal/d) capacity standalone dehumidifier with a rated DH energy factor (EF_d) 1.4 l/kWh, and ventilation rate per requirements of ASHRAE Standard 62.2 (ASHRAE 2007). Tables 3.3 and 3.4 provide results for the concept AS-IHP and GS-IHP systems, respectively. Control set points were the same for all three systems. For SH/SC, set points were 21.7 °C and 24.4 °C (71 °F and 76 °F), respectively; set point for WH was 49 °C (120 °F); set point for DH was 55% relative humidity (RH). Each system also included a humidifier set to maintain a minimum indoor RH of 30%. The assumed daily hot water use was ~245 l/d (~64.5 gal/d), consistent with the Department of Energy (DOE, 2010) daily hot water draw totals for electric resistance and heat pump water heater (HPWH) Energy Factor (EF) ratings testing.

Tab. A 1: Estimated annual site HVAC/WH system energy use and peak kW for baseline HVAC/WH system

Location	Heat pump cooling capacity [tons]	HVAC/WH site energy use, [kWh]	HVAC/WH hourly peak kW demand (W/S/SA)
Atlanta	1.25	7230	8.6/4.6/2.1
Houston	1.25	7380	6.1/4.4/2.2
Phoenix	1.50	6518	6.1/3.9/2.1
San Francisco	1.00	4968	5.7/5.6/1.6
Chicago	1.25	10773	9.7/6.1/2.4

* W – winter morning; S – summer maximum; SA – summer mid-afternoon

Tab. A 2: Estimated annual site HVAC/WH system energy use and peak kW for AS-IHP system

Location	Heat pump cooling capacity [tons]	HVAC/WH site energy use, [kWh]	HVAC/WH hourly peak kW demand (W/S/SA)*	% energy savings vs. baseline
Atlanta	1.25	3349	2.2/1.5/1.2	53.7
Houston	1.25	3418	1.9/1.1/1.1	53.7
Phoenix	1.50	3361	2.1/1.7/1.7	48.4
San Francisco	1.00	1629	1.8/1.6/0.8	67.2
Chicago	1.25	5865	7.3/1.6/1.0	45.6

* W – winter morning; S – summer maximum; SA – summer mid-afternoon

Tab. A 3: Estimated annual site HVAC/WH system energy use and peak kW for GS-IHP system

Location	Heat pump cooling capacity [tons]	HVAC/WH site energy use [kWh]	HVAC/WH hourly peak kW demand (W/S/SA)*	% energy savings vs. baseline
Atlanta	1.25	3007	2.0/1.1/1.0	58.4
Houston	1.25	3290	1.8/1.1/1.0	55.4
Phoenix	1.50	2909	1.7/1.2/1.2	55.4
San Francisco	1.00	1699	1.8/1.6/0.6	65.8
Chicago	1.25	5126	6.9/1.7/0.8	52.4

* W – winter morning; S – summer maximum; SA – summer mid-afternoon

A.2 Development process GS-IHP

In early 2008 an industry partner, ClimateMaster, Inc. (CM), and ORNL began a series of GS-IHP system design iterations resulting in two generations of GS-IHP prototypes for lab and field testing. Results of the lab tests performed by CM were used to calibrate the variable-speed research version of the DOE/ORNL heat pump design model (HPDM) (Rice 1991; Rice et al, 2005) which was incorported into the TRNSYS simulation model for estimation of annual performance and energy savings potential. The process is documented by Rice, et al (2013) and Baxter et al. (2013) and summarized in this subsection.
A nominal 2-ton (7 kW) design cooling capacity was selected for system development leading to field testing. CM assembled and lab tested two generations of prototype systems in their laboratory over a wide range of ground-source conditions. ORNL used the detailed lab measurements of refrigerant and source/sink conditions to calibrate the HPDM in each of the four operating modes: SH, SC, SC + WH, and dedicated WH. The HPDM was linked to a publicly available optimisation program, GenOpt (Wetter, 2009), to auto-calibrate available heat exchanger (HX) adjustment factors as linear or quadratic functions of compressor speed and/or source/sink temperatures for best match to measured suction and discharge pressures. The test data were also used to determine compressor map power and mass flow corrections, compressor shell heat loss factors, line heat gains/losses and suction superheat levels as similar functions of compressor speed and/or other operating conditions, as well as the indicated active refrigerant charge in each mode. Tab. A 4 summarizes the difference between the calibrated models and CM‘s lab test data for the final prototype in capacity, compressor power, and compressor-only COP.

Tab. A 4: Agreement of Calibrated Models to Prototype 2 GS-IHP Lab Tests

Calibrated Model Results for Prototype 2 GSIHP				
Operation Mode	**Calibration Statistics**	**Capacity**	**Compressor Power**	**Compressor Only COP**
		[%]	**[%]**	**[%]**
Space Cooling	ave. diff.	4.8	1.3	3.5
	std. dev.	2.1	1.9	2.6
Space Heating	ave. diff.	4.8	1.4	3.4
	std. dev.	1.2	1	1.4
Dedicated WH	ave. diff.	-3.9	-0.9	-3
	std. dev.	3	1.5	3.4

Baseline equipment modeling

To determine the energy savings potential of the GS-IHP design, two baseline cases were also defined. First, a minimum efficiency standard, electric-driven equipment set was defined. This included a 7 kW (2-ton) fixed capacity air-source heat pump with a rated SEER of 13 (cooling SPF=3.8) and US Region IV HSPF of 7.7 (heating SPF=2.3), represented as a function of ambient and indoor conditions based on a manufacturer’s published data, and an electric water heater with a rated efficiency or energy factor (EF) of 0.90. This is essentially the same as the baseline system used in the IHP concept development (see IHP Background section above) but without the dehumidifier and humidifier units.
Next a high-efficiency commercially available two-capacity 7 kW (2-ton) ground source heat pump with desuperheater (GSHPwDS) was modeled in HPDM, which was calibrated based on manufacturer’s lab data as was done for the GS-IHP case. The two-capacity GSHP has a rated full load cooling COP of 5.4 (EER of 18.5 Btu/Wh) and a rated full load heating 4.0 COP per ISO standard 13256-1 (1998). Part load ratings are 7.6 COP cooling (26 EER) and 4.6 COP heating. Full- and part-load GSHP cooling capacities are 7.80 and 6.25 kW (26.6 and 21.3 MBtu/h) with full- and part-load heating capacities of 5.80 and 4.84 kW (19.8 and 16.5 MBtu/h).

The desuperheater function was modeled in TRNSYS as a fixed HX effectiveness based on the manufacturer's test data, pump operation logic, and recommended control settings for the domestic hot water (DHW) tank element thermostats for a 49°C (120°F) set point. The ground and DHW loop pumps were typical single-speed induction-motor designs used by the manufacturer.

GHX modeling

The GHX configuration for both the GS-IHP and GSHPwDS was modeled in TRNSYS as two vertical bore loops connected in parallel. Soil properties were assumed or measured for the 5 U.S. locations. Ten-year sizing runs were made at multiple bore lengths for each system and used to determine the required length to stay within the minimum (winter) and maximum (summer) 10-year design daily average entering water temperatures (EWTs). (As the minimum and maximum EWTs are approaching asymptotic values at 10 years of operation, 20-year values would be only slightly higher.)
Tab. A 5 shows the assumed soil characteristics and grout types for the 5 U.S. locations, the loop fluid, the minimum and maximum design temperatures, and the required bore lengths and specifications.

Tab. A 5: TRNSYS 10-year bore sizing results for GSHPwDS and GS-IHP units in reference house in 5 different U.S. locations

	Soil Characteristics, Assumed* or Measured[M]		Loop Fluid	Min 10-yr EWT	Max 10-yr EWT	Grout Type	Bore Length / Unit Cap. GSHPwDS	Grout Type	Bore Length / Unit Cap. GSIHP
	k	diffusivity							
Location	Btu/hr-ft-F [W/m-ºC]	ft²/day [mm²/s]		ºF [ºC]	ºF [ºC]	GSHP	ft/ton [m/kW]	GSIHP	(ft/ton) [m/kW]
Atlanta	1.2 [2.1]	0.90 [0.97]	Water	42 [5.6]	95 [35]	Std	313 [27.1]	Enh	294 [25.5]
Houston	1.2 [2.1]	0.90 [0.97]	Water	42 [5.6]	95 [35]	Std	294 [25.5]	Enh	220 [19.1]
Phoenix	0.8[M] [1.4[M]]	1.65[M] [1.77[M]]	Water	42 [5.6]	95 [35]	Std	572 [49.6]	Enh	449 [38.9]
San Francisco	1.4 [2.4]	1.02 [1.10]	Water	42 [5.6]	95 [35]	Std	268 [23.2]	Enh	310 [26.9]
Chicago	1.4 [2.4]	1.02 [1.10]	20% PG	30 [-1.1]	95 [35]	Std	233 [20.2]	Enh	299 [25.9]
	*per soil property data on GEOKISS site (http://www.geokiss.com/res-design/GSHPDesignRec2.pdf)								

Bore Specifications:
Number of Bores = 2
Bore Diameter = 4.5"[11.4cm], Borehole Separation = 15'[4.57m], Nominal HDPE Pipe Size = 0.75"[1.9cm]
Grout Conductivity Assumptions:
Standard grout, 0.4 Btu/hr-ft-ºF [0.69 W/m-ºC]
Enhanced grout, 0.9 Btu/hr-ft-ºF [1.56 W/m-ºC]

Standard grout was assumed for the conventional 2-capacity GSHPwDS and enhanced grout for the GS-IHP. Enhanced grout was found to more than pay for its higher cost by reducing the required bore length, which was especially beneficial in balanced and cold climates due to the added heat extraction from the ground loop in the winter and shoulder months to meet the domestic hot water (DHW) load. In Atlanta, the required bore length for the GS-IHP with the enhanced grout was 33% less than for standard grout; however, the annual energy use for the GS-IHP was found to be nearly the same regardless of grout used since both cases stayed similarly within the minimum and maximum loop design temperatures. Had standard grout been used for the GS-IHP Atlanta case, however, 25% more bore depth was predicted to be required than for the 2-capacity GSHPwDS case.
The relative bore depth requirements between the GS-IHP and two-capacity GSHPwDS given in Tab. A 5 show a 6% shorter bore for the GS-IHP in Atlanta, 22 and 25% less depth needed in Phoenix and Houston, and 16 and 28% longer bores needed in San Francisco and Chicago.

System control set points

For SH/SC, indoor set points were 21.7 °C and 24.4 °C (71 °F and 76 °F), respectively; the set point for WH was 49 °C (120 °F). The system's DHW controls for heat pump WH operation for the analysis were set to operate until the lower tank temperature was 49 °C (120°F) and the upper electric element was set to minimize electric element use while maintaining the upper tank delivery temperature above 41 °C (105 °F). The assumed daily water use schedule shown in Fig. A 1 includes discrete tempered (@ 41 °C) and untempered (@ 49 °C) hot water draws totaling ~245 l/d (~64.5 gal/d).

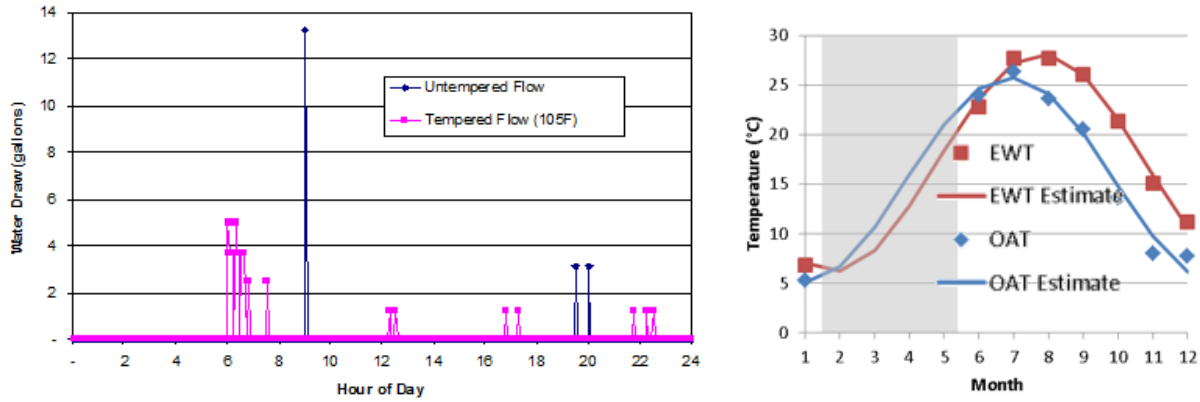

Fig. A 1: Assumed daily hot water draw schedule from DHW tank (left) and OAT and EWT measured Data and estimates (2012-2013) (right)

Performance simulation results

Predicted total annual energy savings for the GS-IHP prototype 2 design are shown in Tab. A 8 based on TRNSYS analyses in five Building America locations. The predicted energy savings range from 57.2% to 61%. Average savings are 58.7% over the 5 climates.
Electric resistance energy use for space and water heating is predicted to be essentially eliminated in all but the northern climate case, where it was reduced by 97.4%. Water heating savings relative to resistance units range from 68 to 79%.

GS-IHP field performance observations

Both the 1st and 2nd generation prototype IHPs were field tested in a research house in Oak Ridge, TN with simulated occupancy loads (Munk et al., 2014). Fig. A 2 left is a photo of the house along with thermal envelope. Fig. A 2 right shows the GHX layout (a horizontal trench GHX, part of which was located in existing foundation and utility trenches).

Fig. A 2: Test site (left) and GHX layout (right)

The home was split into four zones, upstairs, downstairs living space, master bedroom, and basement, which were all controlled to same set points of 21.7°C for heating and 24.4°C for cooling. The GHX had a total of 796 m of high density polyethylene (HDPE) pipe placed around the foundation of two of the basement walls in addition to two utility trenches and a rain garden in the backyard.
Tab. A 6 shows the four operating modes of the prototypes. During the cooling season, the unit can operate in three of the four modes: SC, SC+WH, or WH. If there are coincident space cooling and water heating demands, the unit will run in the SC+WH mode. If there is only a demand for water heating, the unit will run in WH mode. During the heating season, the unit only operates in two of the four modes: SH and WH. There is no combined space heating and water heating mode, so the unit gives water heating priority unless the indoor space temperature falls by a preset number of degrees below the heating set point.

Tab. A 6: Prototype GS-IHP Operating Modes

Mode	Heat Source	Heat Sink
Space Cooling	Indoor Air	Ground Loop
Space Heating	Ground Loop	Indoor Air
Space Cooling plus Water Heating	Indoor Air	Domestic Hot Water
Dedicated Water Heating	Ground Loop	Domestic Hot Water

The 1st generation prototype was monitored for the 2011 year (January through December) with details summarized in Baxter et al (2013). Several technical issues were encountered during the year that resulted in frequent interruption of GS-IHP operation.

While this limited the extent of the collected performance data, what was available provided invaluable information to CM, enabling them to develop a much improved 2nd generation prototype.
The 2nd generation prototype was installed at the test site on May 7, 2012 with the help of CM personnel. Monitoring of the 2nd generation system took place from June 2012 through January 2013. Since an entire year's worth of data was not able to be collected during the project, approximations were made for months where data was not available, so that the annual performance could be estimated. The first step in this process was to fit a sinusoidal wave to the daily average outdoor air temperature (OAT) and daily average entering water temperature (EWT) data. These waveforms were then used to generate average monthly OATs and EWTs for the months without data, Fig. A 1 right. The load in each mode was then estimated by plotting the monthly delivered output in kWh against the average OAT for the month. A linear fit was applied and, along with the estimated OAT, a delivered load was estimated for months without data. Similarly, the COPs for each mode were estimated by plotting the existing data against the average EWT for each month.

Tab. A 7: 1st generation GS-IHP vs. Baseline Equipment; Estimated Annual Performance Comparison

Operation mode		GS-IHP	Baseline Equipment	Percent Savings Over Baseline
Space Cooling	COP	4.9	3.7	
	Delivered [kWh]	8432	8432	
	Consumed [kWh]	1707	2298	25.7%
Space Heating	COP	4.1	2.4	
	Delivered [kWh]	10524	10524	
	Consumed [kWh]	2539	4337	41.5%
Water Heating	COP	3.8	1	
	Delivered [kWh]	2733	2733	
	Consumed [kWh]	726	2733	73.4%
Total	**Consumed [kWh]**	**4972**	**9368**	**46.9%**

The estimated annual energy use of the GS-IHP was then compared to that of a baseline system at the same site.

The baseline consisted of an ASHP with a rated seasonal cooling COP of 3.8 (SEER of 13 Btu/Wh) and rated seasonal heating COP (in US Region III) of 2.4 (HSPF of 8.3 Btu/Wh), as rated per AHRI 210/240 (AHRI 2008), coupled with an electric resistance water heater.
The ASHP rated cooling performance was degraded by 4.7% based on manufacturer's performance data to account for site return air temperatures that were lower than those used to determine the ratings. Results are shown in Tab. A 7.
The space cooling performance for the GSHP is similar to the performance seen from high end ASHPs that have been tested in this climate. However, the water heating COP of 3.8 and space heating COP of 4.1 are very high relative to standalone heat pump water heaters (HPWH) and ASHPs, respectively. Since the tank losses from the DHW storage tank were not accounted for in the GS-IHP field measured performance, they were also omitted from the baseline equipment efficiency for the performance comparison in Tab. A 7 (baseline WH energy factor (EF) of 1.0).

Tab. A 8: Energy Use and Savings for Prototype 2 Relative to Minimum Efficiency Equipment Suite in Residential 7kW Cooling Application

Operation		ASHP	GSHP w DS	Savings from Base	VS GSIHP	Savings from Base
Space Cooling	Con-sumption [kWh] **Atlanta**	1608	1177	26.8 %	754	53.1 %
Space Heating		2388	1660	30.5 %	1155	51.6 %
Water Heating		3293	2672	18.8 %	848	74.3 %
Ventilation		189	189		189	
Total		7479	5699	23.8 %	2946	60.6 %
Space Cooling	Con-sumption [kWh] **Houston**	2548	2154	15.5 %	1542	39.5 %
Space Heating		1102	754	31.6 %	495	55.1 %
Water Heating		2813	2030	27.8 %	619	78.0 %
Ventilation		189	189		189	
Total		6653	5128	22.9 %	2845	57.2 %
Space Cooling	Con-sumption [kWh] **Phoenix**	3450	2756	20.1 %	1921	44.3 %
Space Heating		762	542	28.9 %	306	59.9 %
Water Heating		2470	1731	29.9 %	510	79.4 %
Ventilation		189	189		189	
Total		6871	5218	24.1 %	2926	57.4 %
Space Cooling	Con-sumption [kWh] **San Francisco**	23	4	83.9 %	10	57.0 %
Space Heating		1366	1142	16.4 %	813	40.5 %
Water Heating		3766	3405	9.6 %	1070	71.6 %
Ventilation		189	189		189	
Total		5344	4741	11.3 %	2082	61.0 %
Space Cooling	Con-sumption [kWh] **Chicago**	651	333	48.8 %	251	61.5 %
Space Heating		6448	4052	37.2 %	3139	51.3 %
Water Heating		4140	3309	20.1 %	1309	68.4 %
Ventilation		189	189		189	
Total		11429	7884	31.0 %	4888	57.2 %

The table shows that the largest percentage and absolute savings come from water heating, at 73.4% and 2007 kWh respectively. The energy savings in the space heating mode come in a close second at 1798 kWh due to both the high efficiency and high heating load (higher than normal for the test site location).
The total annual savings when compared to the Baseline equipment is predicted at about 47%, which is very close to the 50% targeted savings for the project. One should note that the actual daily hot water use at the test site was only ~185 l/day vs. the ~245 l/day used for the prototype 2 simulations summarised in Tab. A 8. Had the DHW usage at the test site been at the higher level, the annual savings would have been about 50%.

The HPDM was calibrated against lab data for the 2nd generation unit and used to develop performance maps and these, in turn, were input to the TRNSYS/HPDM (T/H) annual performance simulator along with the site weather data for the 2012 heating and cooling seasons, the site hot water usage averaging ~185 l/d (~49 gal/d), average GHX loop EWTs and water mains temperatures during heat pump operation, and test house specifications to estimate annual performance compared to a baseline minimum efficiency equipment suite (the same baseline suite as described in the Background section minus the dehumidifier and humidifier). The GHX loop EWTs and water mains temperatures for 2012 are shown Fig. A 3.

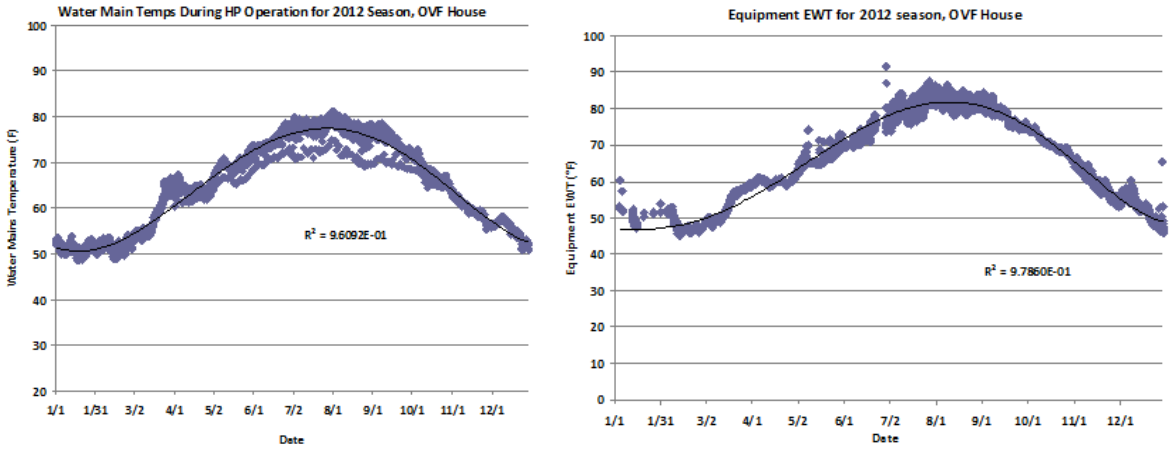

Fig. A 3: Average return ground loop temperatures (left) and average water mains temperatures (right) during heat pump operation for 2012 season, ZEBRAlliance house 2 in Oak Ridge, TN

Results of the T/H simulations follow in Tab. A 9 and Tab. A 10. Tab. A 9 shows the projected energy savings for the 2nd generation prototype where predicted total HVAC/WH savings are 57.8%. Space conditioning savings approach 50% while water heating savings exceed 76% compared with the baseline electric resistance water heater (WH tank losses were accounted for in the simulation).

Tab. A 9: Projected 2nd generation GS-IHP prototype energy savings vs. baseline systems for House 2 in 2012 season

Operation mode		GS-IHP	Baseline Equipment	Percent Savings Over Baseline
Space Cooling	COP	6.77	3.38	
	Delivered [kWh]	5202	5202	
	Consumed [kWh]	768	1539	50.1%
Space Heating	COP	5.19	2.68	
	Delivered [kWh]	8765	8765	
	Consumed [kWh]	1690	3265	48.2%
Water Heating	COP	3.79	0.89	
	Delivered [kWh]	2313	2313	
	Consumed [kWh]	610	2605	76.6%
Total	**Consumed [kWh]**	**3177**	**7519**	**57.8%**

Tab. A 10 shows the predicted seasonal COPs (performance factors). Converting the seasonal performance numbers to US SEER and HSPF indices, the GS-IHP had a predicted SEER of 23.1 Btu/Wh and HSPF of 17.7 Btu/Wh.

Tab. A 10: Projected 2nd generation seasonal COPs

Predicted Seasonal COPs, OVF House, 2012 Season			
	SC COP	SH COP	WH COP
Baseline ASHP	3.38	2.68	0.89
2nd Gen. GSIHP	6.77	5.19	3.79

GS-IHP product development status and preliminary payback analyses

A new product based on the beta unit design was announced by CM in 2012 – the Trilogy® 40 Q-Mode™ (http://www.climatemaster.com/residential/geothermal-heat-pumps/trilogy/). The unit was formally introduced in a March 2012 press release and was available for order beginning in December 2012. It is available in two nominal SC capacity sizes: 7kW (2 ton) and 14 kW (4 ton).

Preliminary payback analyses for the GS-IHP system concept were reported in Murphy et al (2007b). These analyses were based on the assumption of large quantity production and mature market competition. The simple payback for the GS-IHP vs. the baseline system ranged from 7 to 14 years. These estimates are subject to significant uncertainties primarily related to the GHX installation costs, which can vary widely depending on local site geologic characteristics.

A.3 Load profile of the Net Zero Residential Testing Facility

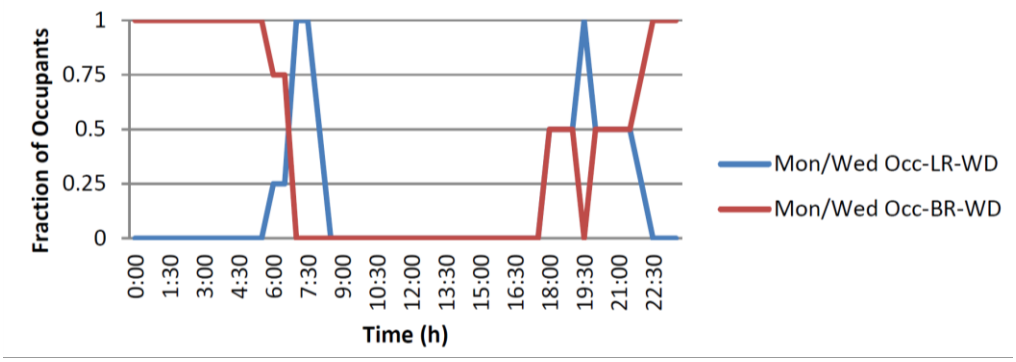

Fig. A 4: Load profile NZERTF for Mondays and Wednesdays

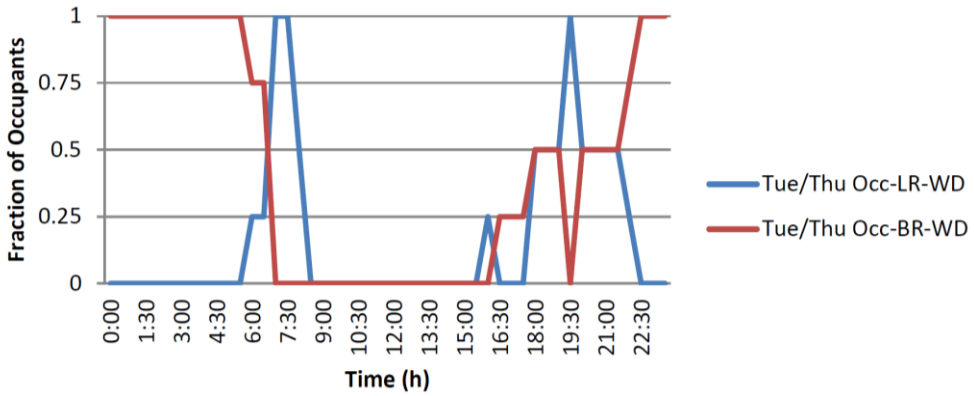

Fig. A 5: Load profile NZERTF for Tuesdays and Thursdays

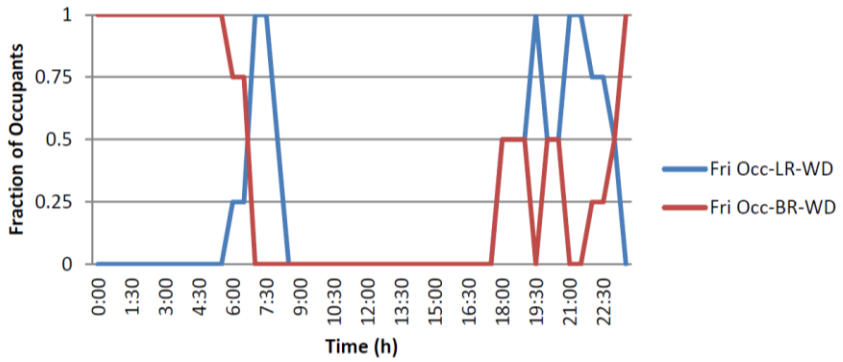

Fig. A 6: Load profile NZERTF for Fridays

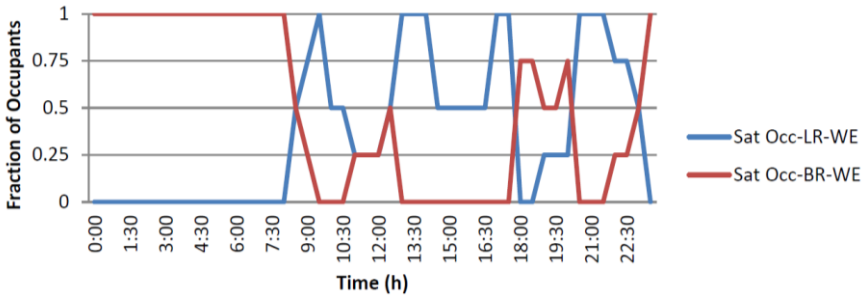

Fig. A 7: Load profile NZERTF for Saturdays

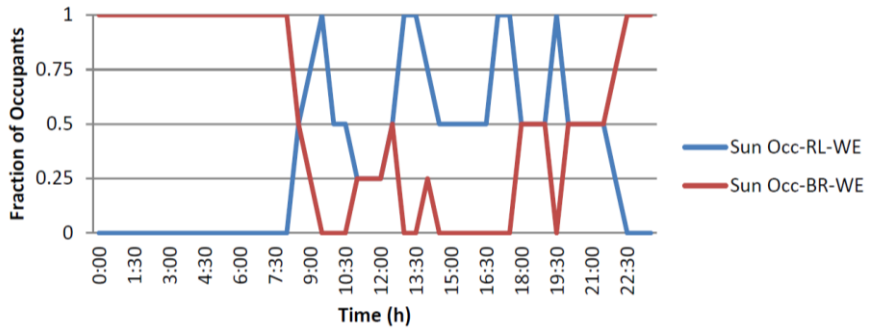

Fig. A 8: Load profile NZERTF for Sundays

A.4 Instrumentation Net Zero Energy Residential Testing Facility

Tab. A 11: Instrumentation installed on ASHP

Instrument	Model [2]	Range	Total Uncertainty at a 95 % Confidence Level
Transducer voltage measurement	National Instruments, cDAQ-9205	0 to 10 VDC	±5 mVDC
T-type thermocouples	National Instruments, cDAQ-9214	-10 °C to 55 °C	±0.6 °C
Barometric pressure	NA	67.0 to 101.5 kPa	±1 % of reading
High pressure transducer	Omegadyne PX309-1KGI	6895 kPa	±0.25 % of reading
Low pressure transducer	Omegadyne PX309-500GI	3447 kPa	±0.25 % of reading
Air pressure differential (ESP[1])	Ashcroft CX8MB	0 to 187 Pa	±0.8 % of reading
Indoor blower and controls power meter	Ohio Semitronics W-002X5	0 to 300 VAC, 5 Amps, 1000 W	±5 W
Indoor total power meter	Ohio Semitronics W-059E	0 to 300 VAC, 100 Amps, 20 000 W	±100 W
Outdoor unit power meter	Ohio Semitronics W-110X5	0 to 300 VAC, 20 Amps,4000 W	±20 W
Supply air dry-bulb temperature sensor	General Eastern Humi-DP-XR-D	-28.8 °C to 49 °C	±0.5 °C
Supply air dewpoint temperature sensor	General Eastern Humi-DP-XR-D	-28.8 °C to 49 °C	±1.0 °C
Return air dry-bulb temperature sensor	Vaisala HMT330-3	-40 °C to 60 °C	±0.2 °C
Return air dewpoint temperature sensor	Vaisala HMT330-3	-20 °C to 100 °C	±1.5 % of reading
Outdoor air dry-bulb temperature sensor	Vaisala HMT330-3	-40 °C to 60 °C	±0.2 °C
Outdoor air dewpoint temperature sensor	Vaisala HMT330-3	-20 °C to 100 °C	±1.5 % of reading
Coriolis refrigerant mass flow meter	Micromotion Coriolis Elite Sensor, CMF025	0 to 2180 kg h^{-1}	±0.15 % of reading

1- External Static Pressure

2- Identification is not intended to imply recommendation or endorsement by the National Institute of Standards and Technology, nor is it intended to imply that the entities, materials, or equipment are necessarily the best available for the purpose.

A.5 Detailed results of the NZERTF in the first year of operation

Tab. A 12: Monthly NZERTF thermal loads and energy consumption [kWh] by end use

Month/Year	Jul/13	Aug/13	Sept/13	Oct/13	Nov/13	Dec/13	Jan/14	Feb/14	Mar/14	Apr/14	May/14	Jun/14	Annual
Heating Load	0.0	0.0	0.0	56.4	830.4	1351.0	2156.9	1634.7	1423.5	252.7	0.0	0.0	7705.7
Cooling Load	2122.9	1392.1	937.2	306.4	1.7	0.0	0.0	0.0	0.0	66.8	603.0	1559.7	6989.7
DHW Load	252.4	217.8	238.2	268.5	283.2	325.9	343.1	330.0	340.5	300.3	276.9	250.6	3427.5
Heat Pump Heating	0.0	0.0	0.0	33.6	396.4	581.5	1254.8	753.1	650.4	113.2	0.0	0.0	3783.1
Heat Pump Cooling	700.8	481.0	345.4	142.3	15.7	0.0	0.0	0.0	0.0	13.6	177.7	511.3	2387.8
Heat Pump Water Heater	53.3	70.8	57.0	82.5	129.8	156.3	142.8	125.0	120.7	72.7	55.2	46.1	1112.2
Solar System Circulators	35.7	27.1	31.4	24.2	22.0	18.2	20.4	19.8	22.6	29.0	34.3	34.8	319.6
Lighting	37.5	31.9	36.1	37.8	36.3	36.6	36.9	32.9	36.2	38.1	39.5	35.6	435.4
Plug Loads	202.5	167.1	199.7	210.2	208.5	210.2	214.0	193.8	216.7	206.3	208.2	202.5	2439.5
Heat Recovery Ventilator	42.4	35.6	42.3	44.4	43.7	44.3	46.4	38.7	45.3	42.8	45.4	43.1	514.4
Refrigerator	36.2	30.3	36.0	35.4	32.3	34.0	34.4	31.1	34.7	34.2	35.9	35.7	410.2
Dish Washer	7.8	6.4	7.8	7.8	8.8	8.6	8.6	7.8	8.9	8.0	7.9	7.9	96.3
Cooktop	19.2	16.4	19.7	19.2	19.6	19.7	19.3	17.8	20.9	19.2	20.1	19.4	230.4
Oven	30.0	27.0	31.7	30.0	33.7	31.9	30.0	29.3	35.8	31.7	33.7	31.7	376.6
Clothes Washer	5.2	4.6	6.2	6.2	6.1	6.3	6.2	5.6	6.4	6.0	6.1	6.0	70.8
Clothes Dryer	47.6	39.8	45.9	44.8	46.8	46.9	45.7	41.2	50.8	44.1	44.2	44.0	541.8
Microwave	12.3	10.4	12.3	12.5	12.2	12.4	12.6	11.4	12.7	12.2	9.2	11.1	141.3
Total PV AC Energy	1492.7	1162.4	1399.7	994.4	839.2	481.1	800.9	729.3	965.2	1425.1	1600.0	1633.3	13523.4
Total Energy Consumed	1262.7	968.3	888.9	747.9	1025.0	1193.7	1891.4	1324.5	1269.4	689.2	733.7	1044.5	13039.2
Net Energy Export	230.1	194.2	510.8	246.5	-185.8	-712.6	-1090.6	-595.3	-304.2	735.9	866.3	588.8	484.1

Tab. A 13: Monthly photovoltaic system performance

Month	Jul/13	Aug/13	Sep/13	Oct/13	Nov/13	Dec[a]/13	Jan[a]/14	Feb[a]/14	Mar[a]/14	Apr/14	May/14	Jun/14
Average Daily Incident Solar Energy on Array[b] (kWh)	292.4	270.1	283.0	190.3	160.0	108.0	149.7	183.3	207.3	271.8	309.1	325.0
Average Daily Solar Insolation on Array[b] (kWh/m^2)	5604.0	5176.0	5424.0	3648.0	3067.0	2069.0	2868.0	3513.0	3972.0	5209.0	5924.0	6228.0
Average Ambient Temperature (C)	25.7	23.6	19.7	15.0	6.8	4.3	-1.9	1.1	4.1	12.7	18.7	23.6
Average Cell Temperature During Energy Generation (C)	38.6	36.7	35.1	26.5	15.9	11.1	7.2	10.8	15.1	24.2	32.8	37.6
Average Daily Delivered DC Energy (kWh)	51.4	47.8	49.8	34.4	30.0	16.3	27.4	27.9	33.5	50.9	56.1	58.2
Array Efficiency (%)	17.6	17.7	17.6	18.1	18.8	15.0	18.3	15.2	16.2	18.7	18.1	17.9
Average Daily Delivered AC Energy (kWh)	49.3	45.7	47.7	32.8	28.6	15.4	26.0	26.7	31.9	48.6	53.7	55.7
Inverter Efficiency (%)	95.9	95.6	95.8	95.5	95.3	94.5	95.1	95.4	95.2	95.6	95.7	95.7

[a]For 8 days in December, 8 days in January, 12 days in February, and 10 days in March the PV array was fully or partially covered with snow. If these days had been excluded the array efficiencies would have been 19.2 %, 19.7 %, 19.5 %, and 19.2 %, respectively, for December, January, February, and March.
[b] The Average Daily Incident Solar Energy on Array was determined using the framed area of an individual module (1.63 m^2) multiplied by the number of modules (32).

Tab. A 14: Monthly ASHP performance

Month	Jul/13	Aug[a]/13	Sep/13	Oct/13	Nov/13	Dec/13	Jan/14	Feb/14	Mar/14	Apr/14	May/14	Jun/14
Thermal Load[b]	0.0	0.0	0.0	56.4	832.1	1351.0	2156.9	1634.7	1423.5	252.7	0.0	0.0
Heating Mode (kWh)	2122.9	1392.1	937.2	306.4	1.7	0.0	0.0	0.0	0.0	66.8	603.0	1559.7
Cooling Mode (kWh)												
Heat Pump Energy Usage	0.0	0.0	0.0	33.6	396.4	581.5	1254.8	753.1	650.4	113.2	0.0	0.0
Heating Mode (kWh)	700.8	481.0	345.5	142.3	15.7	0.0	0.0	0.0	0.0	13.6	177.7	511.3
Cooling Mode (kWh)												
Resistive Heat (kWh)	0.0	0.0	0.0	13.6	103.0	117.0	547.6	196.4	169.4	10.2	0.0	0.0
Avg. Outdoor Temp (°C)	26.6	24.6	20.7	15.5	7.1	4.5	-1.5	1.0	4.1	13.1	19.7	24.5
Avg. Indoor Temp (°C)	23.6	23.5	23.5	22.4	21.0	21.0	20.9	20.9	21.0	21.2	22.9	23.3
Degree Heating Days	0.0	0.0	30.7	218.8	610.0	773.5	1107.3	873.3	792.6	301.0	45.9	0
Degree Cooling Days	924.9	682.5	580.5	325.0	61.4	39.1	0.0	0.0	22.8	196.3	542.1	785.4
Heating Run Time (hr)	0.0	0.0	0.0	14.9	181.5	314.1	460.9	370.7	305.1	10.2	0.0	0.0
Cooling Run Time[c] (hr)	492.1	347.2	256.3	81.2	17.5	0.0	0.0	0.0	0.0	52.6	133.8	395.6
Dehumidification Mode (hr)	164.9	143.8	70.0	38.0	17.5	0.1	0.0	0.0	0.0	0.0	13.8	133.2
Dehumidification (l/kWh)	1.35	1.30	1.20	1.10	0.29	0.70	-	-	-	-	1.04	1.23
Coefficient of Performance												
Heating Mode (-)	0.00	0.00	0.00	1.68	2.10	2.32	1.72	2.17	2.19	2.23	0.00	0.00
Cooling Mode (-)	3.03	2.89	2.71	2.15	0.11	0.00	0.00	0.00	0.00	4.90	3.39	3.05
COP1 (Dehumidification)[d]	0.93	0.89	0.91	0.76	0.20	0.48	-	-	-	-	0.71	0.84

[a]Missing data Aug 2 through Aug 6, 2013
[b]Heat pump thermal load includes electric resistance heat.
[c]Cooling run time includes the time the unit operated in the dehumidification mode.
[d]Dehumidification COP equals the average of the daily dehumidification COP values (total latent energy divided by electrical energy during active dehumidification)

Tab. A 15: Monthly heat recovery ventilator performance

Month/Year	Jul/13	Aug/13[a]	Sept/13	Oct/13	Nov/13	Dec/13	Jan/14	Feb/14	Mar/14	Apr/14	May/14	Jun/14
Energy Consumption (kWh)	42.4	35.6	42.3	44.4	43.7	44.3	46.4	38.7	45.3	42.8	45.4	43.1
Average Ambient Temperature (°C)	26	24	20	15	7	4	-2	1	4	13	19	24
Average Outdoor Air Temp to HRV (°C)	26	24	20	16	8	6	1	4	6	13	19	24
Average Indoor Temp to HRV (°C)	24	24	24	22	21	21	21	21	21	21	23	24
Average HRV Exhaust Temperature (°C)	26	24	22	18	13	12	9	11	12	16	21	24
HRV Effectiveness (-)	0.62	0.61	0.71	0.75	0.76	0.74	0.73	0.74	0.75	0.75	0.75	0.74
Average Flow Rate (m^3/hr)	174	192	180	194	186	206	208	205	207	195	201	193
Sensible Load[b] Introduced by HRV(kWh)	-18.7	4.9	54.4	106.8	204.5	244.5	314.3	245.4	243.5	122.0	62.2	4.8
Latent Load[c] Introduced by HRV (kWh)	511.7	282.9	40.1	-23.5	-138.4	-106.0	-106.8	-70.7	-58.2	-76.0	-23.4	233.1
Additional Heat Pump Electrical Energy Used to Meet HRV Ventilation Load (kWh)[d]	229.6	191.6	-5.4	-30.7	32.1	154.9	417.1	201.1	189.5	-16.9	-77.0	165.0
Sensible Load Introduced by Balanced Ventilation System, No HRV (kWh)	-81.1	-10.1	122.5	236.2	491.0	591.9	763.0	593.6	591.3	293.0	133.4	-21.1
Latent Load Introduced by Balanced Ventilation System, No HRV (kWh)	513.6	290.4	62.3	12.3	-113.1	-80.4	-80.1	-52.7	-38.1	-54.3	3.7	262.1
Additional Heat Pump Electrical Energy Used to Meet Balanced Ventilation System (No HRV) Load (kWh)[e]	201.7	167.2	-15.6	1.7	58.6	198.6	538.5	229.1	232.3	29.9	-64.5	154.1
Difference in Heat Pump Energy – No HRV vs HRV Ventilation relative to HRV Ventilation (%)	-4.0	-5.0	-1.8	18.4	6.4	7.5	9.6	3.8	6.6	35.9	7.0	-2.1

[a] Missing data for Aug-2 through Aug-8, 2013

[b] Sensible loads are the sum for the month with positive sensible indicating cooling and negative indicating heating the house.
Some days the HRV or the mechanical ventilation system helped the cooling or heating system and some days the HRV or mechanical system worked against the heating or cooling system.

[c] Latent loads should be equal but differ due to using living room relative humidity and temperature for the exhaust air when doing calculations for mechanical ventilation.
HRV calculations where done with living room relative humidity and the temperature measured at the HRV for the exhaust air. A negative latent load occurred when moisture was removed from the house

[d] Heat pump electrical is the reduction or increase in the energy consumed by the heat pump as the result of introducing outdoor air utilizing the HRV

[e] Heat pump electrical is the reduction or increase in the energy consumed by the heat pump as the result of introducing the same quantity of outdoor air as the HRV case but with no heat recovery

www.heatpumpcentre.org

IEA Heat Pump Centre
c/o SP Technical Research Institute of Sweden
PO Box 857
SE-501 15 BORÅS
Sweden
Tel: +46 10 516 5512
E-mail: hpc@heatpumpcentre.org

www.heatpumpcentre.org

Report no. HPP-AN40-3